11-2015

Biomechanical Investigation of Elite Place-Kicking

Chase M. Pfeifer
University of Nebraska-Lincoln, chasepfeifer@gmail.com

Biomechanical Investigation of Elite Place-Kicking

by

Chase M. Pfeifer

A DISSERTATION

Presented to the Faculty of

The Graduate College at the University of Nebraska

In Partial Fulfillment of the Requirements

For the Degree of Doctor of Philosophy

Major: Biomedical Engineering

Under the Supervision of Professors Jeff A. Hawks and Shane M. Farritor

Lincoln, Nebraska

November, 2015

Biomechanical Investigation of Elite Place-Kicking

Chase M. Pfeifer, PhD

University of Nebraska, 2015

Advisors: Jeff A. Hawks, Shane M. Farritor

Many studies aim to understand the fundamentals of kicking commonly displayed by soccer players [4,6,10,16,17,18,24,25,28,29,30,34,36,38,40]. Of those studies, most are limited to a two-dimensional (2D) analysis using high-speed cameras for position tracking or utilizing electromyography to observe the activity of select muscles [4,6,18,25,29,36]. The few studies that investigate kicking using a three-dimensional (3D) model are limited in their position tracking capabilities and focus mainly on joint flexion potentials and foot speed.

This dissertation is a comprehensive biomechanical analysis (kinematic and EMG) of the field-goal place-kicking techniques of four elite kickers in American football. Data were compared and contrasted with ball flight trajectories created using a motorized mechanical place-kicker to elucidate the influence of impact location on ball flight. A novel tracking software was developed to quantify ball flight trajectory. Human subject testing revealed that the ideal timing of proximal-to-distal motion (application of the summation of speed principle) plays a key role in achieving maximum kicking potential. However, the quality of a place kick cannot be determined solely on foot speed but also other impact conditions such as foot orientation, impact location, and the energy created by the kicking leg through impact. The findings emerging from human subjects' testing were reinforced by data emerging from the mechanical kicker, demonstrating that

impact location is the driving factor influencing the football's flight. These findings correlate with the results of the human subject testing.

To the author’s knowledge, this work is the first published study to date that comprehensively analyzed kinematic and electromyography patterns generated by elite American football place kickers and compared these data to patterns emerging from a motorized mechanical model of place kicking.

To my wife, Charity L. Pfeifer

Acknowledgements

The completion of this dissertation would not have been possible without the guidance and assistance of several people. First, I would like to acknowledge the opportunity given to me by the Department of Mechanical & Materials Engineering to be funded and perform this research. I would also like to acknowledge Dr. Wieslaw Syzdlowski who helped to direct me through my master's research and has played a pivotal role in my development as an instructor.

This research would not be possible without the equipment, knowledge, and expertise of the Nebraska Athletic Performance Lab and the researchers. Specifically Dr. Judith Burnfield, Dr. Guilherme Cesar, and Ryan Hasenkamp. Without their expertise in biomechanics and research procedures, this project would still be in its infancy. A number of student volunteers put countless hours into performing kicks with the mechanical kicking machine and processing the projectile tracking data. I would like to thank Andrew Palmesano and Margret (Maggie) Clay for all their help on this front.

I would also like to acknowledge my dissertation committee for all their guidance. Dr. Jeff Hawks for peaking my interest in biomechanics many years ago, taking me under his wing and supporting me over the years, as well as constantly networking for me to ensure that I am in touch with the right people to surpass all my road blocks. Dr. Judith Burnfield for continuing to teach me the more clinical side of biomechanics and looking at the bigger picture. You have stepped in over the last year and have given my goals and aspirations direction and I cannot thank you enough. Dr. Shane Farritor for making time for me at a moment's notice and opening your lab and resources of tools and knowledgeable students to help me along the way. Your lab's mechanical field-goal

kicker has allowed for the development of interesting and meaningful studies. Dr. Timothy Gay who wrote the book on football physics and I am sure will continue to be a resource and colleague down the line.

Finally, I would like to thank my family and friends for their love, encouragement, and support over the years. My beautiful wife Charity who has been by my side over the last 8+ years as we have moved across the country time after time always supportive of my goals and dreams. My father, Brian Pfeifer, has always been a call away for me to bounce a theory off of or to work out a concept. You have always made it clear that the sky is the limit and if I work hard enough I can do anything. My mother, Susan Pfeifer, and my sister, Blake Michaels, you are always there in a time of need and constantly make my life brighter. Last of all I would like to thank my friend and colleague Matt Kalus for conducting the first stage of study with me back in 2011, which seems like a lifetime ago... Without that first step, none of this would be possible.

Table of Contents

List of Figures

List of tables

Chapter 1: Introduction

The kicking motion, similar to that for throwing, starts to develop in human beings at a young age. This skill often grows through adolescence as youth play games such as soccer and kick-ball or participate in martial arts. At the college and professional level there are a number of popular sports that require someone to perform a kicking motion such as soccer, football, rugby, kick-boxing, and mixed martial arts. Given the diversity of kicking techniques and projectiles (e.g., round, oblong, inflated, hard, human body), this dissertation has selected to focus primarily on the complex motion of place-kicking in American football. However, it is expected that some aspects of the results and conclusions will have implications for other kicking applications.

1.1 Background

American football (from now on referred to as football) came to life in the United States in the late 1800s, having its core roots in rugby and soccer. A football team is commonly split into three units which include an offense, defense, and special teams. Every special teams play (kick-off, punt, and field-goal/point after touchdown) involves one of three different types of kicking. Each of these kicks occurs in different situations and requires different skills and mechanics of movement by the individual performing the kick (the "kicker"). A snapshot of these motions can be observed in Figure 1.

A punting situation occurs when the offense has one remaining chance to advance the ball past the first down marker and wishes to kick the ball down the field in hopes of giving the receiving team a field position that is more advantageous to the kicking team. In most cases the punter desires to kick the ball as far as he can with the most hang time,

in order to allow his team to advance down the field and tackle the opposing player who is attempting to catch and return the punt. In order to make the ball travel as far as possible it is desired that the ball travel in a spiral to reduce air drag. Numerous studies have been performed on the flight of a spiraling football, most notably, how an increased rotational velocity increases the stability of the ball through flight and reduces turbulent airflow along the surface of the ball, thus reducing the drag on the ball [45]. Knowing the velocity and trajectory of the ball leaving the foot, along with the aerodynamic properties of air around the ball, it is possible to estimate how far the ball will travel.

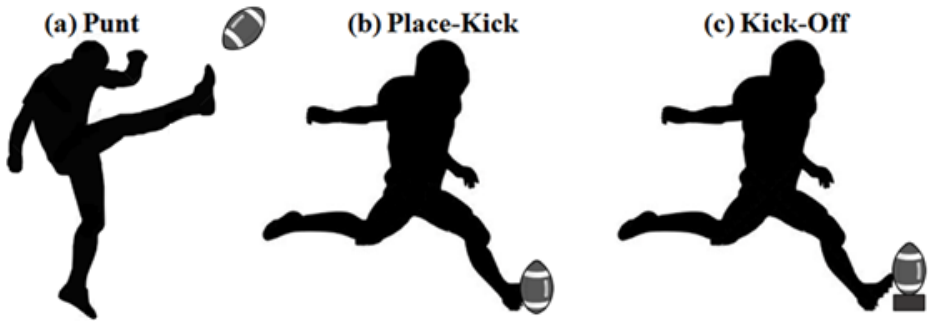

Figure 1 - Types of kicking in football (a) the punt (b) the place-kick (c) the kick-off

Kick-offs and field-goals greatly differ from punts in approach and ball flight. A punter takes two to three steps and, while dropping the ball, swings his leg straight up, leaning back to impact the falling ball while attempting to have his kicking foot end up near his ear on the same side of his body during his follow through. On a kick-off or field-goal the ball is placed on a tee or the ground respectively. A kicker approaches the ball and strikes it with their foot sending it on an end-over-end (aka, toppling) trajectory. This end-over-end flight is quite unpredictable. Therefore it is commonly accepted that a large striking velocity and momentum is desirable for kicking the ball further in a kick-

off or field-goal. When examining ball flight in punting, the tightness of a spiral may enable a punter to kick a ball farther with less applied force. This highlights that both the technique of creating an aerodynamically efficient spiral and force of impact can significantly influence the distance and speed of a football's flight.

Though more similar to each other than punts, kick-offs and field-goals have several key differences as well. First, though the ball is similarly oriented, a kick-off requires the ball to be placed on a tee while in a field-goal the ball is held on the ground by a teammate. The ball is generally orientated with its long axis vertical and depending on the kicker slightly tilted to the side or front/back. Field-goals require three people, a snapper, holder, and kicker. The ball is hiked to the holder who orients the ball on the ground for the kicker to kick. In this situation a kicker impacts the ball off of the ground and relies on their teammates to properly prepare the ball while the other team rushes towards them in an attempt to block the kick. The advantage of a kick-off is that the ball is stationary and placed off the ground on a tee. Placing the ball on a tee allows the kicker to have more freedom with impact location on the ball because the ground does not impede the motion of the kicking foot.

Second, as eluded to, there is a good deal of urgency and stress placed on a kicker during a field-goal. In contrast, a kicker typically has plenty of time to perform a kick-off. This correlates to the differences in approaches for the two kicks. Given the time constraints, a kicker usually travels 10-15 yards before making contact with the ball on a kick-off. For a field-goal the kicker only takes 2-3 steps (2-3 yards) before making contact with the ball. The limited amount of time a field-goal kicker has to kick the ball

forces quick accelerations and a high foot impact velocity, requiring quick reaction time and superb timing. This aspect of timing to create ideal velocities and accelerations is thoroughly investigated in this study.

1.1 Scope

The goal of this dissertation is to evaluate collegiate kickers and determine factors that contribute to more effective place kicks (point-after attempts and field-goals). I hypothesize that:

1) Individuals who demonstrate greater kinematic consistency across multiple kicks will launch the football with more similar trajectories.
2) Kicking movement patterns (kinematics and muscle demands) that more closely follow the summation of speed principle will result in a larger foot velocity potential and in turn a greater potential for increased kick distance.

These factors have been quantified by simultaneously recording lower body kinematics (joint and body segment motion) and electromyography (muscle activation patterns), as well as the resultant ball trajectory. Biomechanical factors of the lower body of four elite kickers (Division I college football kickers) were quantified and used to analyze the motion of field-goal kicking.

A secondary goal of this dissertation research was to refine and test a prototype mechanical kicking machine to assess end-over-end football flight patterns resulting from variations in impact location and angle while maintaining consistent impact speed and momentum. A projectile tracking technique developed for this study was used to track a

total of 135 trajectories from the mechanical kicking machine. This dissertation utilizes this same tracking technique to evaluate the elite kicker's point-after attempts (PAT) and field-goals. The evaluation of the kick quality is based on a number of trajectory factors including launch angle, ball speed, kick distance, and accuracy.

Using this evaluation the *best* (defined as the kick that went the furthest and most nearest to the center of the goal-post) and *worst* (defined as the kick that was either furthest from the center of the goal-post or traveled the least distance) field-goal kicks were selected from each participant and more comprehensively examined and compared. In addition to the kick-by-kick analysis, an average kinematic model was also produced for each participant for both field-goals and PATs to compare biomechanical factors and deviation of movement between the participants. These average kinematic models allowed for an investigation in kinematic consistency across multiple kicks from the same category, either PATs or 50-yd field-goals.

Chapter 2: Instep Kicking Technique

Kicking is a propulsive action in which the leg or foot is used to strike an object; therefore, kicking may be considered a unique, highly specialized form of striking that may be classified into two general categories, the place-kick and the punt [12]. In terms of developmental sequence, it has been observed that a two-year-old child is capable of kicking a ball (in a place-kicking fashion) but not an 18-month-old who simply walks into the ball [21]. Other studies report similar observations, showing that kicking the ball forward by its full circumference or more is usually attained by age 2 while the basic kicking pattern, which includes preparatory backswing of the kicking foot, is usually apparent by age 4 [41]. Studies have also outlined a sequence of kicking development that in the advanced stages include rapid forward extension of the lower leg, increased arm-leg opposition, and pronounced follow-through with a hop on the support leg [22]. A rudimentary form of these kicking stages in place-kicking are present in most children by age 5 or 6 [19]. It can be seen that the complexities of the kicking mechanics start to develop at a young age.

The instep (or "soccer-style") kicking technique is a place-kick where the individual impacts the ball with the top or side of the foot as opposed to a toe-kick where the person impacts the ball with their toe while the foot is oriented perpendicular to the shank. The toe-kick was the only technique for place-kicking when football started until Pete Gogolak, a soccer player from Hungary, became the place-kicker for Cornell University in the early 1960's (he was later drafted by the Buffalo Bills in 1964). It took a while for this technique to be accepted but by the late 1980's toe-kicking in the NFL was

all but extinct. The reason for transitioning to the instep technique was that kickers were making longer field-goals at higher success rates. For comparison, toe-kickers were making less than 60% of their field-goal attempts while instep-style were making around 80%.

Given the ubiquitous nature of instep kicking, the biomechanics of this technique is thoroughly investigated in this dissertation. Many studies have been performed with regard to the instep kicking technique within the sport of soccer, as it is the most popular sport worldwide, but little has been investigated with regard to the place-kick in football. The basic kinematics of the kick is similar for both sports but the ideal foot placement, ball shape, and ultimate goals are quite different.

Foot placement when impacting a football or soccer ball can differ because soccer balls and footballs have very different shapes. A soccer ball is a sphere and a football is considered a prolate spheroid (i.e, the axis of symmetry is longer than the other axes). Therefore, the location in which one strikes the football for a successful kick can be much more sensitive than that of a soccer ball. The difference in overall goals is quite obvious as well. A soccer player may have several different intentions when he/she performs an instep kick (distance, hang-time, location, etc.). A place kicker in football wishes to get the ball through the field goal without being blocked by the opposing team. Some mechanical factors that influence the trajectory of the kick include impact location, magnitude and angle of impact force, orientation of the football, and the size and orientation of the kicking foot.

2.1 Instep Kinematics

2.1.1 Segmental and Joint Rotations of the Kicking Leg

The instep kick is commonly broken down into a series of phases. In this study these phases are defined as the backswing, swing, impact, and follow-through (illustrated in Figure 2). At the start of the backswing phase the plant foot (non-kicking foot) is traveling in the direction of the ground, headed towards its planted position, and the kicking leg begins to elevate. The hip is slowly adducted and externally rotated [30] while the knee flexes and internally rotates [34]. The ankle is plantar flexed, abducted and slightly pronated. This backswing phase is completed shortly after the plant foot makes contact with the ground (becomes planted), with the hip extended and knee flexed [30].

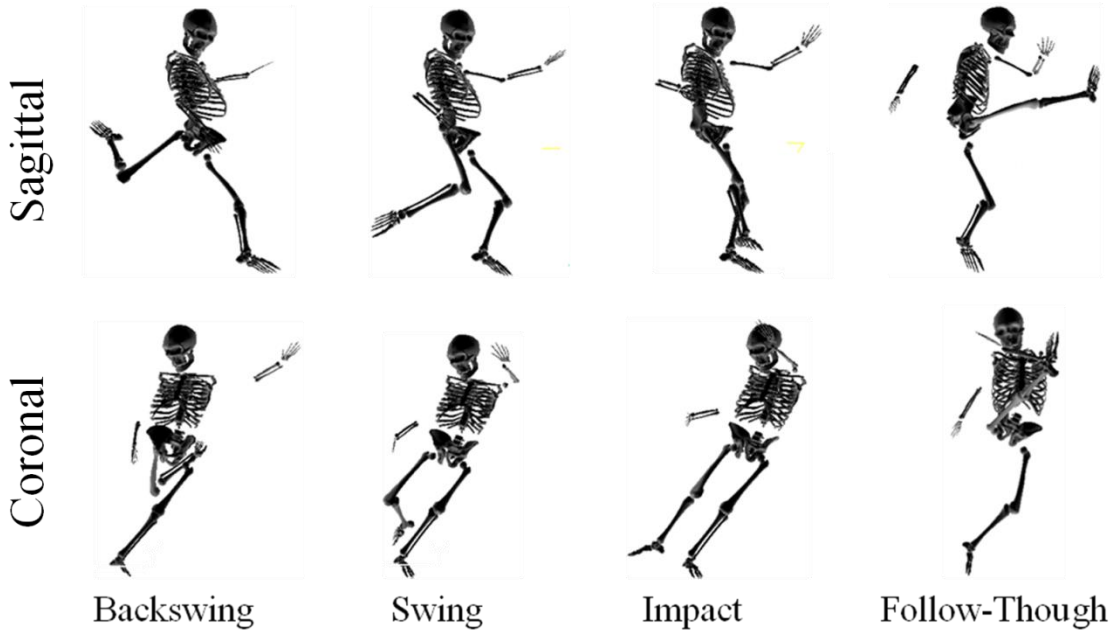

Figure 2 - Phases of the instep kicking motion in the sagittal (top) and coronal (bottom) planes

The next phase will be referred to as the swing phase. During the swing phase forward motion is initiated by rotating the pelvis around the plant leg and by advancing the kicking leg's thigh forward while the knee continues to flex [46]. The hip starts to flex and abducts while it remains externally rotated [30]. During this motion the ankle is adducted and plantar flexed whereas supination and pronation is minimal. Simultaneously, knee extension velocity is maximized while external/internal tibial rotation values are generally low [34]. When impact occurs, the hip is flexed, abducted and externally rotated while the ankle is planter flexed and adducted [30].

2.1.2 Proximal-to-Distal Motion

In sports as well as many day-to-day activities, a number of movements rely on a proximal-to-distal sequence of motions. Depending on the application, this type of movement can be incredibly important for performance. Proximal-to-distal motion can be described as a motion that initiates in the larger, heavier proximal body segments and, as energy increases, proceeds outward to the smaller, lighter distal segment [31]. These mechanics are associated with final maximal speeds of the distal member. Bunn's "Summation of Speed Principle" explains the theory of this movement, stating that each succeeding segment initiates motion at the time of maximum speed of its proximal segment, generating higher distal endpoint speeds than the latter [11]. This idea is graphically represented in Figure 3.

The left plot in Figure 3 shows the speed curve of the foot crossing that of the shank at the shank's maximum speed. The right plot in Figure 3 shows the speed curve of the foot crossing that of the shank earlier in time, before the shank reaches maximum

speed. With this example, the difference in timing of foot movement results in the foot achieving a higher speed in the left plot of Figure 3. One can see how optimizing proximal-to-distal movement to increase the velocity of the hands or feet could be beneficial for many athletic endeavors, whether throwing, striking, or in the case of this study, place-kicking.

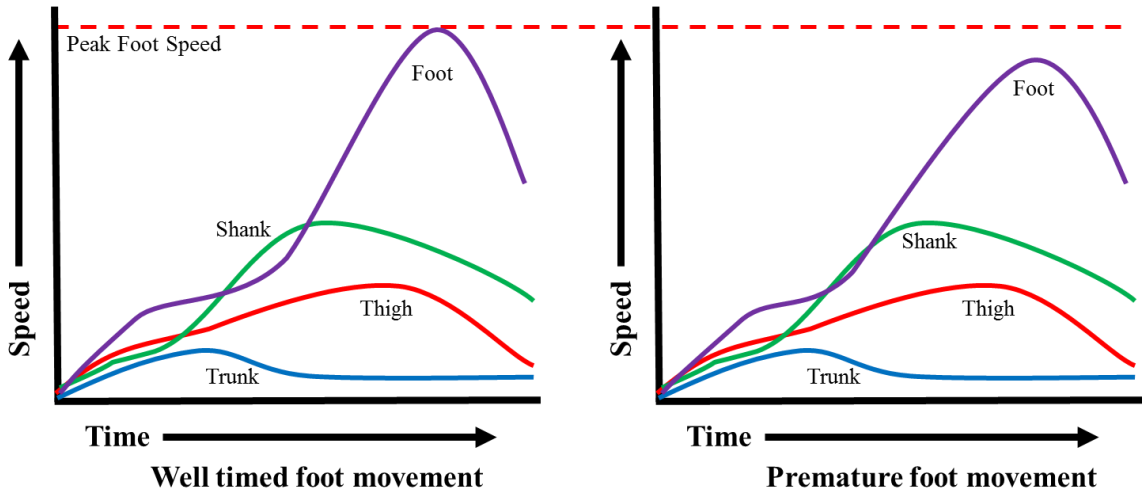

Figure 3 - Summation of Speed Principle illustrated for a kicking motion

During the backswing phase the angular velocity of the hip is minimal to negligible while the shank displays a negative velocity (traveling away from the body's center of mass). Through the start of the swing phase the hip begins to exhibit angular velocity while knee flexion continues to move the shank backwards until maximum knee flexion is achieved. Though the velocity of the shank is negative in relation to the body's center of mass, the whole body is moving forward, building momentum towards the ball.

The hip continues to extend and reaches its peak extended position just before the knee starts to extend. At this instant the velocity of the thigh and shank are equal and therefore the angular velocity of the knee is zero. As the hip begins to flex, the knee starts

to extend and the velocity of shank increases until striking the ball [18]. At impact with the ball the angular positions of the hip and knee align the leg into a more rigid orientation “whipping” the foot to reach a peak linear and angular velocity [24].

Therefore, a kicker’s maximum foot velocity significantly depends on the velocities of the more proximal members. If a kicker can accelerate a distal member (i.e., the foot) when an adjacent proximal member (i.e., the shank) is at maximum velocity, from the trunk to the foot (Figure 2), then ideal proximal-to-distal timing has been achieved and the kicker’s foot will have its highest velocity potential.

2.2 Two-Dimensional Kinematic Studies

Again, the majority of existing studies on the instep technique have been limited to soccer and therefore the information presented in this chapter deals with kicking a soccer ball. However, the mechanics of the instep technique are very similar between the two sports. Thus the studies that have been performed for soccer can be related to place-kicking in football.

Since soccer is a team sport and the ball is constantly moving from player to player, some necessary assumptions and simplifications need to be made to evaluate the kicking motion. One of these simplifications is that the ball is stationary before it is kicked. This simplification makes the studies of soccer kicking mechanics much more comparable to place-kicking in football. A common theme in soccer studies investigating the instep kick is asking the participants to perform a “maximal” instep kick, in which the participant kicks the ball as hard as he/she can [25].

Two-Dimensional (2D) motion analysis of kicking using a high-speed camera was done as early as the 1970's and focused on kinematic quantification of the kicking leg. Therefore, most of the results delivered have been limited to partial body analysis in the sagittal plane. The most common parameters analyzed using this method were ball speed, joint position, joint angle and angular velocity. In 1971 Plagenhoef determined that if the thigh quickly decelerated during the swing phase, the subsequent acceleration of the lower leg required less muscle power. On the other hand, if the thigh slowly decelerated the knee extensors had to increase the shortening speed in order to develop more power for achieving an equivalent foot kicking velocity [35].

In 1983 Kollath investigated the maximal instep kick in 2D using professional soccer players by tracking the path of the hip, knee, ankle, and toe in the sagittal plane. Figure 4 displays the measured velocity of the leg through an instep kick of one elite athlete in this study. Figure 4 illustrates that the hip and knee gradually decelerate from the backswing phase to ball contact.

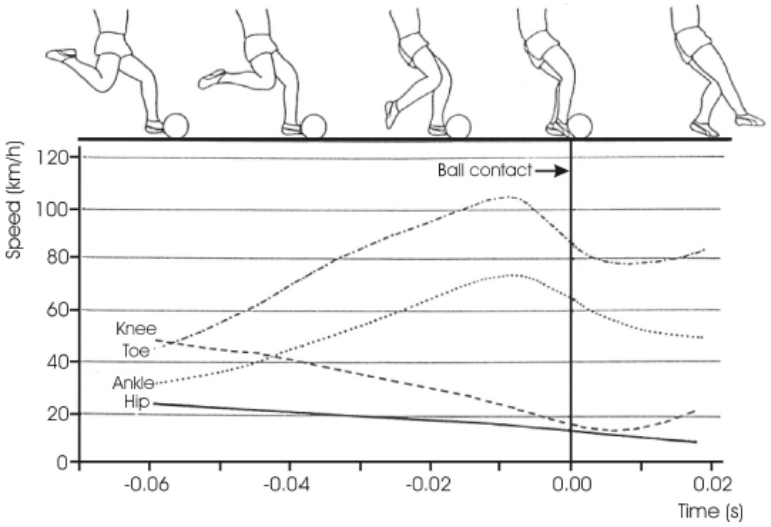

Figure 4 - Speed-time excursion of the hip, knee, ankle, and toe of a German national soccer player (adopted from [12])

The majority of 2D kicking studies are restricted to the sagittal plane, thus the media-lateral movement of the kick cannot be investigated. Therefore the rotational component of velocity is not included in the results of Kollath's study [26]. A 2D study by Roberts and Metcalfe in the transverse plane was able to investigate this media-lateral movement. Their study revealed that the path of the kicking foot forms an S-curve when approaching the ball (Figure 5). Roberts and Metcalfe also concluded that approaching a ball with a certain angle would benefit hip rotation, which is important for the lateral movement during the kick [36].

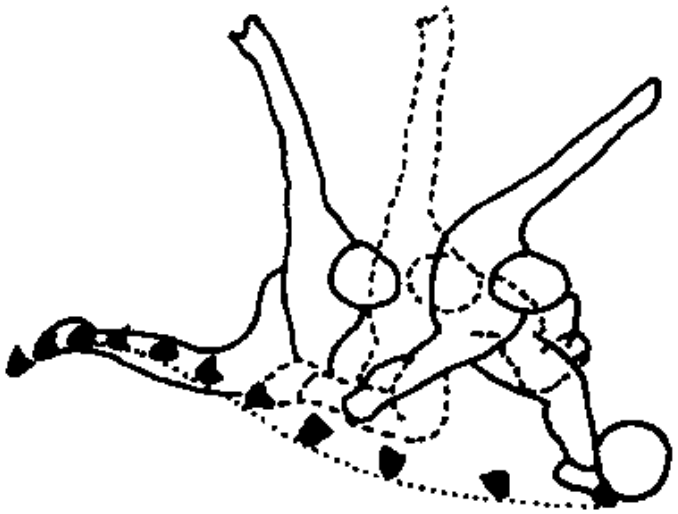

Figure 5 - Transverse view of the kicking foot during a maximal instep kick [adopted from 36]

Other useful results obtained from previous 2D studies are the quantifications of foot velocity and soccer ball launch speed. In general the maximum foot speed for advanced players was found to be 6.9 m/s (15 mph) with a ball launch speed of 8.3 m/s (18.6 mph), although it was unclear how advanced these players were [28]. The maximum foot speed for elite athletes is more than 27.7 m/s (62.1 mph) with a ball launch speed of more than 33.3 m/s (74.6 mph) [28].

This information is useful to help understand an instep kick and provides a range of athletes' foot velocities. Currently there is no quick decisive way to quantitatively analyze an athlete for coaches and scouts. Therefore researchers wished to develop user-friendly methods to simplify evaluation by measuring one or two parameters during an instep kick. Some examples include EQ 1 and 2:

$$V_{ball} = 0.34\,\frac{m}{s} \times V_{foot} + 0.76\,\frac{m}{s} \qquad \{\text{EQ 1}\}$$

where V_{ball} is the velocity of the ball (at maximum velocity after impact) and V_{foot} is the velocity of the foot (at impact) in m/s [47]. EQ 2 is a bit more complicated,

$$V_{ball} = \frac{V_{foot} \times M \times (1+e)}{M+m} \quad \{EQ\ 2\}$$

where M is the effective striking mass of the leg, m is the mass of the ball, and e is the coefficient of restitution [29,10]. Though these equations were proven relatively accurate in their respective studies they still do not produce an efficient and simplified method of quantitative analysis because high-speed analysis of their kick needs to be performed in order to find one of the velocities.

2D analysis of the soccer instep technique from the sagittal and transverse planes has laid the foundation for researchers to quantify the skill. There is room for improvement in preparing full body kinematic models as well as using findings to instruct athletes. However, a 2D analysis cannot completely describe full-body movement, and may be missing important characteristics of the instep technique.

2.3 Three-Dimensional (3D) Kinematic Studies

Similar to the 2D and electromyography (EMG) studies, the first 3D analysis of the instep technique was limited to a partial body model, focusing on only the kicking leg. Nearly all the studies that have been performed are limited to examining only the kicking leg. This is mainly due to the difficulty involved in tracking high-speed, relatively unpredictable movements in a large capture volume when using a full body kinematic model [39]. It is also expected that including the upper body introduces a number of complicated variables in which the researchers did not wish to address until

the kinematics of the lower body are better understood. With that being said, Rodano and Tavana used an opto-electronic system at 100 Hz for recording marker positions strategically placed on the leg joints in 3D [38]. Their results however did not reveal new aspects of the instep technique when compared to the 2D studies that were previously performed.

The first full body 3D analysis of the instep technique was performed by Shan and Westerhoff [40]. Their study was performed in a lab environment with 2 cm thick wrestling mats on the floor to simulate grass and a vertically hanging wrestling mat to stop the ball after impact. A nine-camera VICON motion analysis system tracked motion of the kicker (fully body model consisting of 42 reflective markers; 120 Hz) and soccer ball (3 markers).

Similar to previous studies, their results revealed that the key characteristics of the instep technique could be extracted as the formation of a tension arc, and the fast release of this tension arc in a quasi-whip-like fashion with complimentary upper body movement. This finding was original in that the upper-body had never been examined and thus the tension arc modeled from previous studies ended at the athlete's hip. Furthermore, by comparing different levels of athletes, Shan and Westerhoff confirmed that the tension arc created by the kicking leg and upper-body generated an explosive muscle contraction through muscle pre-lengthening in the backswing, increasing the power of the kick [40]. From this analysis they concluded that the maximal distance between the hip of the kicking leg and the opposite shoulder provided a quantitative

means to judge kick quality, therefore demonstrating that full body 3D analysis may be more advantageous when compared to the 2D model for studying the instep technique.

Unlike the conclusion of Smith and his colleagues [43], Shan and Westerhoff found that more skilled players demonstrated much greater range of motion in both the hip and knee joints which lead to higher foot velocity. However, a novice kicker used the knee as the primary source of inertia for creating foot velocity [40]. This suggests that there are more factors than just knee extension, such as flexibility and timing of body segment movement (Summation of Speed Principle), making up an effective instep kick.

2.4 Electromyography Studies

EMG has been used to examine muscle activity during an instep kick to help explain the role of a muscle through the kick as well as the magnitude of muscle activation. The use of surface EMG is quite appealing to researchers because it offers a means to acquire *in vivo* data about muscle processes with a non-invasive approach. EMG captures muscle activity during movement by measuring the activation potentials released. Therefore, in the studies presented all EMG values are expressed as a percentage of the EMG recorded during a maximum isometric effort in order to compare findings between athletes (Table 1) [39,25].

Using this method to examine muscle excitation through an instep kick gives the researcher very useful information on the timing of muscle activation through the kick and as a result, which muscles contribute to an athlete's kicking performance, and in turn can, be trained to increase strength. In the same way that this information is used to

identify muscle groups for training, it can also be used to point out areas of high stresses and potentially assist in injury prevention.

Table 1- Characteristic EMG activity values as reported in previous studies evaluating the instep kick in soccer

Muscle	Backswing Phase	Swing Phase
Iliopsoas	60-80%[1]	65.1-100.9%[2]
Rectus femoris	25-60%[2]	32.5-68.7%[2]
	47.8-51%[3]	78.6-85.5%[3]
Vastus lateralis	0-40%[2]	64-102%[2]
	70%[1]	80%[1]
Vastus medialis	90%[1]	80%[1]
	33.1-40.8%[3]	66.9-70.4%[3]
Biceps femoris	15-25%[2]	5.2-30%[2]
	70%[1]	<30%[1]
	38.9-50%[3]	39.8-40.1%[3]
Gluteus maximus	5-15%[2]	2.1-32.1%[2]
	65-70%[1]	<30%[1]
Semitendinosus	70%[1]	30%[1]
Tibialis anterior	40%[1]	30%[1]

[1]De Proft et al., 1988, [2]Dorge et al., 1999, [3]Manolopoulos et al., 2006 (adopted from [25])

The iliopsoas is a combination of muscles originating at the lower back and medial pelvis which attaches to the medial femur at the hip joint. The rectus femoris is the central muscle in the quadriceps and acts as a hip flexor and knee extensor. The vastus lateralis and medialis contribute to controlling the knee and are muscles located on either side of the rectus femoris. The biceps femoris is part of the hamstring muscle group and spans two joints to assist with hip extension and knee flexion. Semitendinosus has similar function, and is also part of the hamstring muscles. The gluteus maximus connects the lower back and dorsal pelvis to the dorsal femur at the hip joint.

Inconsistent activation percentages are presented in Table 1. The percentages are a range of values for the subjects tested, but the large variation within and between studies suggests that more research is needed to yield more accurate results. Among other things, variations in EMG data could come from inconsistent placement of electrodes, cross-talk between muscles, and participants with different body types.

All three studies presented in Table 1 display larger activation for the quadriceps (rectus femoris, vastus lateralis, and vastus medialis) during the swing phase. This would suggest that the rotation about the knee (flexion) at the final stages of the kick is the limiting factor in foot velocity [16]. Finally, similar to 2D motion analysis, EMG can only examine certain aspects the instep technique. Outside of the muscles encompassing the thigh, studies leave many relevant muscles uninvestigated.

Chapter 3: Projectile Tracking

Understanding the 3D trajectory of ball flight and its relationship to environmental (wind, humidity, temperature) and human factors (kinematics and EMG) is essential to optimizing an elite athlete's performance. Unfortunately, existing technology is often too expensive ($15,000-$100,000), has limited accuracy, and/or lacks the versatility required to track diverse objects (e.g., soccer ball vs. football vs. baseball). The purpose of this portion of the dissertation was to develop and validate an affordable post-processing method that uses computer-vision to track the 3D trajectory of an object. Knowing the trajectory of a football after it is kicked is pivotal in understanding the quality of the kick. Thus, having an end result from the kicking motion allows one to pick out the ideal trajectories and understand what biomechanical factors contributed to producing the desired trajectory.

3.1 Methodology

A golf ball was selected as the initial object for algorithm development. One camera (Panasonic HC-V100, 1080p, 24 Hz), oriented perpendicular to the *x-axis* (Figure 6), produced data relevant to the projectile's motion along the *x* and *z-axis* (longitudinal and vertical position). A second similar camera, oriented parallel to the *x-axis*, produced data relevant to the projectile's motion along the *y-axis* (lateral position). To create a "sight triangle" which was subsequently used to evaluate the projectile's movement in the *y-direction*, a set of calibration lines (1.58x0.39 in or 40x10 mm) was affixed to the ground 30 in (0.762 m) apart in the expected direction of projectile motion (*x-axis*) to

calibrate the video data in the *x-z plane*. A second equidistant set (in the *x-direction*) was placed 12 in (0.305 m) apart in the *y-direction* for calibration of the camera directed down the *x-axis* (Figure 6).

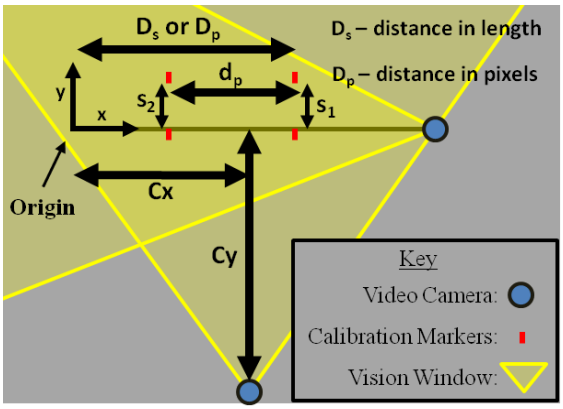

Figure 6 - Data Collection Set-Up/Explanation of Variables

The 2D motion trajectory of the golf ball's flight was calculated from the view of each camera by measuring position with a pixel to distance ratio (Tracker software) [9]. This post-processing technique results in 2D data for the projectile's flight in two perpendicular planes. The camera perpendicular to the ball's flight was used to determine the *x* and *z-position* of the ball (Figure 7), while the parallel camera delivered the *y-position* (Figure 8). These data were then time-synched through identification of the ball to ground impact and an *uncompensated* set of 3D trajectory data points were produced. *Uncompensated* refers to these data points not being yet being adjusted for out of plane movement.

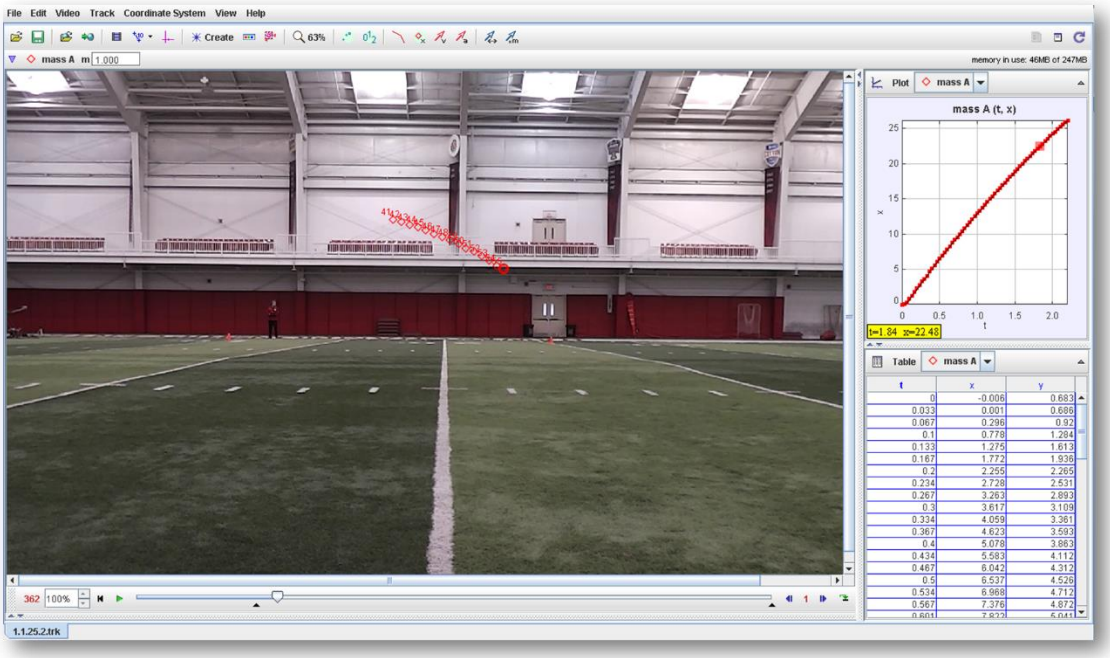

Figure 7 - Example of Tracker Software tracking a football in the x-z plane

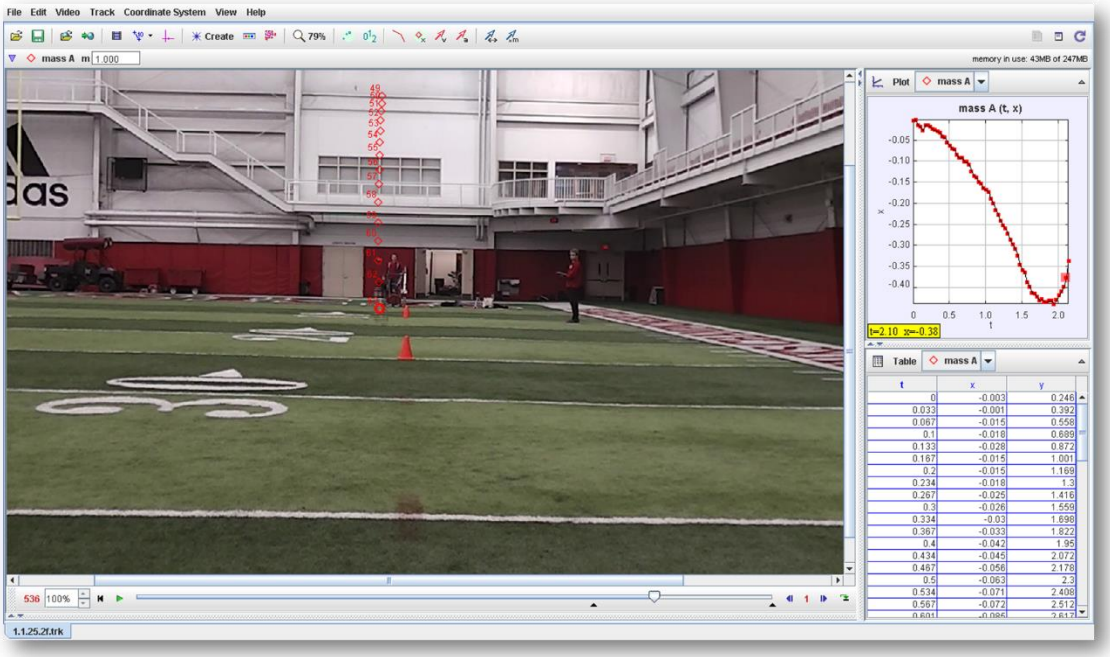

Figure 8 - Example of Tracker Software tracking a football in the y-z plane

To accommodate for the distortion arising from out-of-plane motion for each camera, coordinate data were adjusted using the following methodology to calculate the *compensated* trajectory. The *y-position* was adjusted using EQs 3-5:

$$y_i^{'} = \frac{s_1}{s_1 - y_{c(i)}} * (y_i - y_{c(i)}) \quad \{\text{EQ 3}\}$$

$$y_{c(i)} = \frac{\frac{D_p * D_s}{s_1} - x_{p(i)}}{\left(\frac{\frac{d_p * d_s}{s_1}}{s_1 - s_2}\right)} \quad \{\text{EQ 4}\}$$

$$x_{p(i)} = \frac{D_p}{D_s} * x_i \quad \{\text{EQ 5}\}$$

where y_i is the *uncompensated y-position*, s_1 and s_2 are the distance between the two calibration markers in pixels from the view of the parallel camera (see Figure 6), $y_{c(i)}$ is the correcting *y-factor*, D_s is the distance from the origin of the reference frame to the furthest set of calibration markers, D_p is the distance D_s in pixels from the view of the parallel camera, x_i is the *uncompensated x-position*, $x_{p(i)}$ is the x_i position in pixels, d_s is the distance between the two sets of calibration markers, d_p is the distance d_s in pixels from the view of the parallel camera, and $y_i^{'}$ is the *compensated y-position*.

Next, $y_i^{'}$ was used to calculate the *compensated z* and *x-positions*, $z_i^{'}$ and $x_i^{'}$ respectively. These *compensated* positions are calculated using EQ 6 and EQ 7:

$$z_i^{'} = \frac{z_i - h}{C_y} * \left(C_y + y_i^{'}\right) + h \quad \{\text{EQ 6}\}$$

$$x_i^{'} = C_x - \left(C_y + y_i^{'}\right) * \frac{C_x - x_i}{C_y} \quad \{\text{EQ 7}\}$$

where h is the viewing height of the camera, C_y is the distance from the perpendicular camera to the *x-z plane* (Figure 6), C_x is the longitudinal distance the perpendicular camera is from the coordinate origin, and z_i is the *uncompensated z-position*.

This algorithm was developed by creating a sight triangle in the parallel camera view to more properly account for the depth in the 2D image. Once the new *compensated y-position* is determined the geometric concept depicted in Figure 9 is used to calculate the *compensated z-position* in EQ 6. The same concept is used to calculate the *compensated x-position* in EQ 7.

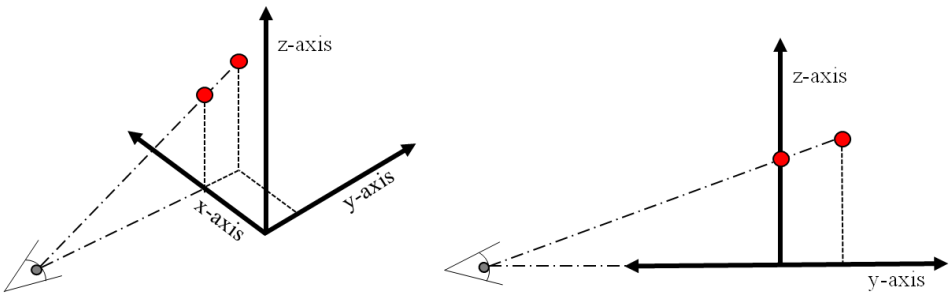

Figure 9 - Geometric concept for compensating for the *z-position*

Algorithm validation was performed using a "*gold standard*" 3D motion analysis system (three Qualisys Oqus 400 series cameras, 200 Hz, calibration residuals < 1mm). A golf ball (42.67 or 1.68 in mm in diameter), covered with retro-reflective tape, was simultaneously tracked during flight through a 3x3x3 m (roughly 10x10x10 ft) capture volume by the 2D Panasonic cameras and the 3D motion capture technology. Ten repetitions were performed and the error in tracking when compared to the *gold-standard* is presented in Table 2.

Table 2 - Average resultant deviation from the control for uncompensated and compensated position.

	Uncompensated Position		Compensated Position	
	Error (mm)	Percent Error	Error (mm)	Percent Error
Trial 01	62.6	6.77%	39.0	4.22%
Trial 02	253.8	14.40%	88.0	4.99%
Trial 03	325.9	19.30%	314.8	16.11%
Trial 04	254.9	12.08%	140.3	6.65%
Trial 05	109.8	10.12%	47.2	4.34%
Trial 06	61.6	3.21%	50.1	2.61%
Trial 07	192.5	9.61%	40.8	2.04%
Trial 08	169.2	8.97%	70.0	3.71%
Trial 09	216.2	17.18%	96.9	7.70%
Trial 10	243.1	12.14%	88.6	4.43%
Average*	173.7	**10.50%**	73.4	**4.52%**
STDEV*	78.3	**4.11%**	33.5	**1.78%**

*Trial 03 was determined an outlier and is not included in the average and standard deviation calculations.

3.2 Results and Discussion

The *uncompensated* coordinate data resulted in an average percent difference from the *gold standard* 3D trajectory of 10.37 ± 3.88%. After applying the discussed geometrical adjustment technique, the average percent difference in trajectory from the *compensated* to the *gold standard* was reduced to 4.20 ± 1.35%. These findings demonstrate that the compensated technique results in a 57% decrease in error when compared to the uncompensated approach at golf ball trajectory tracking. The error presented relates to the average overall error in the system with respect to the distance traveled by the projectile. Calibration markers must be accurately positioned and the cameras need to be directed to clearly view the *x-z* and *y-z planes* to obtain the most accurate position measurements. Similar results are expected for football tracking, the main difference in the procedure is the distance is which the cameras are from the ball.

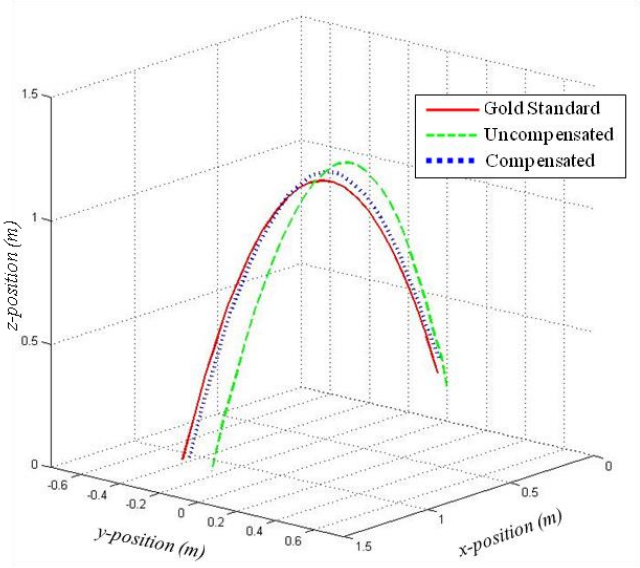

Figure 10 - Example result displaying the *Gold Standard, Uncompensated,* and *Compensated* trajectories. (Trial 05 of the golf ball validation tests)

The low frame rate (24 Hz) of the 2D cameras used in this projectile tracking procedure resulted in projectile blurring in a number of frames. In these instances the center of the blurred projectile was approximated and assessed as the data point. Cameras recording at a higher frequency would be expected to reduce the amount of error resulting from video processing and time-based compiling.

In summary, this work developed and validated an affordable (estimated at $400), accurate (<5% average error) technology for tracking 3D ball flight. More advanced cameras with a higher frame rate may further reduce tracking error but likely increase cost. The remainder of this dissertation utilizes this methodology to track the trajectory of football to assist in determining the effectiveness of a place kick.

Chapter 4: Investigation of Toppling Ball Flight

A toppling ball flight study was performed to better understand the mechanics of end-over-end football flight. As previously mentioned, there is very little in the literature related to toppling ball flight [20,27]. For this study a mechanical kicking machine was used to repeatedly strike the football with a consistent impact velocity. A number of kicks were performed at different impact locations on the football while the ball's long axis remained perpendicular to the field. The experiment was then repeated with the ball tilted either to the left or right 15°. This allows for the examination of ball flight when the ball is not oriented vertically.

4.1 Methodology

4.1.1 Mechanical Kicking Machine

The Department of Mechanical & Materials Engineering at the University of Nebraska-Lincoln has developed a mechanical kicking machine designed to kick 60 times per minute with the hopes of becoming a robotics demonstration for halftime at Nebraska football games. This project has been put on hold due to difficulties creating a ball loading mechanism. For use in this study, the mechanical kicking machine needed to be modified so that it could perform a single kick at a time. The restraints for this new design were mainly cost, thus the spring present on the system was not changed and an affordable winch (under $100) was purchased. As a result, the previously used 2-stroke engine was disengaged, and an electric winch (Superwinch LT2000) was mounted on the frame of the mechanical kicker. After the modifications, the mechanical kicker was able to perform a single kick at the push of a button.

The new mechanical kicker design uses a crank and spring design (Figure 11) to maintain a consistent impact velocity with the football. The point at which the spring was attached to the pulley was optimized to take advantage of the winch's torque and increase the impactor's velocity at impact. This new electric winch design consistently propelled the impactor while maintaining a safety factor of 1.2 for the electric winch (with regards to capable torque).

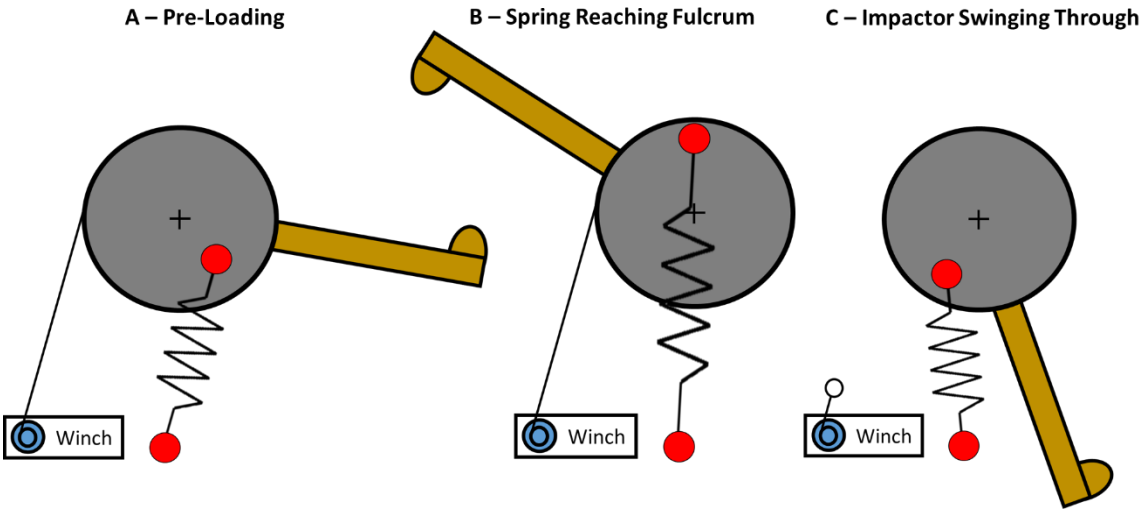

Figure 11 - Crank and spring concept

Figure 12 depicts the final mechanical field goal kicker design utilized for this study. Also present in the image is a custom adjustable tee utilized to manipulate impact conditions on the football. The tee possesses a stationary base and the location of the ball can easily be altered with respect to the base.

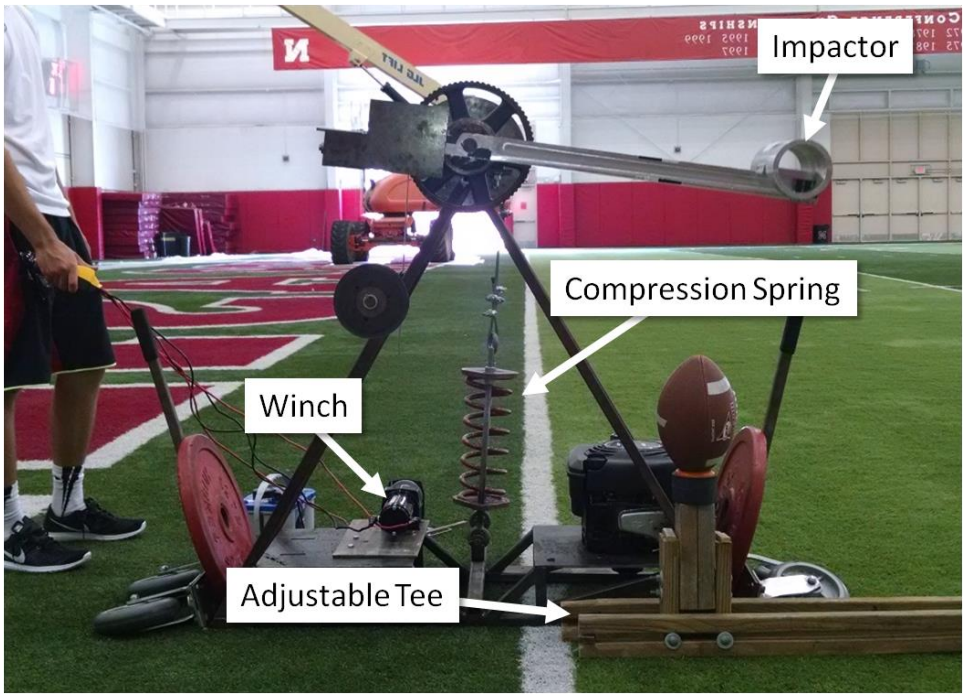

Figure 12 - Mechanical Field Goal Kicker

The impactor was tracked using a *"gold standard"* Qualisys position tracking system (9 Qualisys Oqus 300 series cameras, 200 Hz, calibration residuals < 1.5 mm). Figure 13 depicts Qualisys motion capture data recorded and averaged across 10 impact "kicks". The left vertical axis represents the linear velocity of the impactor head while the right vertical axis represents its vertical position with respect to the global axis. It can be seen from Figure 13 that the impactor reaches a maximum plateau velocity of 12 m/s. A standard deviation of approximately 0.05 m/s was found over the portion of the curve in which impact occurs. The impact angles (20°, 25°, and 30°) presented in Figure 13 are defined in section 4.1.2.

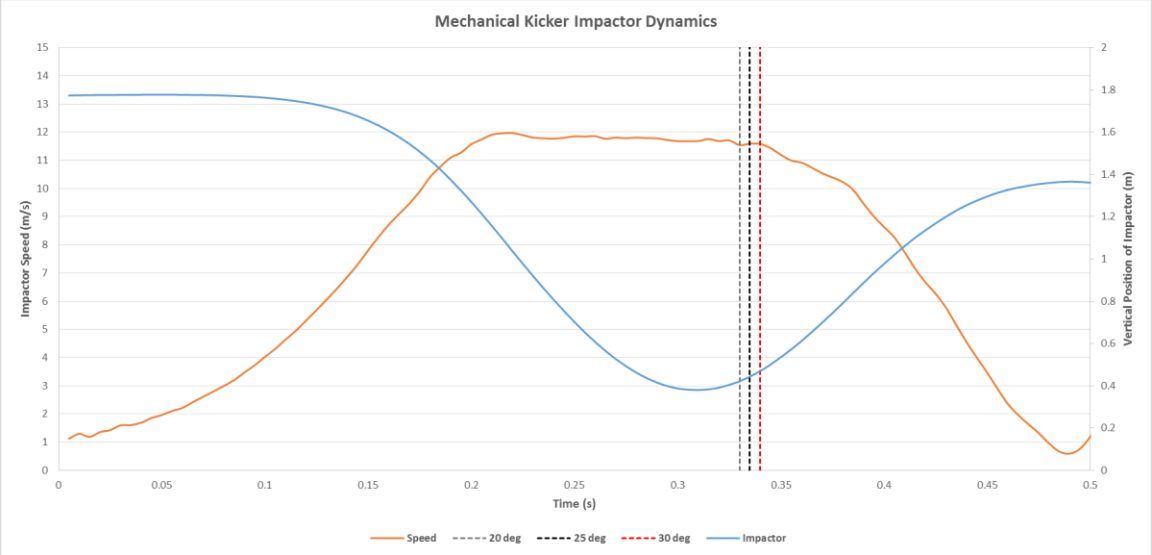

Figure 13 - Dynamics of the impactor through a kick.

4.1.2 Impact Conditions

The ball was impacted in five different locations. The baseline impact location was just below the center of the ball at 13 cm (5.12 in) from the bottom of the ball. The following four impact locations were in 2.5 cm (0.98 in) increments below the baseline location (see Figure 14).

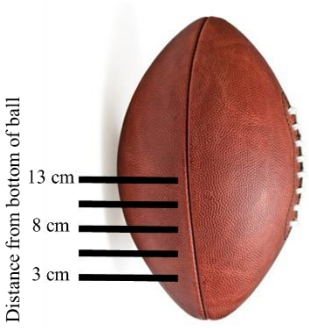

Figure 14 - Football impact locations for the designed experiment using the mechanical kicker

Each of these impact locations were evaluated while being impacted at 20° (gray dashed line in Figure 13), 25° (black dashed line), and 30° (red dashed line) angles off

the horizontal. Literature has shown that soccer players performing an instep kick, impact the ball at around 22° to 27° [28]. Figure 15 illustrates the concept of creating this impact angle with the mechanical kicking machine. The dashed lines in Figure 13 point out the magnitude of velocity and vertical position of the impactor head at 20°, 25°, and 30° impacts. It can be seen that the impact velocity and angles are nearly identical with an impact velocity of 11.54 m/s (37.86 fps) for an angle of 20°, 11.59 m/s (38.02 fps) for an angle of 25°, and 11.58 m/s (37.99 fps) for an angle of 30°. Resulting in a maximum difference of 0.05 m/s (0.16 fps) which is approximately 0.4% off of the average impact velocity.

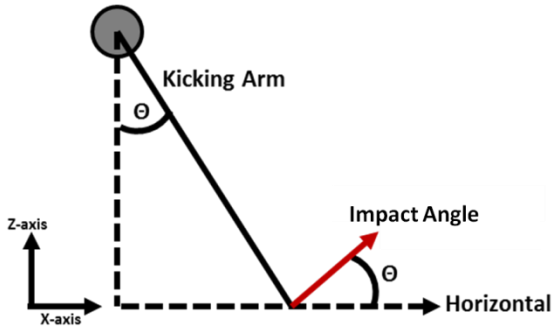

Figure 15 - Calculating the angle of impact.

These variables were controlled by adjusting the position of the ball at impact. Figure 16 depicts how the ball can be manipulated forward/backwards and up/down to allow for the desired impact location and angle. This can be manipulated easily and controlled with the adjustable tee.

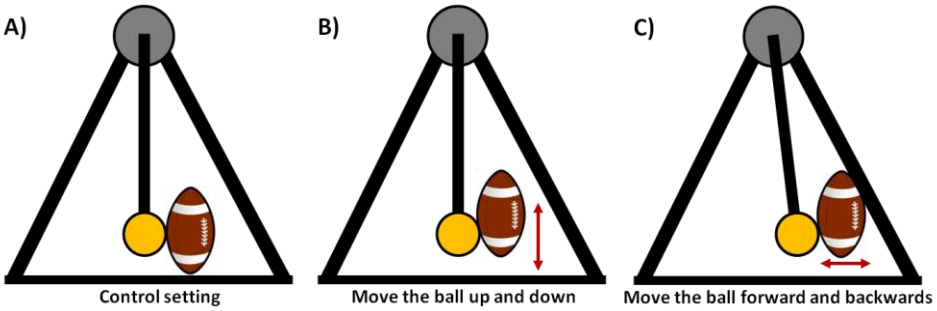

Figure 16 - Mechanical Kicker and football configurations: A) Baseline B) Adjusting the impact location along the long axis of the ball C) Adjusting the directional component of the impact force

The next variable evaluated was the orientation of the ball at impact. It is common for kickers to prefer the ball to be held so that the tip of the ball is tilted slightly to their left or right. Lee et. al (2013) [27] used the coordinate system displayed in Figure 17 and used modeling techniques to predict the flight of the football when initial velocity remained constant and the ball was tilted about the k_b axis. This graphic can be used to demonstrate that the ball will be oriented in the vertical position for baseline testing but will also be tested with 15 degrees of positive and negative tilt about the k_b axis.

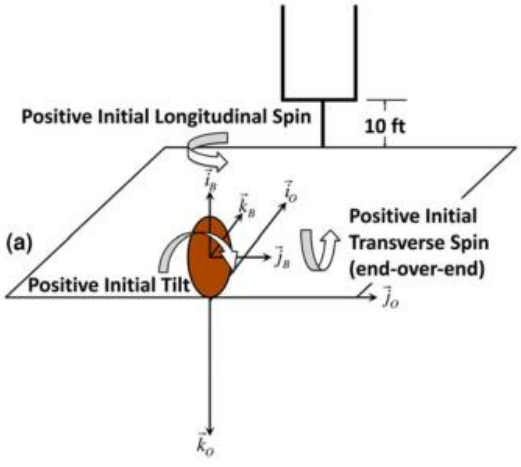

Figure 17 - Local and global coordinate frames (Adopted from [27])

The final variable that was investigated was the size of the impactor (13 cm vs. 6.5 cm in diameter). The impactors utilized for these experiments were cylinders of the same weight but different diameters. In theory, adjusting the diameter of the impactor will affect the area of impact, the deformation of the ball, and thus the impulse of force delivered to the ball.

The five variables examined in this study were: impact location, impact angle, tilt about the k_b axis, and impactor size results in 90 impact conditions or kick variations. Performing each of the proposed kicks three times results in a total of 270 kicks. These kick parameters are laid out in Table 3.

Table 3 - Experimental Design Parameters

l	Impact Location (cm from the bottom of the ball)	13, 10.5, 8, 5.5, 3
Θ	Direction of Impact Velocity (deg)	20, 25, 30
Φ	k-Tilt (deg)	-15, 0, 15
D	Impactor Size (diameter in cm)	13, 6.5

4.1.3 Projectile Tracking

The method outlined in Chapter 3 for tracking the 3D trajectory of a projectile was used to evaluate the ball flight for each impact condition. Using this methodology, 50-yds of field was calibrated for projectile tracking. The setup for data gathering is depicted in Figure 18.

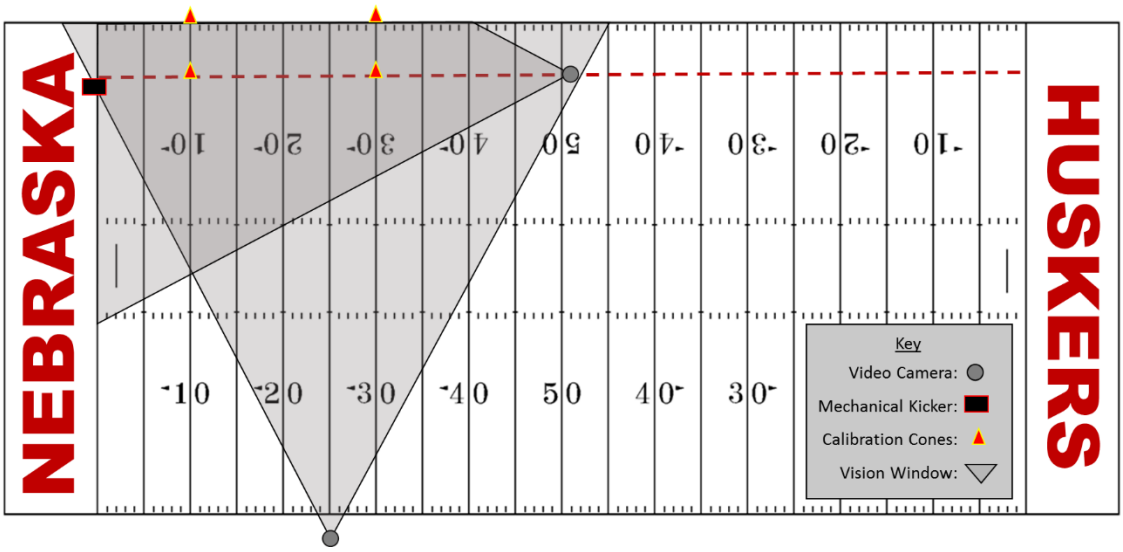

Figure 18 - Camera setup for data gathering

4.1.4 Testing Facility

All data collection took place at the University of Nebraska's Hawks Championship Center, which is an indoor football field. This facility allowed for a controlled environment away from the effects of wind and weather. These factors along with atmospheric pressure within the facility were measured at the beginning of each data gathering session. The average temperature, humidity, and atmospheric pressure observed were 24 ± 2°C, 85 ± 4% rH, and 99.7 kPa respectively.

4.2 Results and Discussion

All 45 impact conditions were completed with the 13 cm impactor, resulting in 135 kicks for the larger impactor. The first 20 kicks for the 6.5 cm impactor head were performed and no significant differences were observed from the 13 cm impactor. Therefore, the following results and analysis are based off impact angle, location, and tilt with a consistent impactor size.

The following figures illustrate the measured trajectories at different impact locations. Each line represents the average trajectory for each of the 45 impact conditions. The solid lines represent an average trajectory with an impact angle of 20°. The blue lines indicate that the ball is oriented with 0° *k*-tilt. The red and green lines represent 15° *k*-tilt and -15° *k*-tilt, respectively. This nomenclature is also used for the 25° and 30° impact angles as well with the dotted and dot-dashed lines, respectively. Impact at 13 cm from the bottom of the ball resulted in a wide range of kicks traveling between 5 m and 14 m across variable impact angles and tilt conditions with an impact angle of 20° resulting in the farthest kicks.

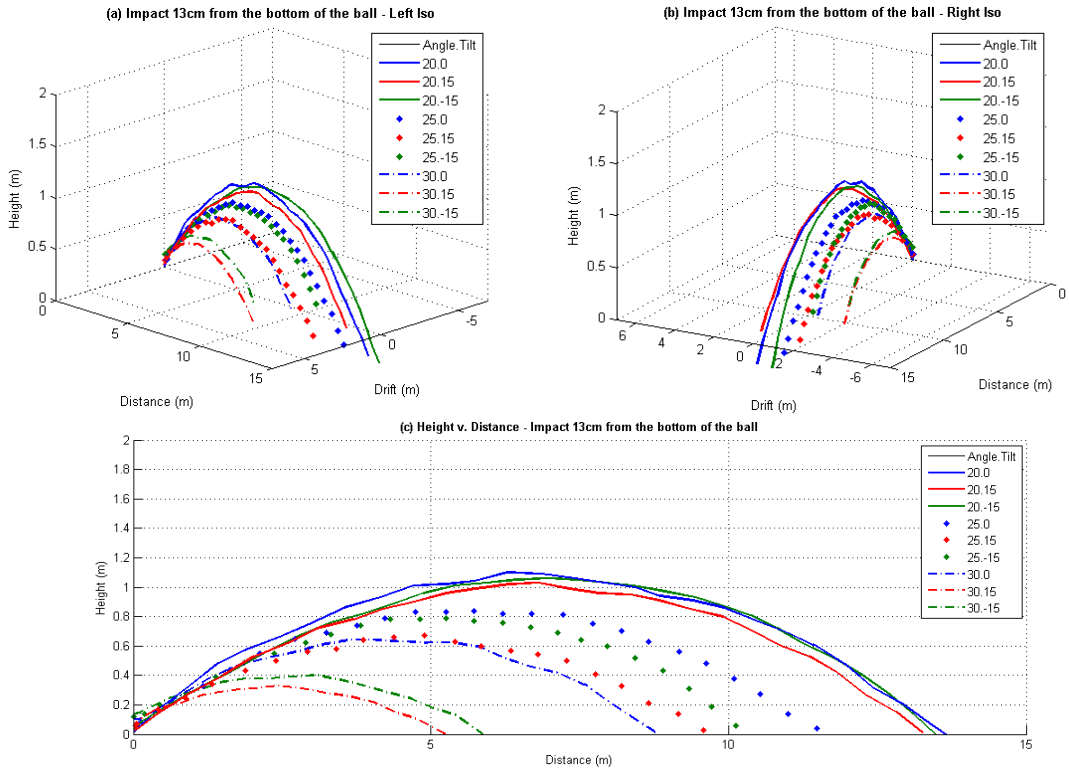

Figure 19 - Football trajectories resulting from impact 13 cm from the bottom of the ball

Figure 19 shows the trajectories for impact at 13 cm from the bottom of the ball, 1.5 cm below the center of the football. At this location a 20° angle or impact causes the ball to travel farther than that of the 25° and 30° impacts. In most instances, impacts with 15° *k*-tilt caused the football to drift off to the right and left of the center-line for positive and negative tilt respectively. With this first impact condition the trajectories do not appear as fluid as the following plots. This is due to the low frame rate (24 Hz) used for projectile tracking. The remaining impact locations (10.5 cm, 8 cm, 5.5 cm, and 3 cm from the bottom of the ball) cause the ball to travel higher and farther, increasing the number of data points and allowing a more zoomed out view when presented.

Trajectories for impact at 10.5 cm from the bottom of the ball are presented in Figure 20. Less separation in distance traveled was observed between the range of impact angles, but the 30° impact angle still showed the shortest distance. Drift to the right and left of the center-line was still observed, but was not as evident as the 13 cm impact location. Impact at 10.5 cm from the bottom of the ball resulted in kicks traveling between 14 m and 19 m across variable impact angles and tilt conditions with an impact angle of 20° resulting in the farthest kicks.

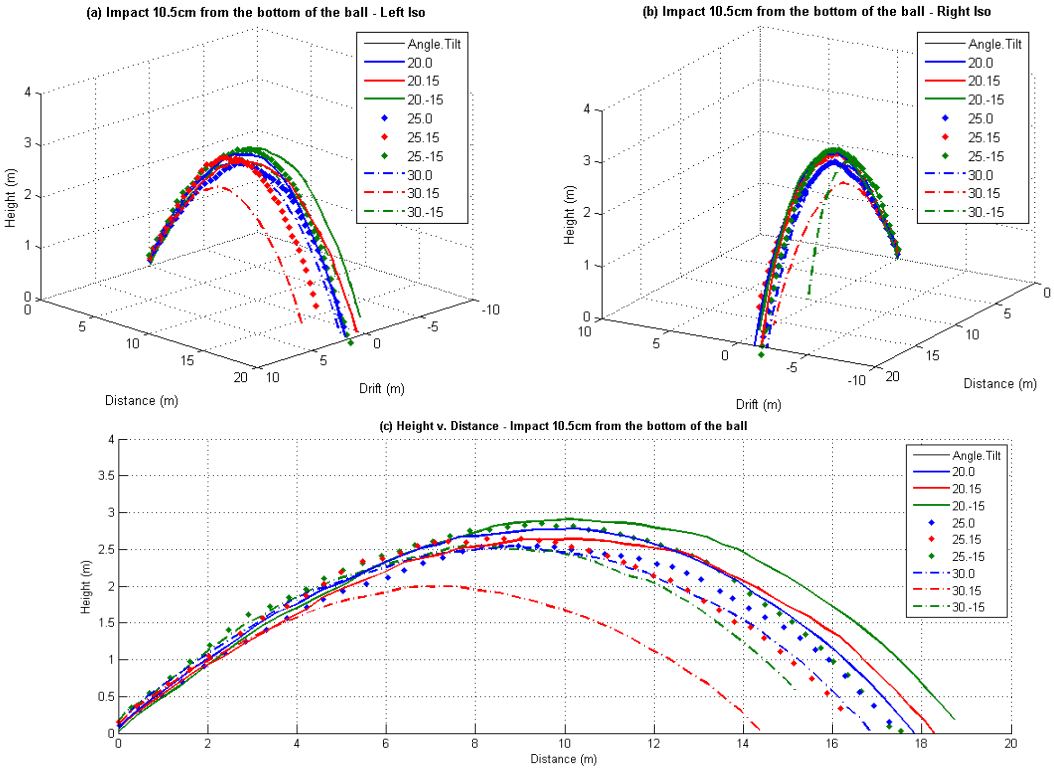

Figure 20 - Football trajectories resulting from impact 10.5 cm from the bottom of the ball

Impact at 8 cm from the bottom of the ball resulted in the ball traveling as far or farther than the 10.5 cm impact location, and achieving a height greater than or equal to the 10.5 cm impact location (Figure 21). For these first three impact locations the ball has traveled the furthest when oriented with 0° *k*-tilt but displayed very different maximum heights. At this impact location, the right and left drift from the center-line is not as evident as in the higher impact locations. Impact at 8 cm from the bottom of the ball resulted in kicks traveling between 16 m and 21 m across variable impact angles and tilt conditions.

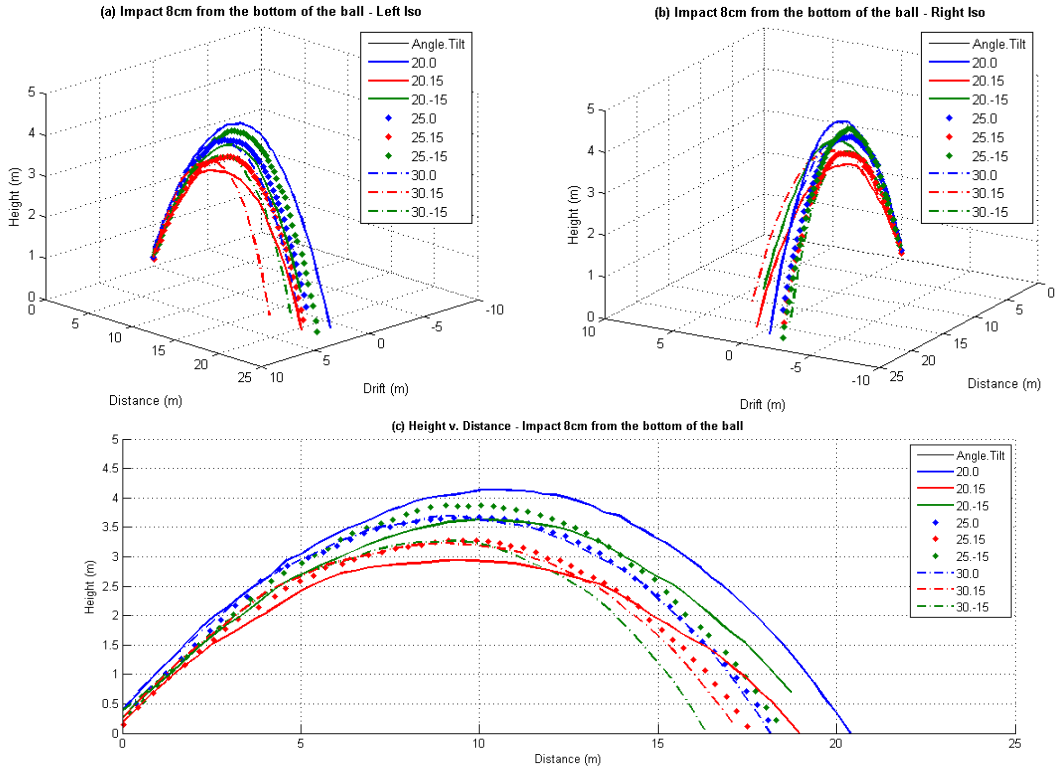

Figure 21 - Football trajectories resulting from impact 8 cm from the bottom of the ball

Figure 22 depicts the impact conditions at 5.5 cm from the bottom of the ball. At this impact location, the variables of impact angle and *k*-tilt make little difference in the trajectory of the ball when compared to the other impact locations. Right and left drift is still evident for positive, and negative *k*-tilt but similar to the 8 cm impact location, it is not as evident as the impact locations higher up on the ball. Impact at 5.5 cm from the bottom of the ball resulted in consistent kicks traveling between 20.5 m and 22 m across variable impact angles and tilt conditions.

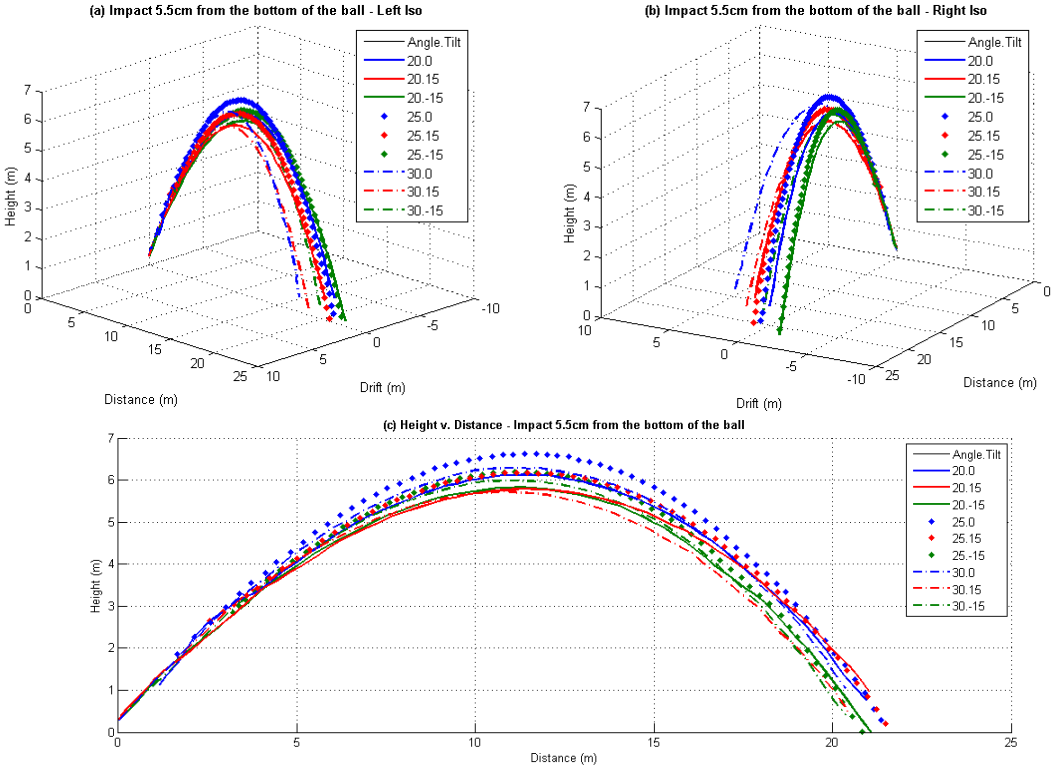

Figure 22 - Football trajectories resulting from impact 5.5 cm from the bottom of the ball

The final impact location was at 3 cm from the bottom of the ball (Figure 22). Impact at 3 cm from the bottom of the ball resulted in kicks traveling between 10 m and 16 m variable impact angles and tilt conditions. These were the shortest measured distances outside of the 13 cm impact and similar to the 13 cm trajectories, the *k*-tilt resulted in more drift as compared to the impact locations between the extremes.

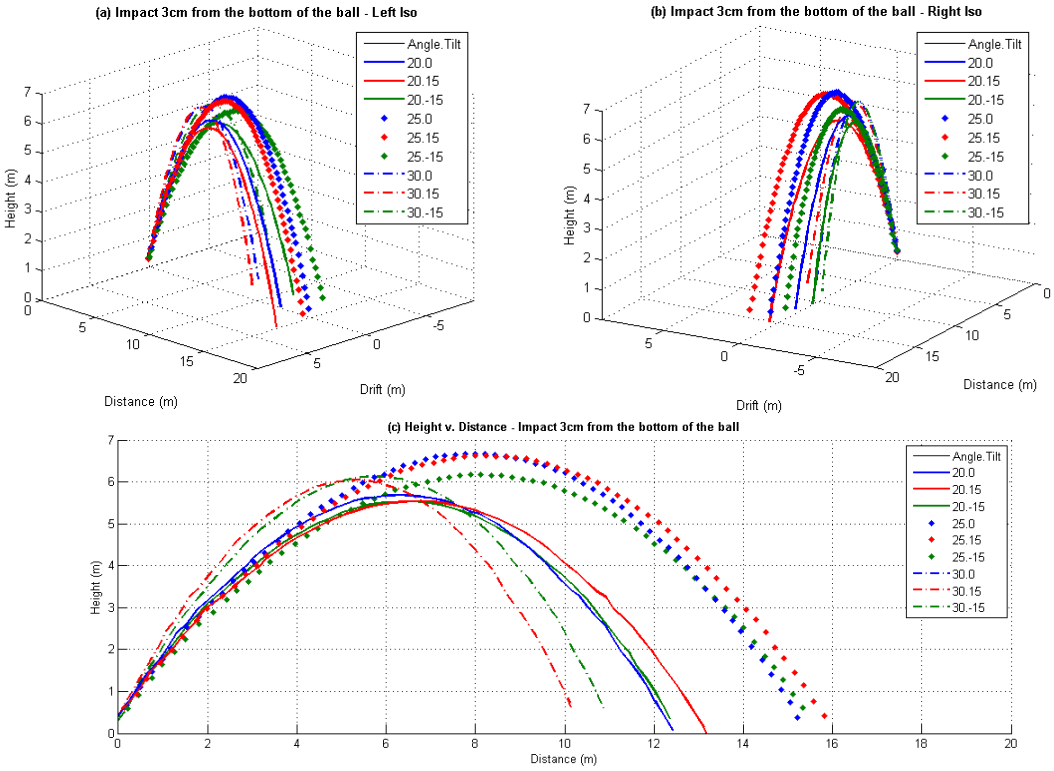

Figure 23 - Football trajectories resulting from impact 3 cm from the bottom of the ball

The results from the impact conditions tested in this experiment showed that the location of impact on a football is a key driving factor in both the launch pitch angle (vertical launch angle off of the horizontal, Figure 25) of the ball as well as the potential for distance. The 2D height versus distance plots in Figure 24 demonstrate that impact at the 5.5 cm location on the ball resulted in the highest, farthest, and most consistent trajectories no matter the angle of impact or the value of *k*-tilt (within -15° to 15°).

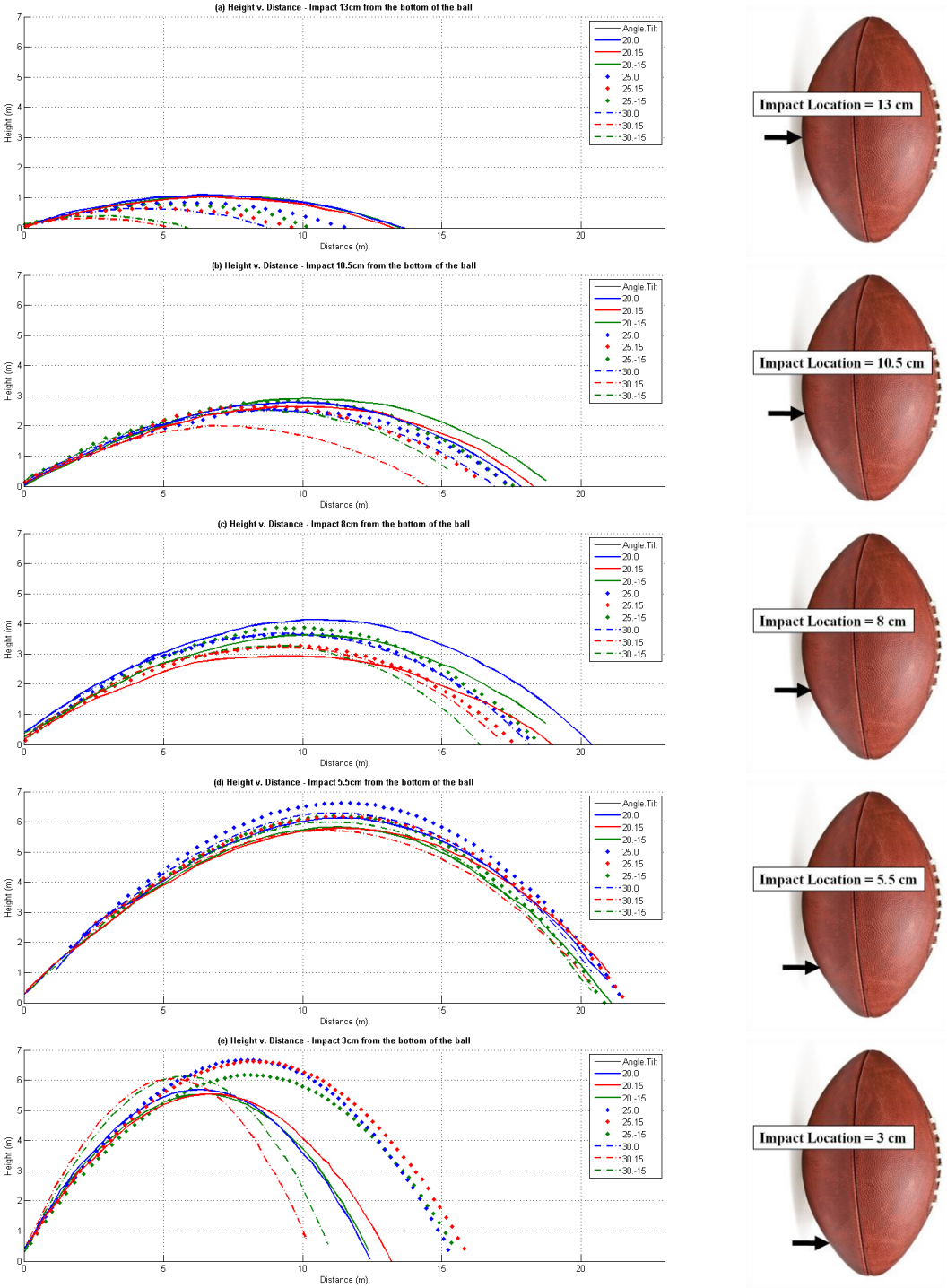

Figure 24 - Football trajectories: Height vs. Distance

Along with the average trajectory for each impact condition the average launch speed, launch pitch angle, and launch roll angles were measured as well. These values were calculated as the average movement over the first 0.2 sec of ball flight and presented in Figure 26, Figure 27, Figure 28. The standard deviations for each average were quite low, averaging out at 0.5 m/s, 1.4°, and 0.2° for launch speed, pitch, and roll respectively. Therefore to ease visual interpretation, the standard deviations are not shown in these plots.

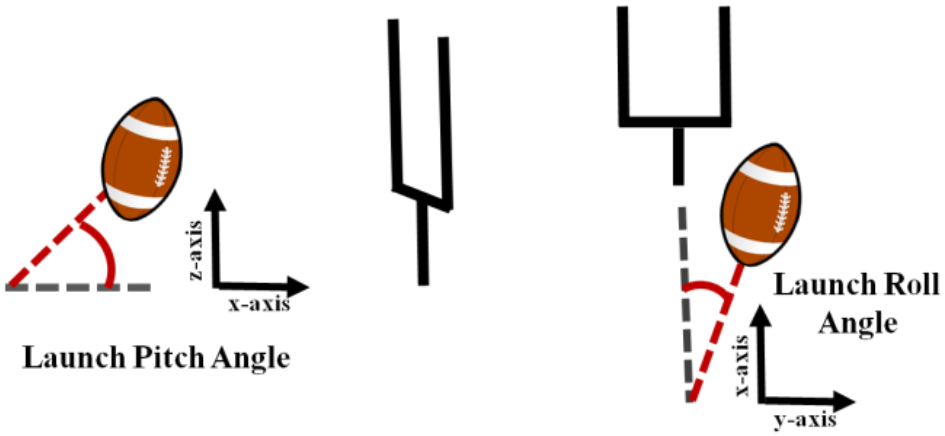

Figure 25 - Launch pitch & roll angles defined

The highest launch speeds are observed when the football is impacted at the 10.5 cm location (Figure 26). Though the football does not travel as far when impacted at this location when compared to the 8 cm and 5.5 cm impact locations it is still expected that this location show the highest launch speeds. This is because the impact conditions are directing the load closest to the center of mass of the ball. Rotation was not measured in this study but a force directed through the center of mass of the football would reduce the moment created about the football's center of mass and allow more energy to be transferred to linear motion.

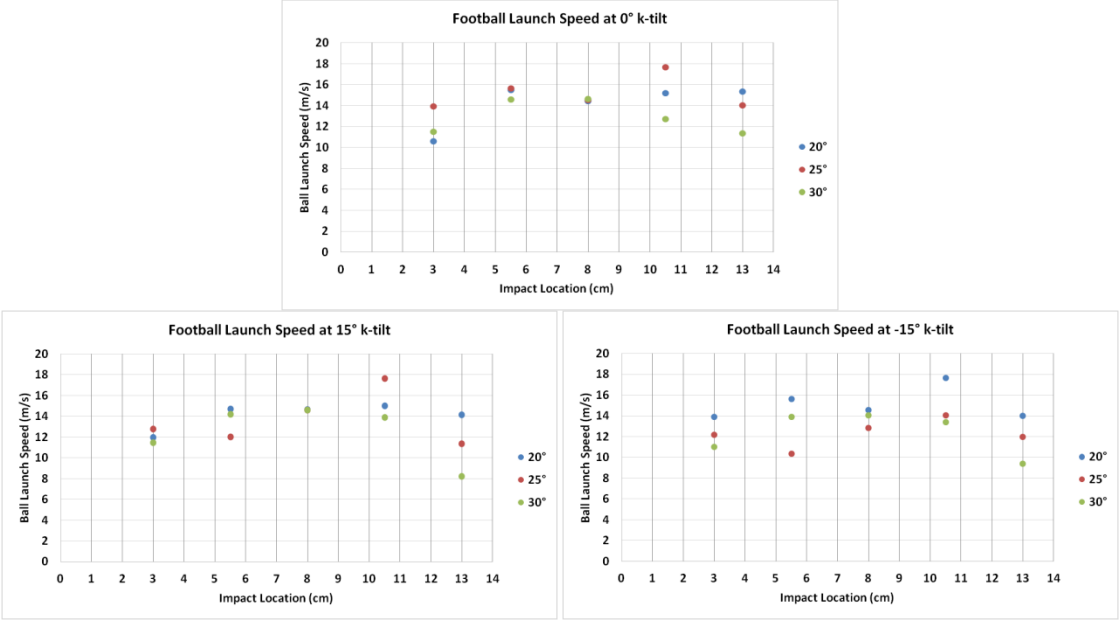

Figure 26 - Mechanical Kicker - Football launch speeds

The tradeoff of this theorized efficiency is that impacting near the center of the ball greatly reduces the launch pitch angle of the football (Figure 27). When looking at the launch pitch angles it can be seen that the 8 cm impact location is the fulcrum point at which the angle of impact does not significantly change the pitch of the ball. In fact, when impacting the ball higher than this point a larger impact angle results in a lower launch pitch angle, when utilized a 6 cm diameter impactor. Though not as evident as observed with 0° *k*-tilt, both the -15° *k*-tilt and 15° *k*-tilt show this trend as well.

Similar to what has been explored in end-over-end football flight simulations by Lee et. al. [27], a negative *k*-tilt results in the football having a lower or more negative launch roll angle. Alternatively a positive *k*-tilt results in the football having a higher or more positive launch roll angle whereas when no *k*-tilt is present a more neutral launch roll angle is observed. Little correlation is seen between the impact location and launch

roll angle, though when studying the trajectories the shorter kicks displayed a more apparent right or left drift from the center-line. The majority of the kicks with *k*-tilt that started out with a significant roll angle and traveled farther (impacts at 10.5 cm, 8 cm, and 5.5 cm) ended up 'hooking' back towards the center-line, thus showing less deviation from the center-line when hitting the ground. This 'hooking' flight pattern is consistent with the simulations presented in Lee et. al. [27].

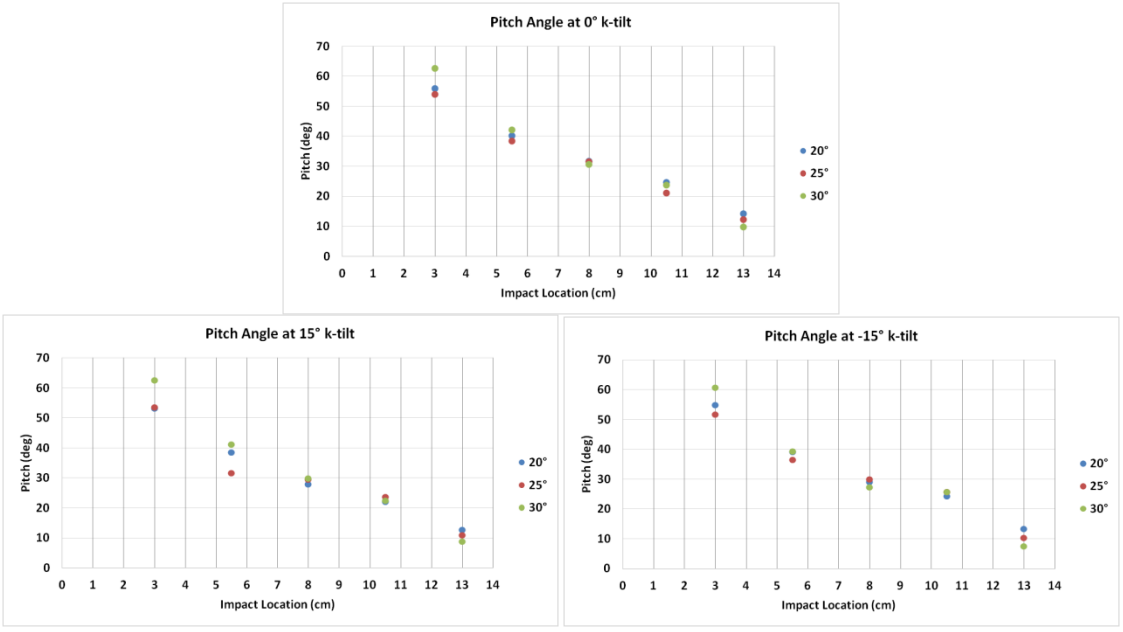

Figure 27 - Mechanical Kicker - Football launch pitch angles

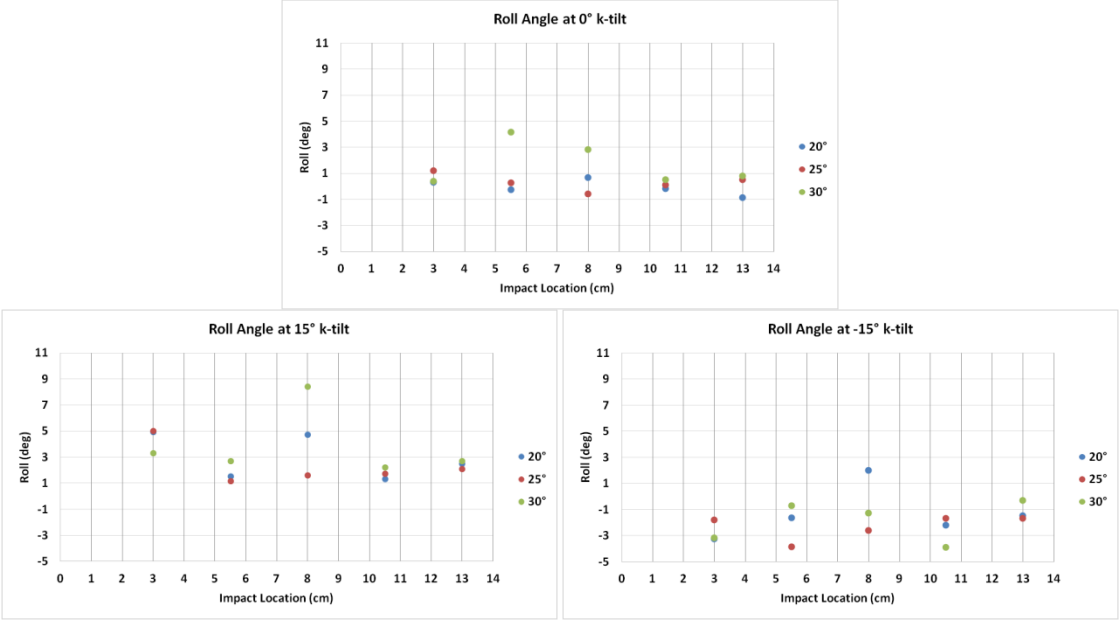

Figure 28 - Mechanical Kicker - Football launch roll angles

Using the pendulum based mechanical kicker with the presented impact conditions, the impact angle of 20° proved to launch the ball the farthest under most impact location and *k*-tilt conditions. The presented impact angles were chosen based on the projectile physics equations (neglecting air resistance):

$$R = \frac{v_o^2}{g} * \sin 2\theta_o \qquad \{\text{EQ } 8\} \qquad\qquad T = \frac{2 * v_o * \sin \theta_o}{g} \qquad \{\text{EQ } 9\}$$

where R, the horizontal distance, and T, the hang time, are calculated using v_o and θ_o which are the launch speed and launch pitch angle respectively [8]. For the most part, a kicker wishes to kick the ball as far and as high as they can. That being the case these equations dictate that a launch pitch angle of 45° would maximize the kick's distance and an angle of 90° would maximize the hang time. Therefore a kicker (governed by these equations and assumptions) would choose a launch pitch angle somewhere between 45°

and 90° that provides the best strategic combination of distance and hang time [8]. This tradeoff is often referred to as the "kicker's dilemma" and though hang time is more relevant in performing punts, in place-kicking it would correlate to kicking the ball above the other players so that it is not blocked.

Using this range as a basis the 20°, 25°, and 30° impact angles were selected and produced launch pitch angles between 7° and 60°. The presented findings support that under these impact conditions, launch pitch angles between 35° and 45° produce the longest kicks. These launch pitch angles correlate with the projectile physics equations that expect a 45° launch pitch angle to produce maximum distance. According to the data trends presented in this chapter, striking a vertically oriented football 5 cm from the ground with an impact angle of 25° are the ideal conditions for both distance and height for an end-over-end kick.

Future studies could repeat the protocols and methodology in this experiment while also altering the impact velocity and/or the impactor's moment of inertia. These additional variables could investigate the tradeoff between mass and speed as well as if there is a cutoff for too fast or too hard of an impact in which no more energy can be transferred to the ball. Other variables such as the angle of the impactor (not perpendicular with the ground) could be investigated and compared to the orientation of a kicker's foot at impact.

Chapter 5: Biomechanical Evaluation of Collegiate Kickers

After approval from the University of Nebraska-Lincoln's Institutional Review Board, four University of Nebraska-Lincoln male college football kickers participated in the study (Height: 1.835 m ± 0.038 m; Weight: 89.0 kg ± 3.4 kg; Age: 21.2 years ± 1.0 year). All testing took place in the Hawks Champion Center, located within the Athletic Department of the University of Nebraska-Lincoln (Lincoln, NE) to prevent the effects of wind and normally uncontrollable elements in an outside environment on the flight of the football. Participants wore kicking cleats of their choosing and spandex shorts during data collection. All the participants were right-footed. Each was instructed to perform 5 to 10 extra-points, 50-yd field-goals, kick-offs, and punts while lower extremity kinematic (motion), electromyography (EMG, muscle activation), and ball trajectory data were gathered. Participants were encouraged to stop and rest if fatigued. A minimum of 3 kicks with complete data sets were recorded from each kicker for each type of kick.

5.1 Methodology

5.1.1 Ball Trajectory Tracking

The projectile tracking system utilizing multiple Panasonic HC-V100 video cameras and calibration cones were arranged in order to capture ball flight for a variety of kicks over different distances. The following figures (Figure 29, Figure 30, Figure 31, and Figure 32) depict the camera set-up for point after attempts, 50-yd field goals, punts, and kick-offs. The graphic of the place kicker in each figure represents the location of the ball at impact and the direction in which the ball was kicked.

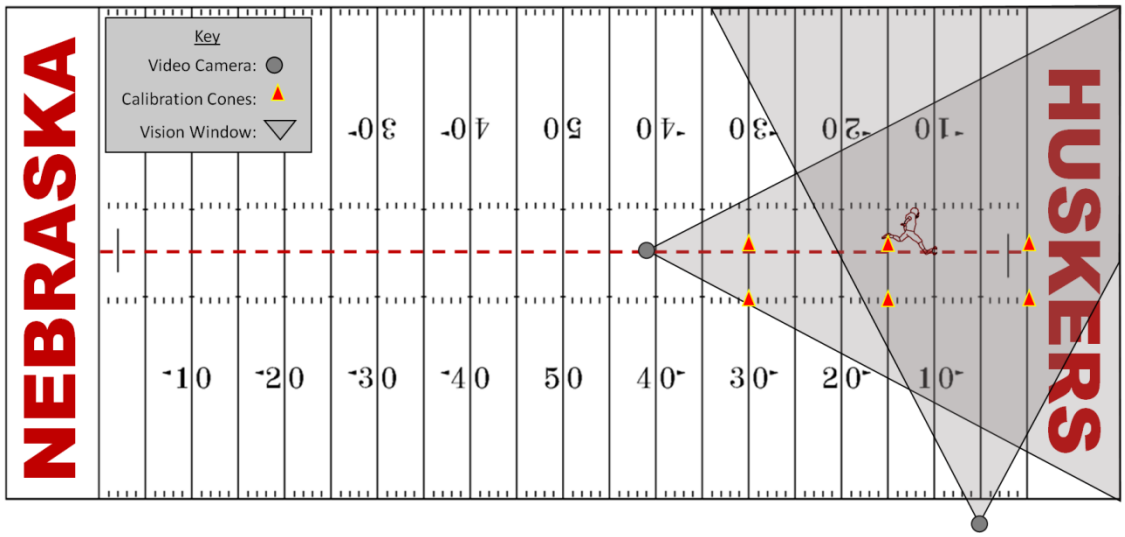

Figure 29 - Camera set-up for point after attempts

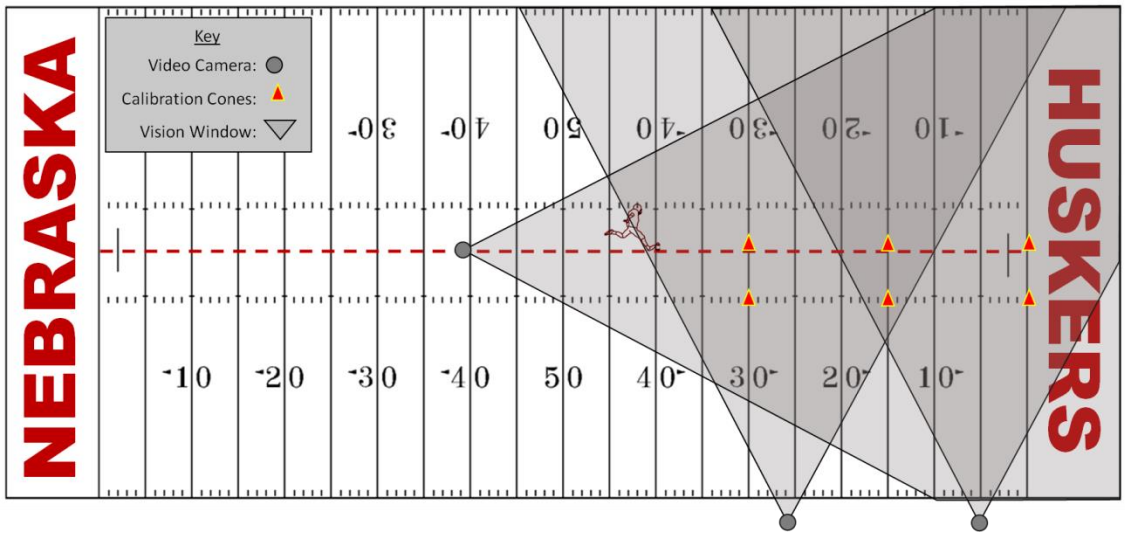

Figure 30 - Camera set-up for 50-yd field goal

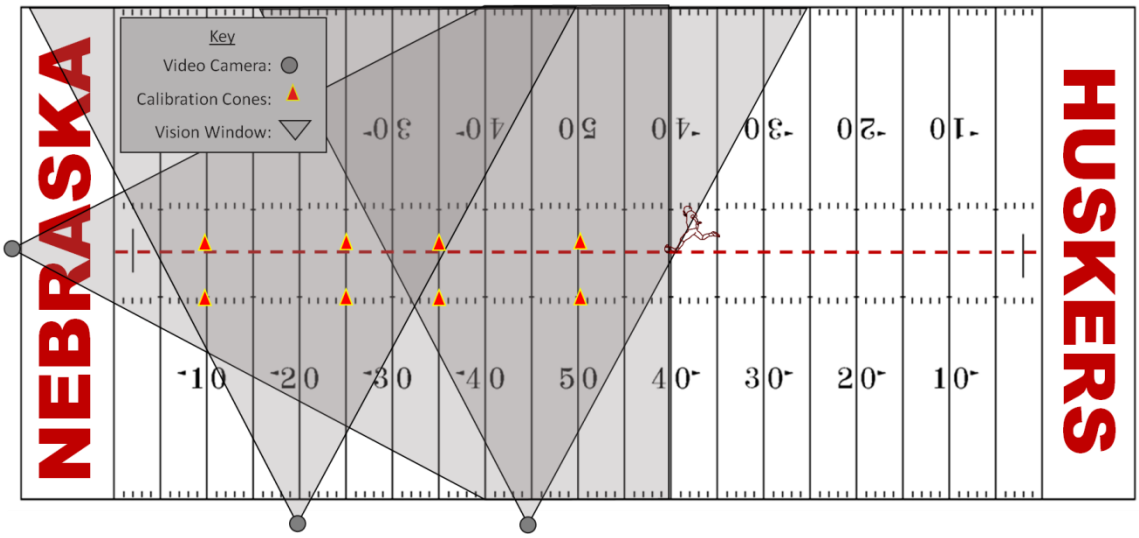

Figure 31 - Camera set-up for kick-off/punt from the 40-yd line

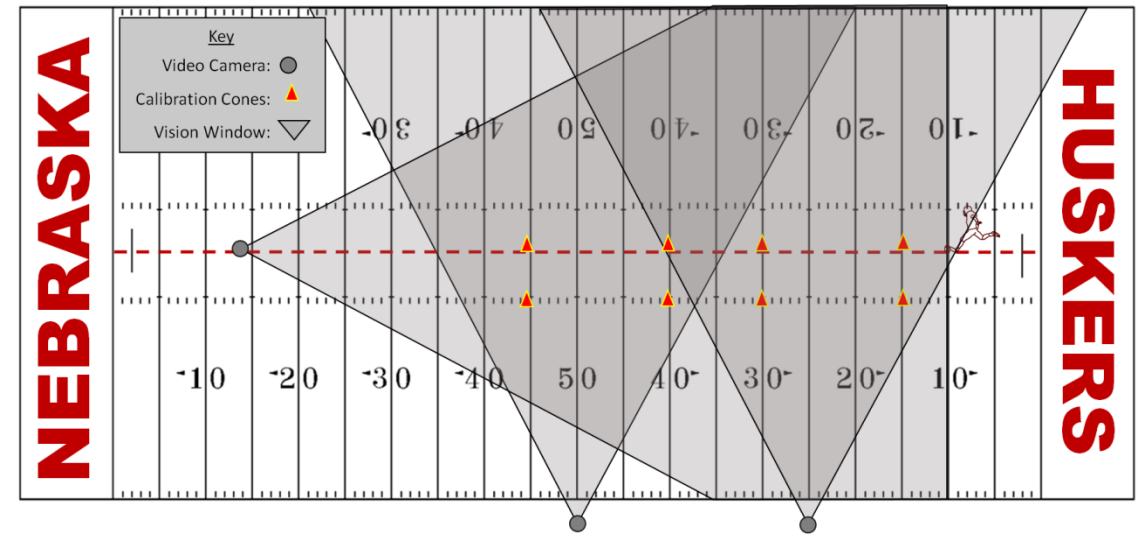

Figure 32 - Camera set-up for kick-off/punt from the 10-yd line

5.1.2 Kinematic Tracking of Elite Kickers

A Qualisys 3D motion analysis system (9 Qualisys Oqus 400 series cameras, 250 Hz, calibration residuals < 2 mm) was utilized for kinematic tracking in this study. This system uses infrared light to triangulate the 3D position of retro-reflective markers (~10 mm in diameter, markers can be observed in Figure 34) strategically placed over anatomical landmarks. The Qualisys cameras were arranged to view activity at the 10-yd

line and the 40-yd line. These locations are based on having the participants kick extra points (PATs) which could also be considered a 20-yd field goal and a 50-yd field goal. Figure 33 displays where these cameras were set up on the indoor football field and an approximated area of calibration for kinematic tracking.

Figure 33 - Qualisys Camera set-up for PAT (top) and 50-yd field-goal (bottom)

Retro-reflective markers were placed over anatomical landmarks to reconstruct the 3D movement of the place-kicker. Despite the scope of this study focusing on lower extremities given challenges with tracking full body movement during such a dynamic

activity, markers were placed on the participants using a full body modified Helen Hayes marker set. This is a commonly used marker set in the field of biomechanics, an example of which can be observed in Figure 34. However, consistent with expectations, the data recorded for the upper extremities, head, and trunk demonstrated large gaps in marker trajectory tracking. Thus, the data were used for graphical snapshots of full body skeleton, but were not analyzed as a part of the dissertation. The marker locations and labels for the utilized model are outlined in Figure 34. In brief, markers were placed bilaterally over the distal end of first toe (on the shoe), medial and lateral malleoli, medial and lateral epicondyles of femur, greater trochanters, iliac crests, and acromioclavicular joints. Markers were also placed over the L5-S1 junction and the cervical process of C7 [13]. Marker clusters mounted on semi-rigid plates were secured to thighs, shanks, and posterior shoes using flexible fabric bands and athletic tape to minimize soft tissue motion artifact [13]. A standing calibration trial was collected with all markers attached. Shoulder, elbow, knee, ankle, and foot markers were removed for dynamic testing. See Figure 34 for further details on marker location, labels, and what markers are present for static and dynamic trials.

Kinematic tracking (also known as inverse dynamics in the biomechanics field) has limitations including some of the underlying assumptions. For example, the distribution of mass in the segment is not uniform and not concentrated at one point. However, the model treats them as such. Second, estimation of joint center of rotation is prone to error [23]. The Helen Hayes model used in this study relies heavily on anthropometry to define the hip joint center due to the joints depth. Joints also often

translate while in rotation (especially the knee) and this methodology is restricted to assuming the joints are purely rotational. Third is the possibility of measurement error such as improper calibration of the system and the movement of skin (where the markers are attached) over the bone. Fourth, body segment parameters are approximations and generalizations. The numbers that define the mass of body parts are based on average human beings and therefore body builder may show different proportions. Error propagation is also possible. For example, if a joint angle is miscalculated at the hip, then the miscalculation may also impact adjacent joints (e.g., the knee). The final limitation pertaining to this study is that this methodology can only determine net joint moments and powers. For instance, equal co-contraction of antagonistic muscles could lead to the forces around the joint summing to zero, and suggest that the joint is not experiencing any forces.

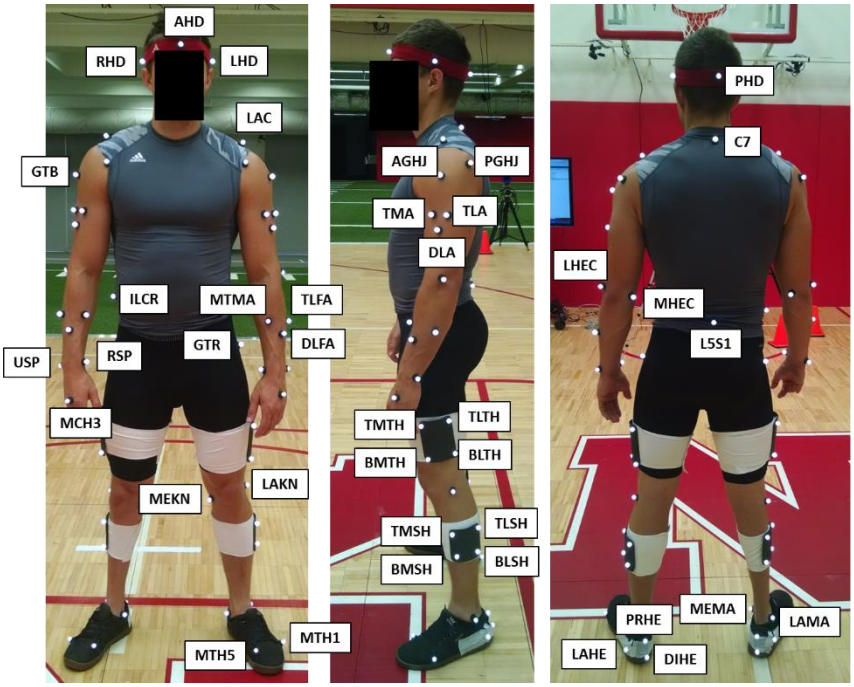

Name	Location	Static	Dynamic
AHD	Anterior Head	x	x
PHD	Posterior Head	x	x
RHD	Right Head	x	x
LHD	Left Head	x	x
AC	Acromioclavicular	x	x
AGHJ	Anterior Shoulder	x	
PGHJ	Posterior Shoulder	x	
GTB	Base of Shoulder	x	
TLA	Top Lateral Arm	x	x
TMA	Top Medial Arm	x	x
DLA	Distal Arm	x	x
LHEC	Lateral Elbow	x	
MHEC	Medial Elbow	x	
TLFA	Top Lateral Forearm	x	x
MLFA	Top Medial Forearm	x	x
DLFA	Distal Forearm	x	x
RSP	Radius side of Wrist	x	x
USP	Ulnar side of Wrist	x	x
MCH3	Hand (3rd knuckle)	x	x
ILCR	Iliac Crest	x	x
C7	C7 Vertebrae	x	x
GTR	Greater Trochanter	x	x
TLTH	Top Lateral Thigh	x	x
TMTH	Top Medial Thigh	x	x
BLTH	Bottom Lateral Thigh	x	x
BMTH	Bottom Medial Thigh	x	x
LAKN	Lateral Knee	x	
MEKN	Medial Knee	x	
TLSH	Top Lateral Shank	x	x
TMSH	Top Medial Shank	x	x
BLSH	Bottom Lateral Shank	x	x
BMSH	Bottom Medial Shank	x	x
LAMA	Lateral Ankle	x	
MEMA	Medial Ankle	x	
PRHE	Proximal Heel	x	x
DIHE	Distal Heel	x	x
LAHE	Lateral Heel	x	x
MTH1	1st Metatarsal	x	
MTH5	5th Metatarsal	x	

Note: Marker names are prefaced with R or L to designate right of left side respectively.

Figure 34 - Full body marker set

After marker identification in Qualisys Track Manager (QTM), Visual™ 3D (V3D) was used to recreate a virtual skeleton of the participants. A custom designed program within V3D is used to process the raw kinematic data for this study was adopted from Cesar (2014) [13] for use with the presented marker set. Each segment of the body was modeled with specific geometry and mass properties. These details can be seen in Figure 35. Again, a full body set model was attempted for all participants but only the lower body (e.g., pelvis, thigh, shank, and foot) markers were dependably tracked throughout the kicks.

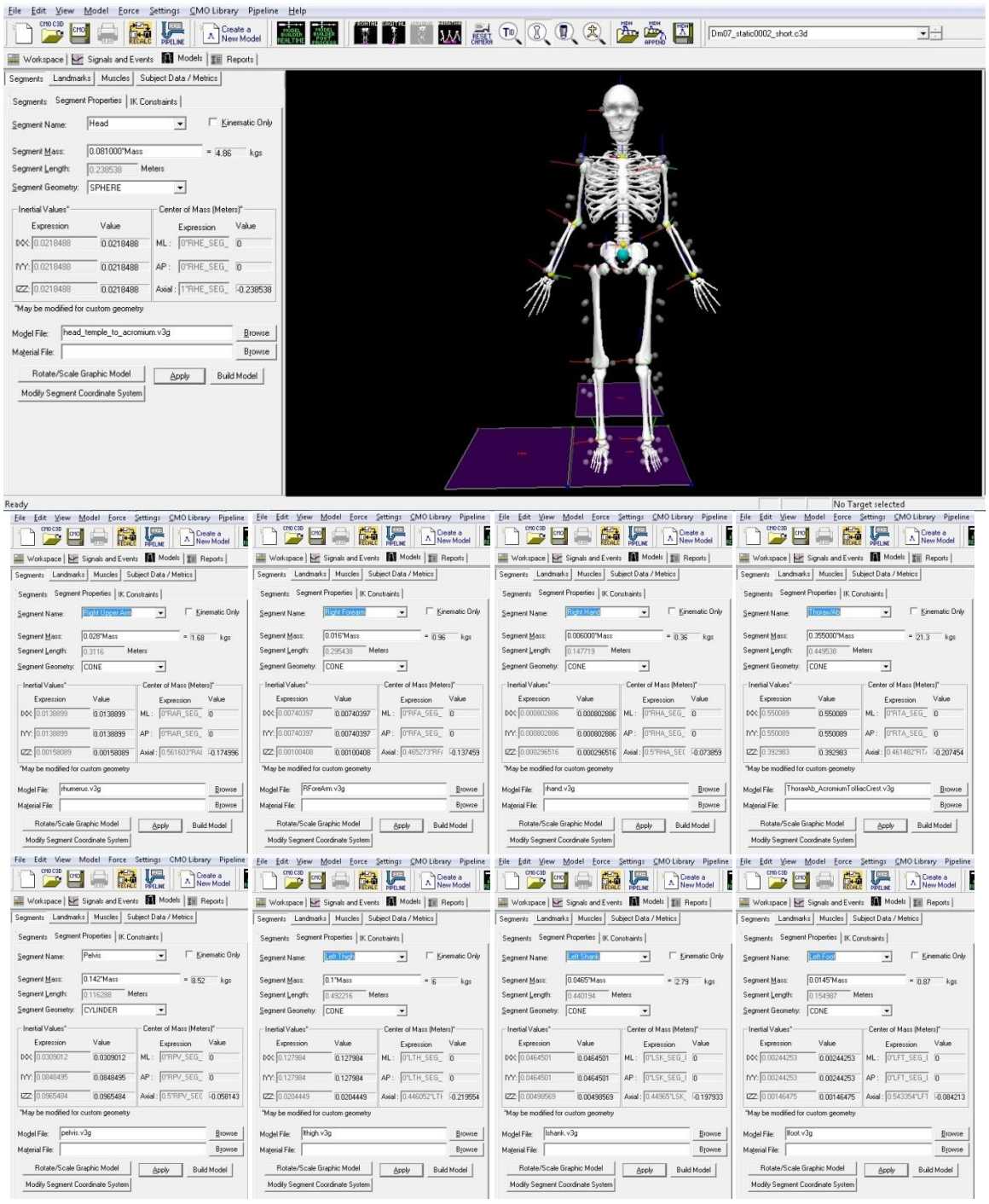

Figure 35 - Model segment parameters (adopted from [13])

5.1.3 Electromyography

Surface electromyography (EMG) data were collected from relevant muscles using a Delsys® Trigno™ Wireless EMG system. As eluded to in Chapter 2, surface

EMG is used to investigate the more superficial muscles and convert their activation into a voltage signal. This surface EMG system wirelessly relays electrical signals generated by the contracting muscle, recorded by each sensor, directly to the QTM software.

EMG data were recorded from 12 muscles that were selected due to their expected role in the kick. Left and right Erector Spinae (central back muscle), the left and right Rectus Abdominus (abs), the right Gluteus Medius (upper thigh), the Gluteus Maximus (buttocks), the Vastus Lateralis (lateral quadriceps), the Vastus Medialis (medial quadriceps), the Rectus Femoris (central quadriceps), the Biceps Femoris (hamstring), the Anterior Gastrocemius (calf), and the Anterior Tibialis (shin). With exception to the Erector Spine and Rectus Abdonminus, all muscles were investigated in the kicking leg only.

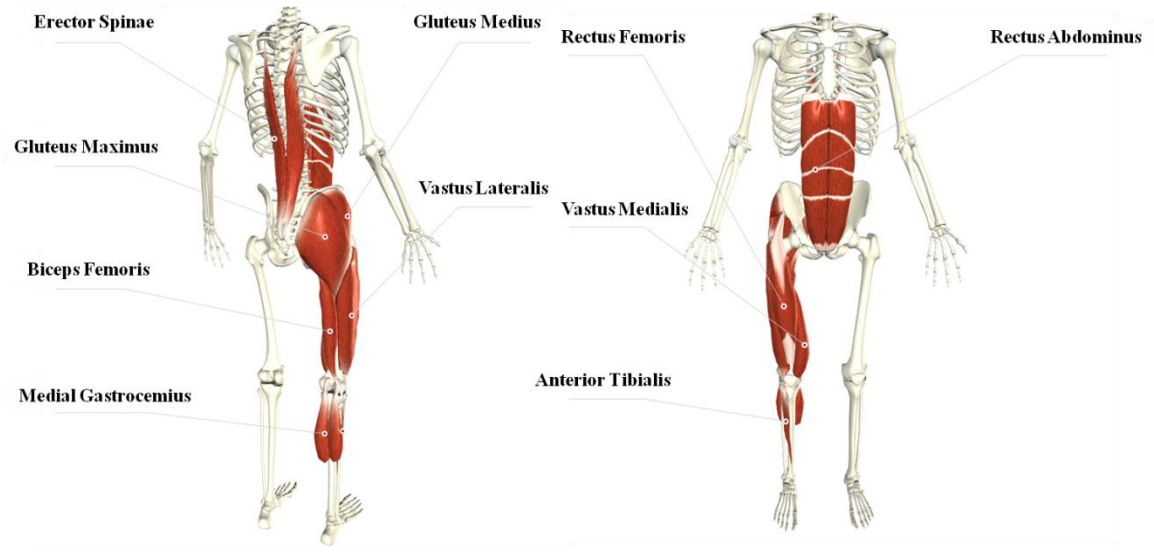

Figure 36 - Muscles investigated with EMG

The Delsys® Tringo™ EMG sensors utilize 4 parallel bar leads, each with a contact dimension of 5 x 1 mm made of 99.9% pure silver (Ag). The overall dimensions

of the sensors are 27.6 x 24.1 x 12.7 mm with an interelectrode distance of 10 mm. The electrodes were positioned longitudinally with respect to the direction of the muscle fibers and located according to the recommendations of Seniam [2]. The participant's skin was shaved, scrubbed with an abrasive, and cleaned with alcohol before the sensor was adhered to the skin with toupee tape (known for its adhesion to skin) and wrapped with an elastic band.

Figure 37 - Delsys® Tringo™ wireless EMG sensor [15]

The raw EMG data was processed in MatLab using a digital Butterworth filter per Mello et al. [32]. This filter is designed to delimitate the frequency band of surface EMG and remove noise in the signal recording during muscle activity. In brief, the Butterworth filter utilized has a passband spectrum between 10 and 400 Hz, with selective stop bands at the fundamental frequency of 60 Hz and its harmonics. [32]. MatLab was used to replicate the filter explained in Mello et al. and perform the filtering process. The filtered EMG signal was then exported to Excel for further processing.

Slight differences in body composition and sensor placement between participants can result in noticeably different voltage readings from subject to subject. Therefore, to

control for differences in EMG signal values across participants, each participant was asked to perform a bodyweight lunge. The bodyweight lunge is an activity regularly performed by college athletes and activates the core and lower body muscles that are used in kicking. EMG signals were recorded from the 12 muscles of interest and the peak value was then used as a normalization reference for subsequent EMG recording during the kicks.

Normalizing the EMG signal with respect to the signal obtained from the bodyweight lunge resulted in place kicks displaying muscle activity from 50% to over 5000%. This means that a muscle may have a level of peak activation while place kicking that is 50 times higher than that of performing a lunge. The mismatch between demands during the lunge activity and the demands of kicking the football indicated that an alternative normalization factor was needed.

To accomplish this, the EMG data for the 50-yd field goals were examined. Consistent with expectations, for most participants and muscles, the muscle activation during the 50-yd field goal attempts were higher than that of the PAT. Therefore, the maximum recorded activation of each muscle from the 5-10 50-yd field goal kicks was found for each muscle and then used as the normalizing factor. This resulted in EMG signal plots ranging from 0% to 100% for normalized muscle activation over time (Figure 39). In instances when the participant showed a larger activation in a PAT than a field-goal, normalized activation of over 100% occurred.

5.1.4 Kicking Phase Definitions

As previously mentioned, kinematic and EMG data was first processed using QTM. During this phase of processing the kinematic trackers for head, arms, and trunk were not consistently tracked. However, the main segments in question, the pelvis and lower limbs, were consistently and accurately tracked throughout each kick. In order to properly cut each data set to consistently line up trials for averaging purposes, four landmarks throughout the PAT and place kicks were defined. These landmarks where defined as foot-off, peak backswing, impact, and peak follow through. Figure 38 illustrates where these landmarks take place in the kicking phase and how they were determined for each kick.

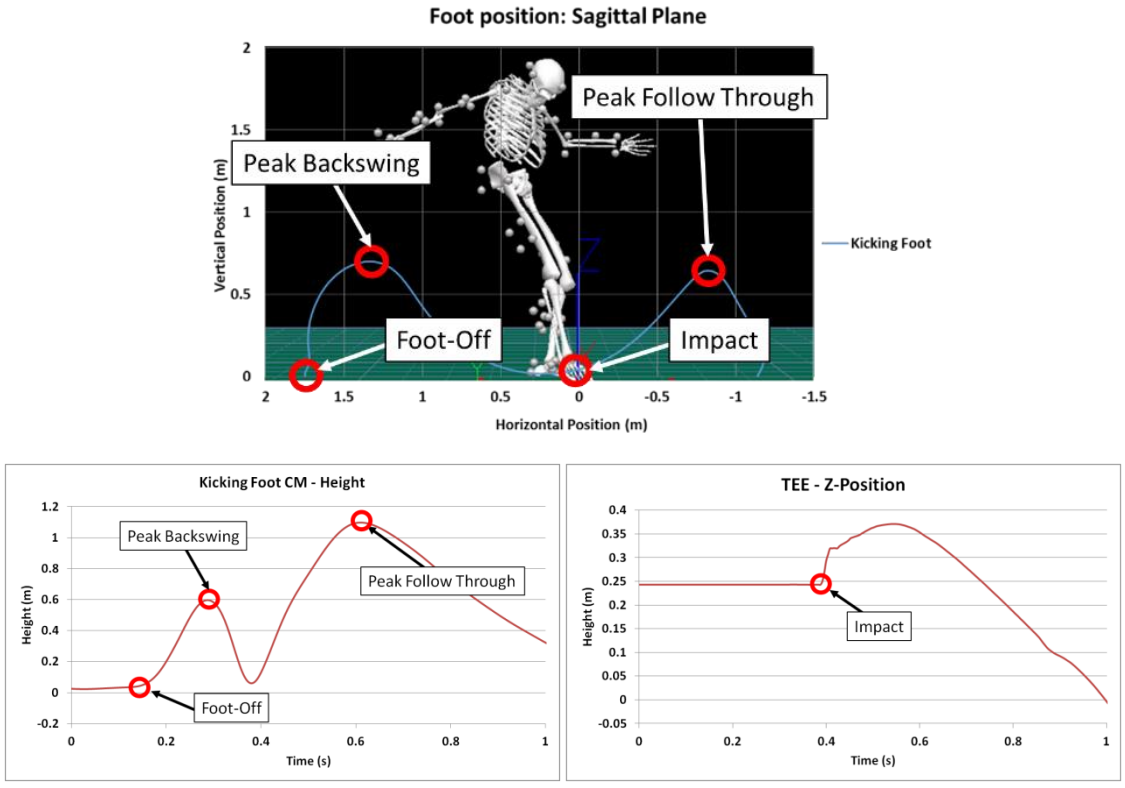

Figure 38 - Phase Defining: Visualization - top; landmarks determined by kicking foot - left; impact - right

These phases are used to trim and synchronize the kinematic and muscle activity data for each kick into a form that can easily be compared from one kick to another, or one participant to another. An example of this is shown in Figure 39. The time component is translated to 0% of phase at *Foot off* and 100% of phase at *Peak Follow Through*. The time or percent phase between each landmark is defined in Figure 39(right) as backswing, swing, and follow-through phases. This terminology will be used to reference portions of the phase throughout this dissertation.

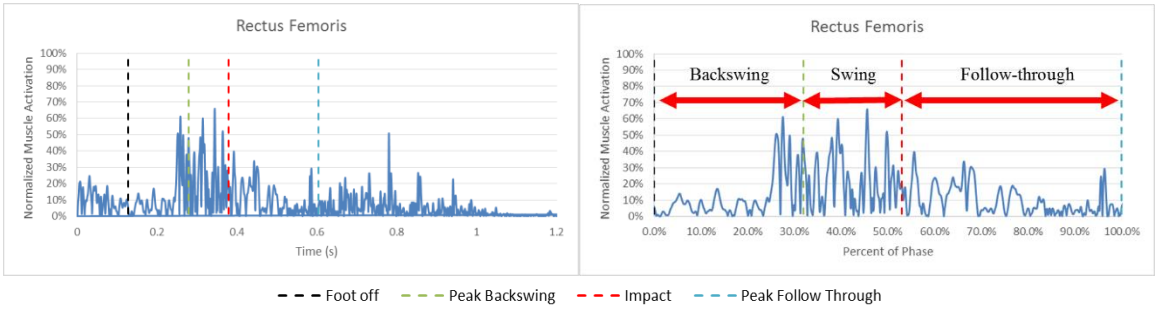

Figure 39 - Example EMG plot. Activation vs. Time (left) and Activation vs. Percent of Phase (right)

5.2 PAT Results and Discussion

5.2.1 Trajectories

Three of the four participants volunteered to kick PATs. The resultant trajectories of these kicks are displayed in Figure 40, Figure 41, and Figure 42. Plots (a) through (c) depict the trajectories from different views while (d) displays the "End Points" or where the ball crossed the plane of the goal post.

Velocity information was tabulated for each set of kicks. This consists of launch angles (pitch and roll) as well as the resultant magnitude of velocity. This information, paired with the "End Points" allows one to make assumptions as to what is a *better* or *worse* kick.

Therefore, what was considered the *best* and *worst* 50-yd field-goal (referred to in the plots as FG) for each participant was investigated in depth as well as the overall average field-goal biomechanics and ball trajectory. The participants made all of their extra points with ease, thus individual kicks will not be examined outside of the average biomechanics and trajectory data.

Participant F01 showed great consistency in his five PATs with an average launch pitch angle of 31.3° with very little roll. Pitch, roll, and speed data for each kick were calculated using the first 0.2 s of the ball's trajectory. This allows for the ball to clearly release from the foot before the launch velocity to be determined. As a reference, it is estimated that the average duration of impact between the foot and a soccer ball is 0.05 s [44].

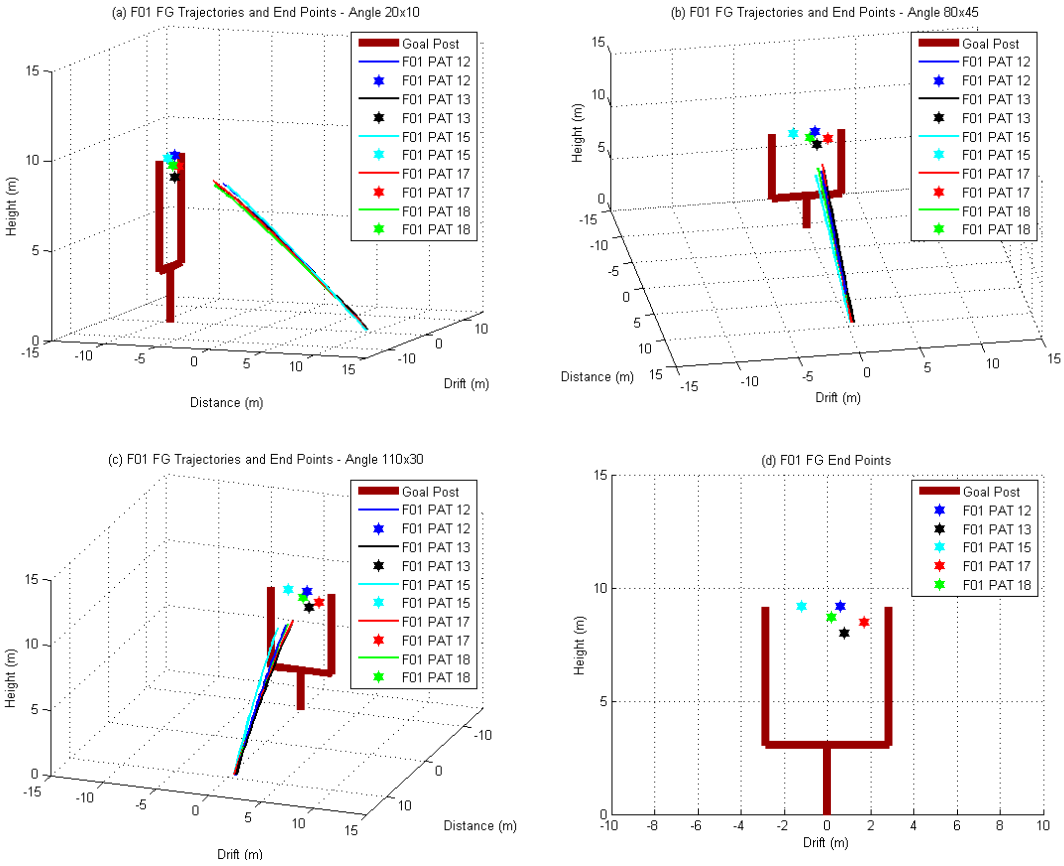

Figure 40 - F01 PAT Trajectories (a-c) Depict trajectories and end points, (d) Depicts the end points

Table 4 – F01 PAT - Ball Launch Mechanics

Kick	12	13	15	17	18	Average	STDV
Pitch (deg)	31.9	31.4	32.6	30.7	30.0	**31.3**	**1.0**
Roll (deg)	-1.9	-0.8	-3.6	-1.0	-1.5	**-1.8**	**1.1**
Resultant Magnitude of Velocity (m/s)	28.6	26.5	27.5	27.9	27.1	**27.5**	**0.8**

Participant F03 showed similar consistency to F01 with his PATs. F03's average launch pitch angle was 33.2°, the highest among the participants. The roll component of the launch angle was negative and less than or equal to 2 degrees with an exception observed in PAT 4. PAT 4 displays a noticeable amount of drift off to the left before ending up in the middle of the goal-post. It is likely this trajectory is largely due to the

higher than average launch roll angle. On average, participant F03 delivered the ball with a resultant velocity magnitude of 26.4 m/s, roughly 1 m/s, or 4% slower than F01.

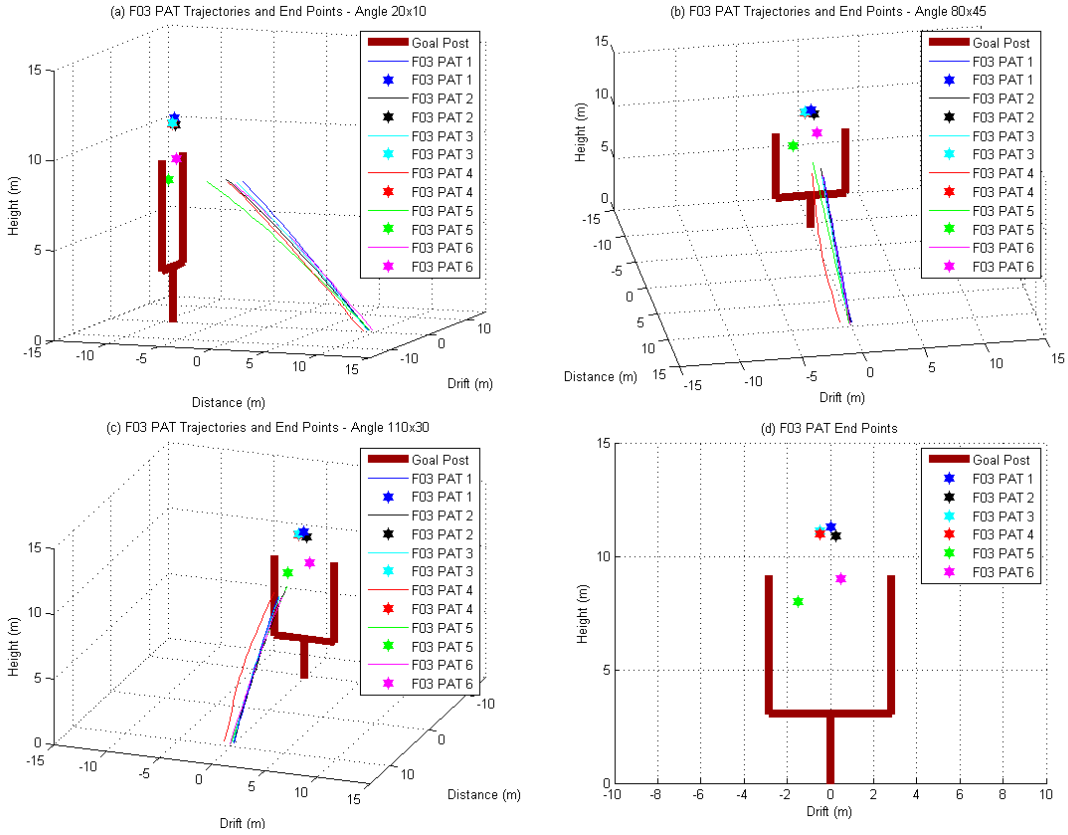

Figure 41 - F03 PAT Trajectories (a-c) Depict trajectories and end points, (d) Depicts the end points

Table 5 - F03 PAT - Ball Launch Mechanics

Kick	1	2	3	4	5	6	Average	STDV
Pitch (deg)	35.4	33.2	34.3	33.6	29.9	32.7	**33.2**	**1.9**
Roll (deg)	-1.7	-2.0	-1.6	-5.2	-2.0	0.0	**-2.1**	**1.7**
Resultant Magnitude of Velocity (m/s)	25.6	24.7	26.6	26.7	27.7	26.9	**26.4**	**1.1**

Participant F04 showed consistency with his PATs as well. His kicks were all to the left of the centerline of the field-goal whereas the other participants' kicks were closer to the center of the field-goal. F04's average launch pitch angle for PATs was 27.1° with

a roll of -3.9°. This pitch angle was lower than that of the other participants and the roll angle was noticeably higher. The magnitude of launch velocity however was much higher than the other participants at 30.9 m/s, an average roughly 12% higher than that of F01.

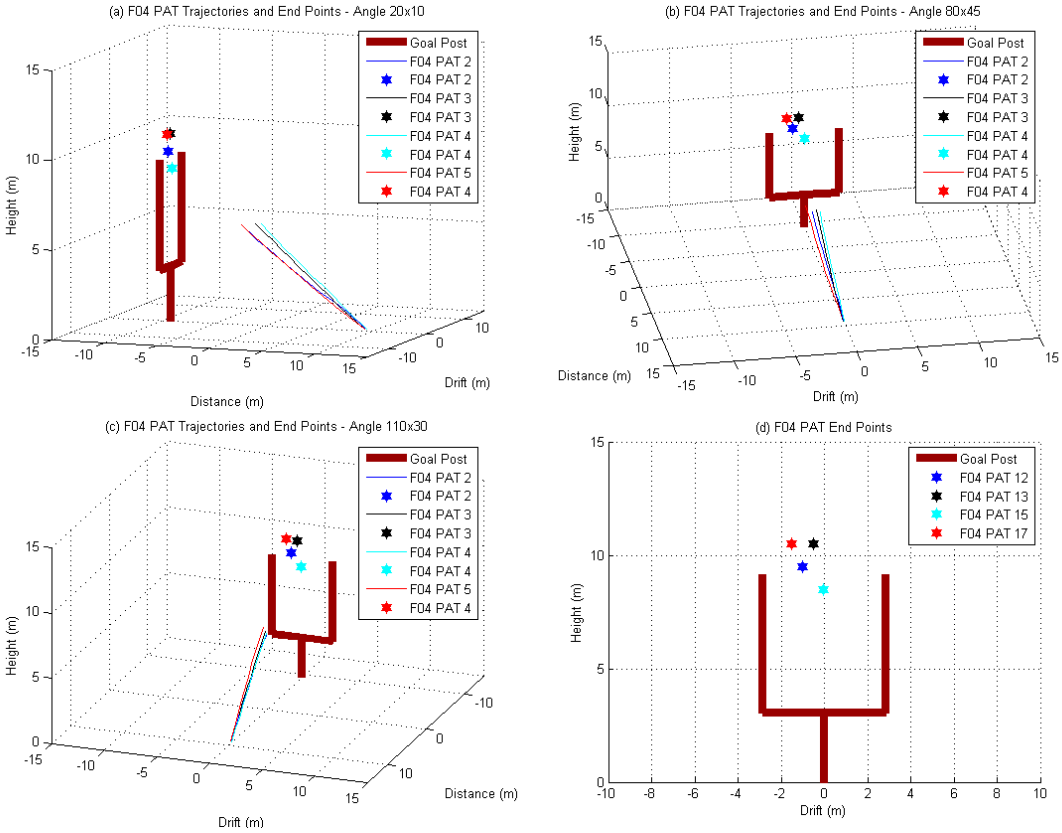

Figure 42 - F04 PAT Trajectories (a-c) Depict trajectories and end points, (d) Depicts the end points

Table 6 - F04 PAT - Ball Launch Mechanics

Kick	12	13	14	15	Average	STDV
Pitch (deg)	24.9	28.8	29.1	26.2	**27.3**	**2.1**
Roll (deg)	-4.4	-2.7	-2.3	-5.8	**-3.8**	**1.6**
Resultant Magnitude of Velocity (m/s)	30.2	30.1	29.9	33.3	**30.9**	**1.6**

A PAT is a situation when a long distance kick is not required, but instead an accurate kick with a large launch pitch angle is ideal. The ball's trajectory must rapidly

ascend vertically to avoid being blocked by the opposing team's players. Therefore, from the data presented participant F03 could be considered the “better” PAT kicker because his kicks have the largest pitch launch angle and accuracy. In this study, accuracy is a measure of how close the end point of the ball is to the center of the field-goal.

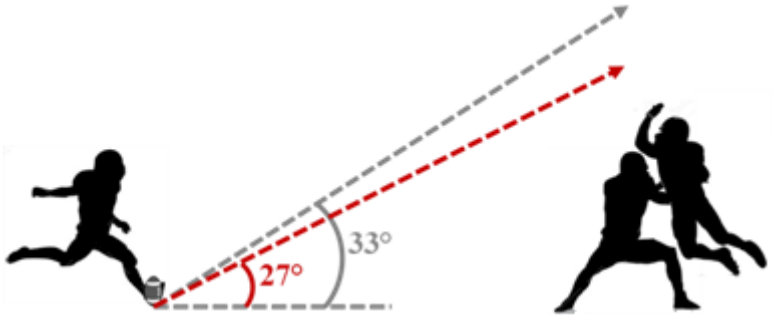

Figure 43 - Difference 6° makes in a field goal (to scale with 6' players)

5.2.2 PAT Kinematic Tracking Data

The kinematic tracking data was processed to output segment speeds, joint angles, and joint power for the kicking leg. The following plots for speed, flexion, and power depict the average value through the investigated kicks from 5% to 95% of phase (as defined in section 5.1.4). A re-sampling process was taken (in MatLab) to ensure that each data set had the same number of data points. This filtering process corrupted a number of data points on the extreme ends of the data ser. Thus, only the middle 90% of the kicking cycle was analyzed and the first and last 5% of the kicking cycle were omitted from subsequent analysis. The shaded portion surrounding the solid line is representative of one standard deviation (SD) from the average at that point in the phase. There are also vertical lines pointing out the average point at which the *Peak Backswi*ng and *Impact* occurred in the phase. The shaded portion around these dashed lines represent the deviation from the average percent of phase in which these events occurred.

Body Segment Velocity

The summation of speed principle, outlined in Chapter 2, describes how proper timing of proximal to distal motion can increase the velocity potential of the more distal body segments. In the current application of place kicking the summation of speed principle is examined as each participant's kicking leg moved through the kick. The average magnitude of the resultant velocity for the pelvis, thigh, shank, and foot are plotted through the defined kicking phase for PATs in Figure 44.

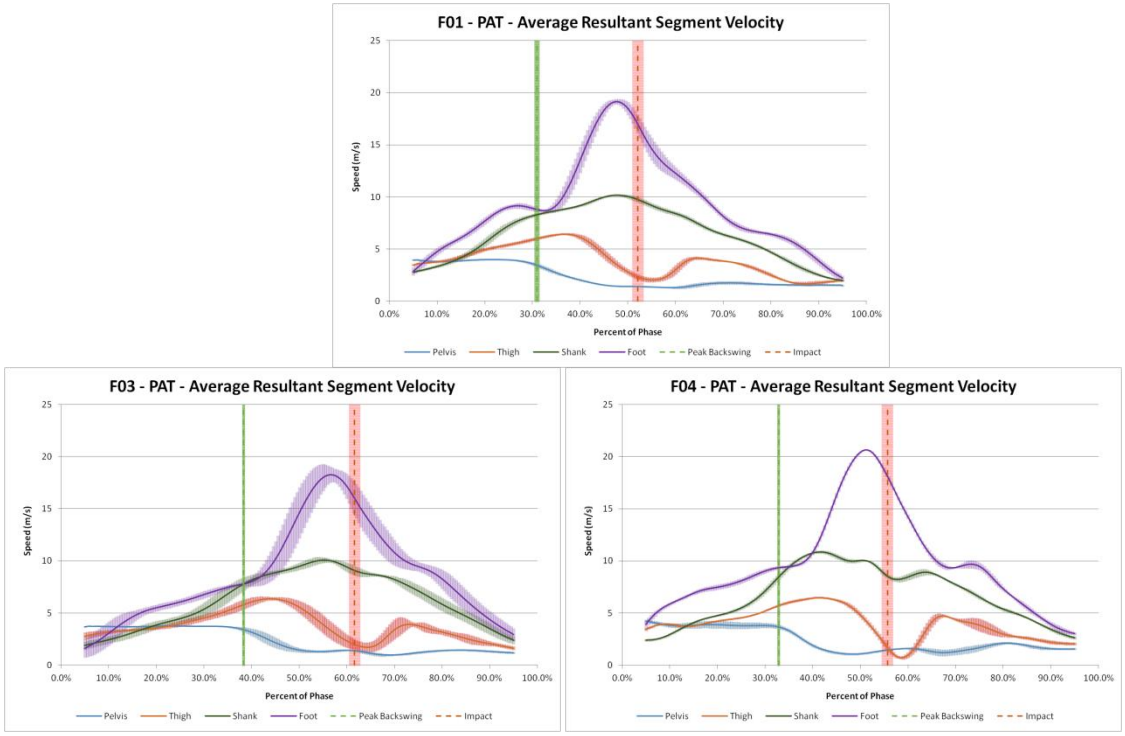

Figure 44 - PAT average magnitude of resultant segment velocity

Figure 44 documents not only the timing of peak segmental velocities across regions of the leg, but also the variability in consistency of velocities across participants. In particular, participant F03 shows a large deviation in segment speed across kicks (as evidenced by the larger width of each of the segment's SD band). In contrast, participant

F04 displays very minimal deviation in segmental velocity, as evidenced by narrow SD bands for each joint.

In accordance with the first hypothesis outlined in the scope of this study, this consistency in movement appears to be linked to consistency in ball trajectory as well. Figure 41(d) and Figure 42(d) highlight that F03 has two kicks that terminated their trajectory well outside of the grouping created by the first 4 kicks. In contrast, F04's PATs all terminate in a similar area within the goal-post. Participant F01 shows very little deviation in his kicking motion as well, however he has a wider dispersion of his kicks than F03 (Figure 45). However, other factors beyond segment velocity may impact accuracy. For example, the variability in F01's approach angle (relative to the environment) may have contributed to the larger deviation for F01 in the horizontal direction.

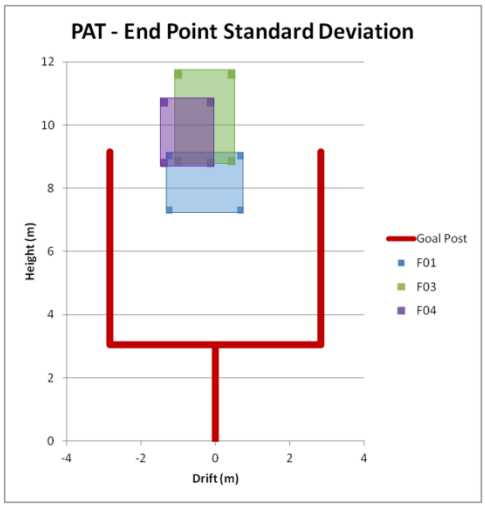

Figure 45 - PAT Deviation from final End Point

The point in which impact occurred in the phase for each participant also varied by approximately 10% of the phase. It should be noted that participants F01 and F04

impacted the ball at an identical time in the phase with respect to peak foot speed (2.4 m/s less then peak foot speed). In contrast, F03 impacted the ball just slightly later in the kicking phase (with respect to peak foot speed) with an average foot speed that was 2.5 m/s slower than his maximum foot speed. Participants F01 and F03 kicked the ball at an average speed of 27.5 m/s and 26.4 m/s respectively, and a launch pitch angle of 31.3° and 33.2°, respectively (Table 4, Table 5, and Table 6). Alternatively, participant F04 kicked the ball at a significantly higher average speed of 30.9 m/s with an average launch pitch angle that was approximately 15% lower (27.3°) than the other participants' pitch angle.

Between peak backswing and impact the kicking foot approaches the ball. To perform this motion a kicker's trunk leans laterally away from the ball and the kicking leg circumducts so that kicking leg extension is able to occur without the foot impacting the ground. This orientation allows a kicker to fully extend their kicking leg, down to the pointed toes, and maximizes the potential for velocity at the distal end of his body (Figure 46). Similar to a swinging pendulum, the foot travels fastest when it is at its lowest point in the swing. Thus as the foot comes up to impact the ball it is slowing down. This concept's relevance in this study is that the point of impact in the kicking phase for participant F03 is later than that of F01 and F04 with respect to peak foot speed. This then relates to the kicking foot being further through the swing and impacting the ball with a larger vertical component of velocity. Depending on the impact location on the ball this may cause the ball to launch with a larger pitch angle.

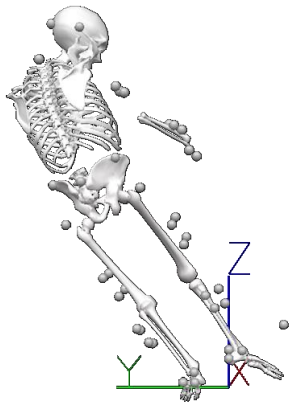

Figure 46 - Example kicker orientation at impact

Along with impacting the ball closer to peak foot speed, participant F04 displays a noticeably higher peak foot speed at over 20 m/s while F01 and F03 reach a peak around 19 m/s and 18 m/s respectively. These data strongly suggest that the difference in foot speed is largely in part due to the timing of segment movement with respect to their more proximal and distal counterparts. Similar to the summation of speed principle visualized in Figure 3, the foot speed for F04 accelerates through the peak velocity of its more proximal counterpart (the shank). This ideal timing of segment motion allows the foot of F04 to have a greater velocity potential, as seen in Figure 44. Both F01 and F03's foot speed starts to increase before the shank has reached its peak resultant velocity, limiting the foot's maximum velocity potential.

Kicking Leg Joint Angles

The joint angles of the kicking leg were examined as well. Figure 48 depicts the average joint flexion for the hip, knee, and ankle in a similar fashion to how segment speed was displayed. Hip flexion refers to the angle between the pelvis and thigh in the sagittal plane with the standing position representing a joint angle close to 0°. If the leg is lifted so that the thigh is perpendicular to the abdomen, similar to a seated position, the

hip joint angle would be around 90°. Knee flexion is defined as 0° when in a standing position and a positive angle is formed when the heel rises towards the buttocks. Ankle flexion is approximately neutral (0°) in a standing position and becomes a negative angle (plantar flexed) when the ankle is extended as if pointing toes. See Figure 47 for an example of lower extremity flexion and extension.

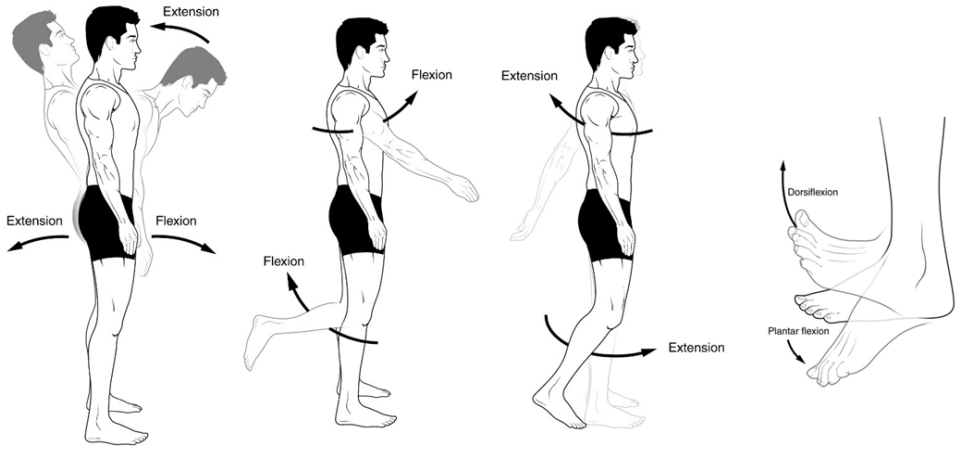

Figure 47 - Flexion/Extension example [3]

Consistency in joint flexion correlates quite well with consistency observed from segment speed. In that both F01 and F04 show lower deviations from the average through the kick (Figure 48). The motion from *peak-backswing* to *impact* (swing phase) largely dictates foot control. Low standard deviations in joint motion during the backswing suggest more consistent foot control across kicks.

Participant F01 shows very little deviation for all three examined joints throughout the kicking phase. F03 shows more knee flexion variation than the others through the entirety of the kicking phase. F04 shows a large amount of deviation in hip flexion in the backswing but shows nearly zero deviation in joint angles in the swing

phase. Larger deviations in knee and ankle flexion for F04 can also be observed in the follow-through phase of the kick.

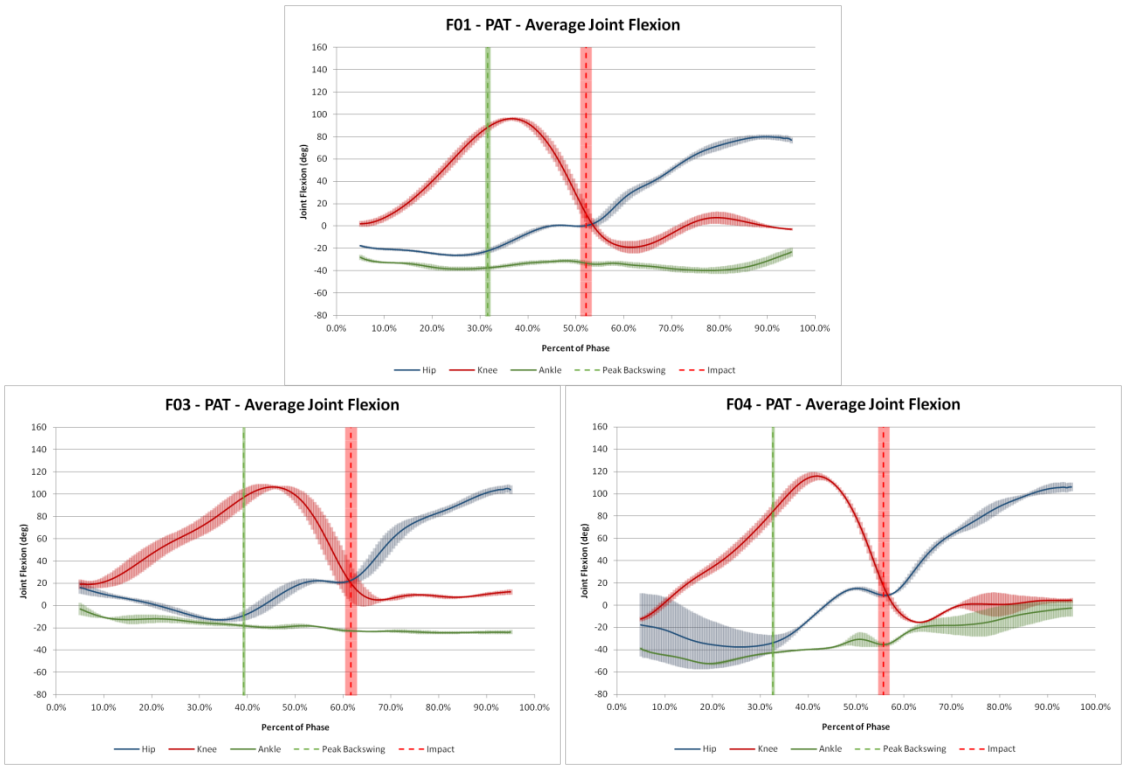

Figure 48 - PAT average joint flexion

Average hip flexion is very similar for all three participants. The hip shows some extension through the backswing, comes to a more neutral position when approaching impact, then climbs in flexion during the follow-through. It is interesting to note that participants F01 and F04 show hip extension at peak backswing (-20° or more) while participant F03 shows an average angle closer to -10°. This is indicative of F03's pelvis being more in line with his thigh at peak backswing. Hip extension in the backswing phase contributes to the tension arc discussed in Chapter 2 [40].

Participants F01 and F03 display peak knee flexion around 100° whereas participant F04 reaches a peak knee flexion nearing 120°. These findings correlate with

Shan and Westerhoff's findings that superior range of motion allows for higher foot speed potential [40]. This larger additional flexion may also contribute to peak knee flexion occurring closer to the middle of the swing phase and the slope of his knee flexion curve contributes to higher joint powers (defined in the following section). It can also be seen that both F01 and F04 show approximately 20° of knee extension after impact. Knee extension in this case is actually hyperextension of the knee (Figure 49). The accepted normal range of hyperextension in flexible adults is no more than 15° [5].

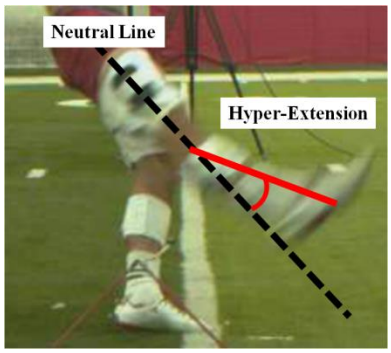

Figure 49 - Knee hyperextension after impact

These athletes are producing foot speeds of 17-20 m/s (38-44 mph) and the buildup of hip flexion and knee extension causes their foot to "whip" near impact and hyperextend the knee. This "whipping" motion between the hip and knee aligns temporally with ball impact for all participants. At impact the hips have just began to flex the thigh upward and the knee is "whipping" into its largest extension. By impacting the ball at this point in the phase the participants are in contact with the ball as they start to go into their maximum knee extension, thus continuing extension through the kick and not losing foot speed to the body's natural mechanisms of decelerating (in this case, maximum extension) before the ball has left the foot.

Joint Power

Power is defined as the rate of work over the change in time. In biomechanics, this same concept can be applied to the joints utilizing the joint angle and segment moment of inertia. Joint power can be defined as:

$$P = I_s * \frac{d\theta^2}{d^2t} * \frac{d\theta}{dt} \quad \text{[EQ 10]}$$

where I_s is the moment of inertia for the segment(s) rotating about the joint in question (defined in Figure 35, segment mass, length, and geometry) and θ is the joint angle (plotted in Figure 48).

Each participant showed a unique power curve through the kick. However, the power about the ankle (Figure 50) remains very close to 0 W at all points in the phase for each participant. This is expected because (1) there is very little joint flexion in the ankle when compared to the other joints, which is because the ankle remains extended through the majority of the kick, and (2) because the mass and size of the foot results in it possessing a much lower moment of inertia when compared to the trunk, thigh, and shank.

Similar to what was observed with the participant's joint angles, F03 shows noticeably more variance in joint power through the entirety of the kick and F04 shows large variance in joint power about the hip approaching peak backswing. This is expected as the joint angle (θ) is the only variable in the power equation that changes through the kick. Participant F01 shows little variance up to impact and a variance in hip power similar to the other participants post impact.

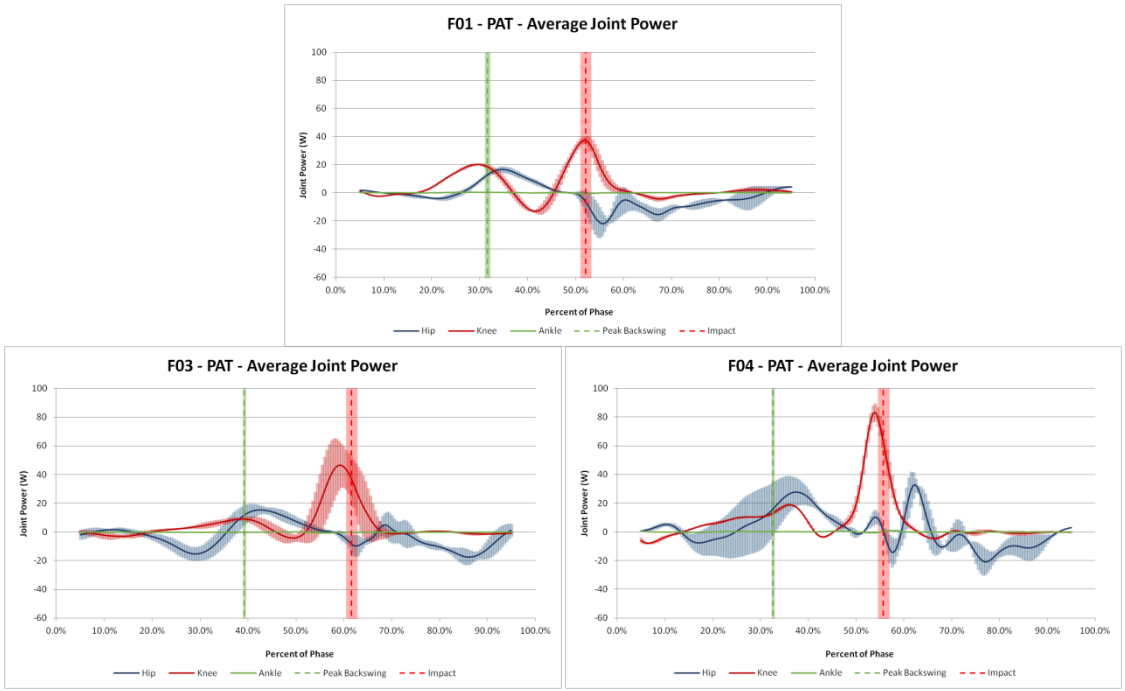

Figure 50 - PAT average joint power

The most noticeable difference in the participants' joint power curves is the magnitude of F04's knee joint power. A maximum energy generation rate of 80 W is observed whereas the average of both F01 and F03 reach a peak around 40 W. F01 and F03 also exhibit energy absorption (negative power) through the hip joint at impact where as F04 shows a more neutral power about the hip joint. It is my belief that this culmination of high joint power at impact, for participant F04, is a result of more proper use of proximal to distal motion (summation of speed principle) and in turn produces higher foot speeds as observed in the segment velocity plot (Figure 44).

During the follow through F04 shows energy generation through the hip meaning that F04 is actively lifting his leg after impact. Alternatively, within 5% phase after impact both F01 and F03's total power becomes zero or negative meaning that their

follow through quickly moves from creating energy to absorbing energy. It is necessary for energy absorption to occur in order to slow the body down after impact but performing this task later in the phase would allow for a larger rate of energy creation through impact. This could be thought of as a sprinter running the 40-yd dash and coming to a stop at the finish line. Running through the finish lines prevents the athlete from decelerating early and therefore allows for a better time.

5.2.3 Electromyography

Electromyography (EMG) records the electrical signal generated by a muscle during contraction. This can include electrical signal arising from concentric, isometric and concentric muscle activity. Concentric and eccentric muscle contractions are depicted in Figure 51, an isometric contraction is when the muscle contracts to prevent movement.

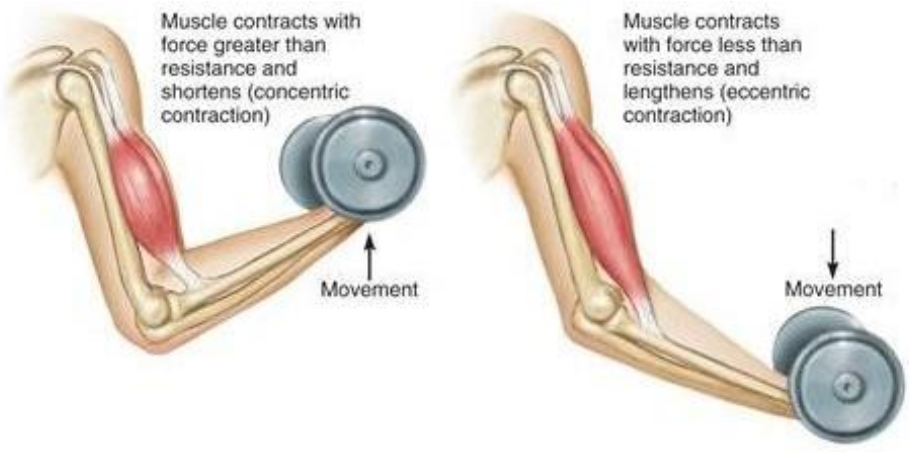

Figure 51 - Concentric (left) and eccentric (right) contraction [14]

A description of segment and joint motion through the instep kick as described in previous studies was presented in Chapter 2. This description is now expanded to include the muscle activation patterns. In brief, at the start of the backswing phase the plant foot (non-kicking foot) traveled towards the ground and the kicking leg began to elevate and

while the pelvis rotated posteriorly, assisted in part by erector spinae (and biceps femoris long head activity in one participant; Figure 52). Activity of the rectus abdominus peaked during the backswing. The ankle plantar flexed, controlled in part by activity of the medial gastrocnemius (Figure 54). During swing, forward motion was initiated by forwardly rotating the pelvis around the plant leg and by advancing the kicking leg's thigh forward while the knee continued to flex [46]. Rectus femoris, vastus medialis and vastus lateralis acted to restrain the rate of knee flexion while approaching peak backswing (Figure 53). Rectus femoris activity also contributed to the initiation of hip flexion while gluteus medius activity was present inconsistently to abduct the thigh [30]. The ankle remained plantar flexed due in part to medial gastrocnemius activity (3 of 4 participants). During swing, rectus femoris activity contributed dynamically to knee extension in all participants, while three of four participants also received assistance from activity in the vastus lateralis and medialis. When impact occurs, the hip is flexed, abducted and externally rotated while the ankle is plantar flexed and adducted [30]. Rectus femoris activity continued to advance the thigh through ball impact and the pretibials and plantar flexors were co-active to create a rigid ankle and hindfoot (Figure 54). During follow-through, activity of the erector spinae, gluteus maximus, and biceps femoris long head decelerated hip flexion and stabilized the pelvis.

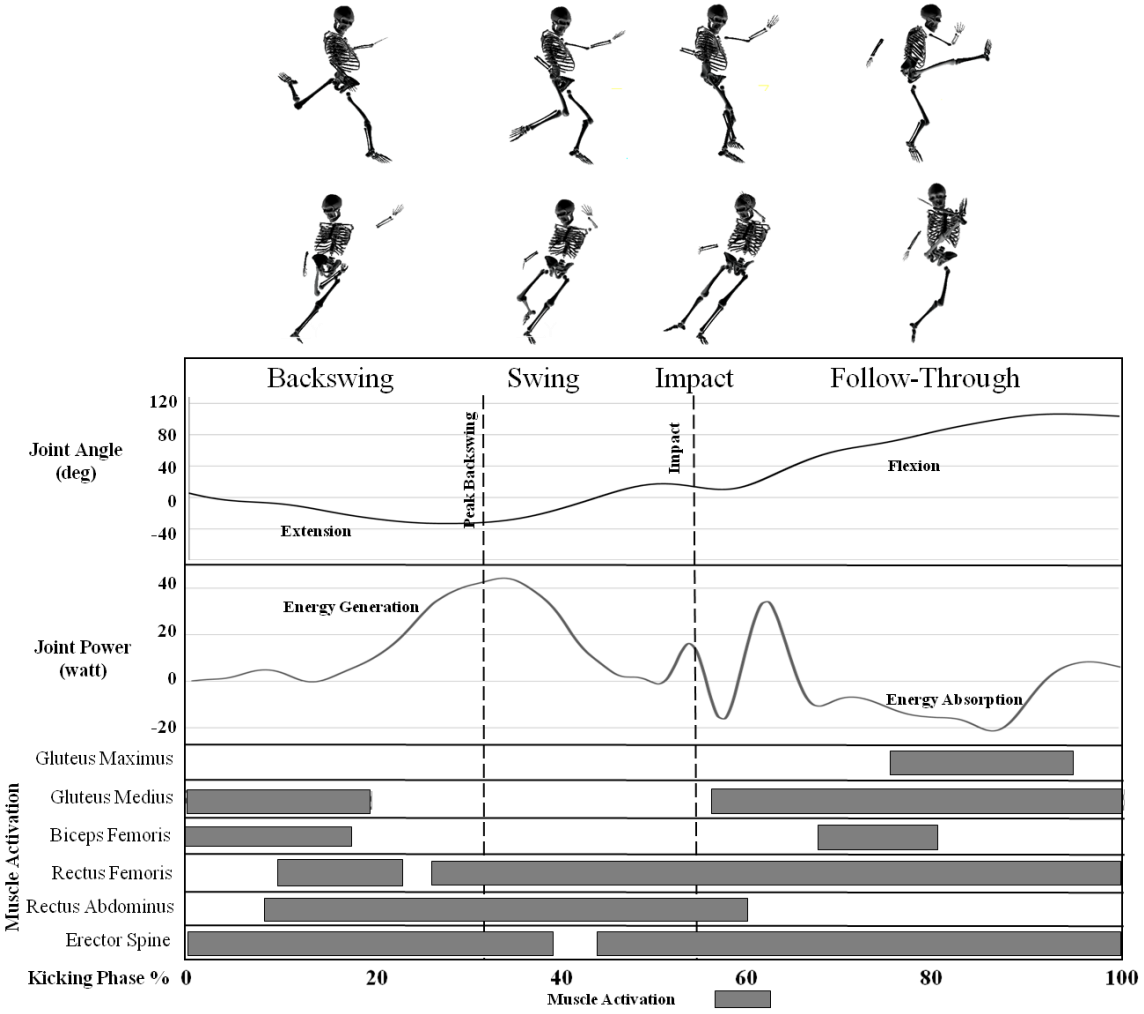

Figure 52 - F04 Hip - Joint motion, power and muscle activation

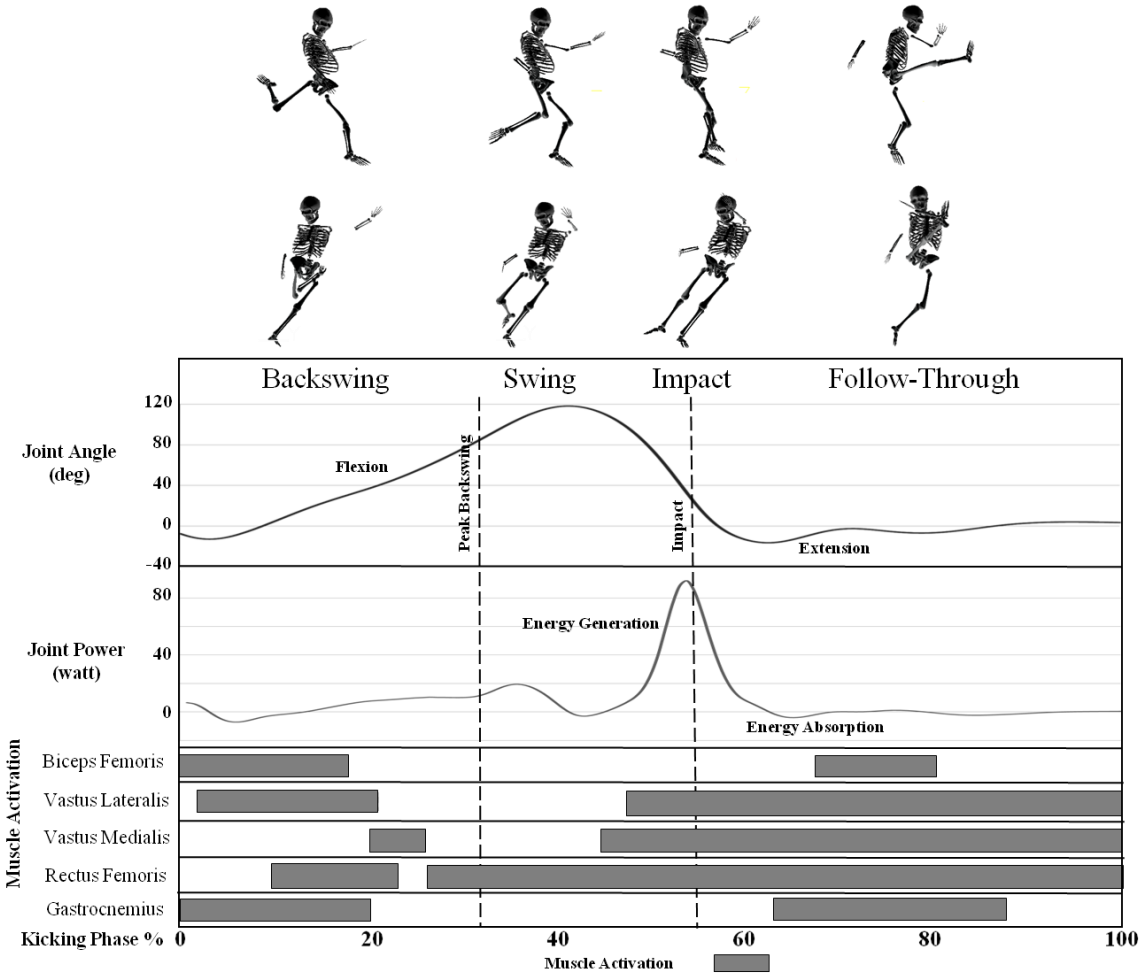

Figure 53 - F04 Knee - Joint motion, power and muscle activation

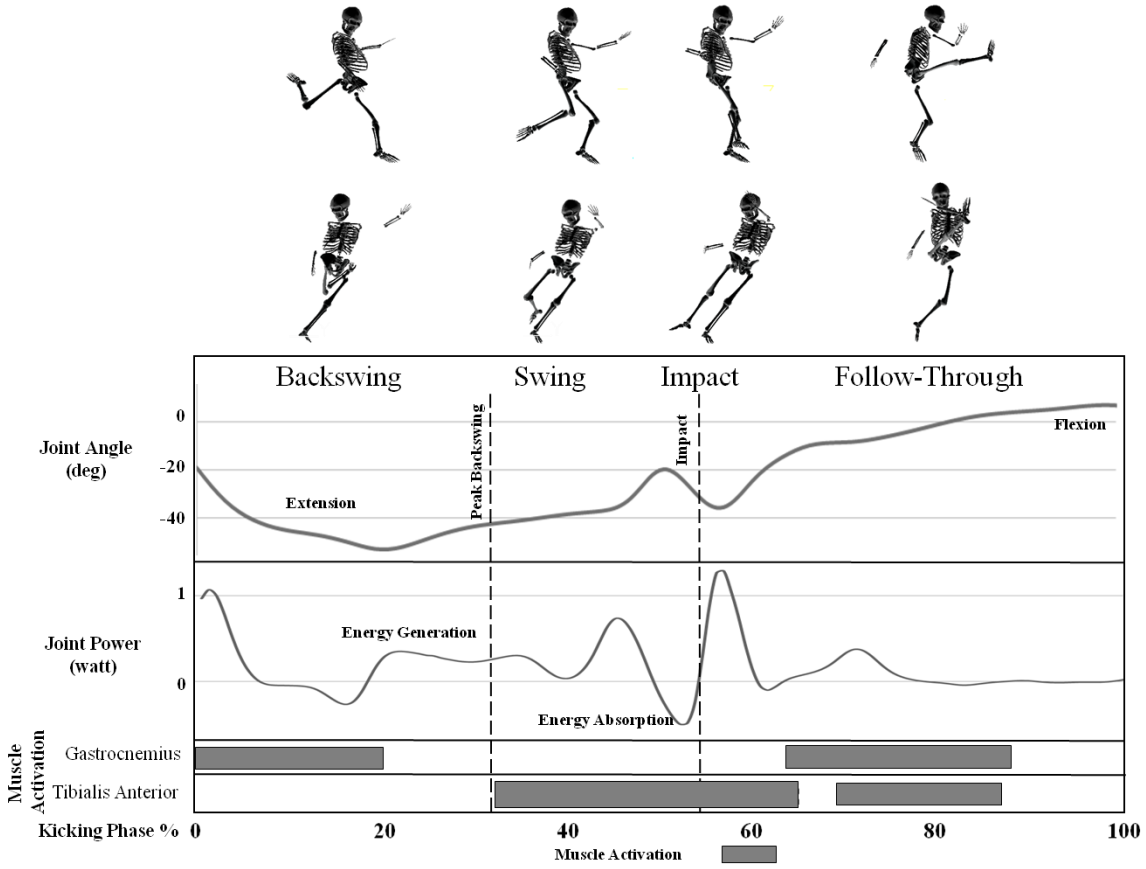

Figure 54 - F04 Ankle - Joint motion, power and muscle activation

Participant F04 displayed joint angle activity and muscle activation most similar to what was found in a number of studies examining the instep kicking technique with elite soccer players and therefore was shown as an example of joint angle, power and muscle activation in the previous figures. The average percent of muscle activation for each participant who performed PATs is present in Figure 55, Figure 56, and Figure 57. For the most part, F01 follows the presented model. There is however, activation of the gluteus maximus just prior to impact. This activation could only slow the kicking leg down and is likely a contributing factor to F01's foot speed being lower than that of F04.

Participant F03 shows a number of discrepancies from the model. First, the biceps femoris shows peak activation through the swing phase. Through this phase the hip is moving towards flexion and the knee towards extension. Activation by the biceps femoris works against these motions thus slowing down the kicking leg. Large activation potentials are present in the gluteus maximus after impact. This is expected as eccentric loading in gluteus maximus will slow down the kicking leg. However, this activation starts prior to impact and therefore also contributes to slowing the kicking leg before impact occurs.

As expected, F03 shows slight abdominal activation approaching peak backswing when the hip starts moving from being in extension to flexion. After peak backswing, there is very little abdominal activation until well into the follow-through phase of the kick. This means that there is very little being done through the participant's core to bring the hip into flexion through impact. This lack of abdominal activation is likely a contributor to F03 exhibiting very little power about the hip joint through impact.

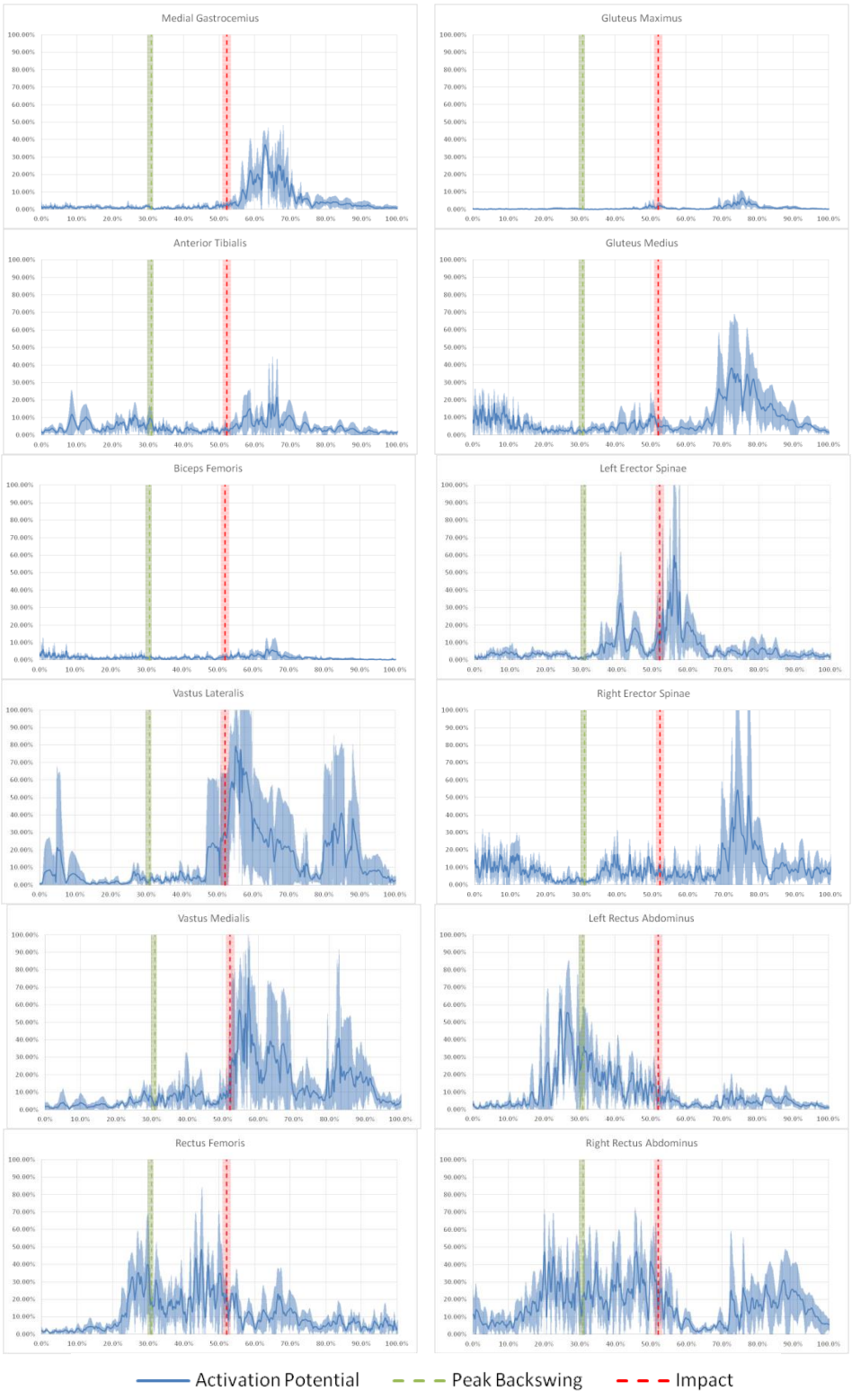

Figure 55 - F01 average PAT EMG activation

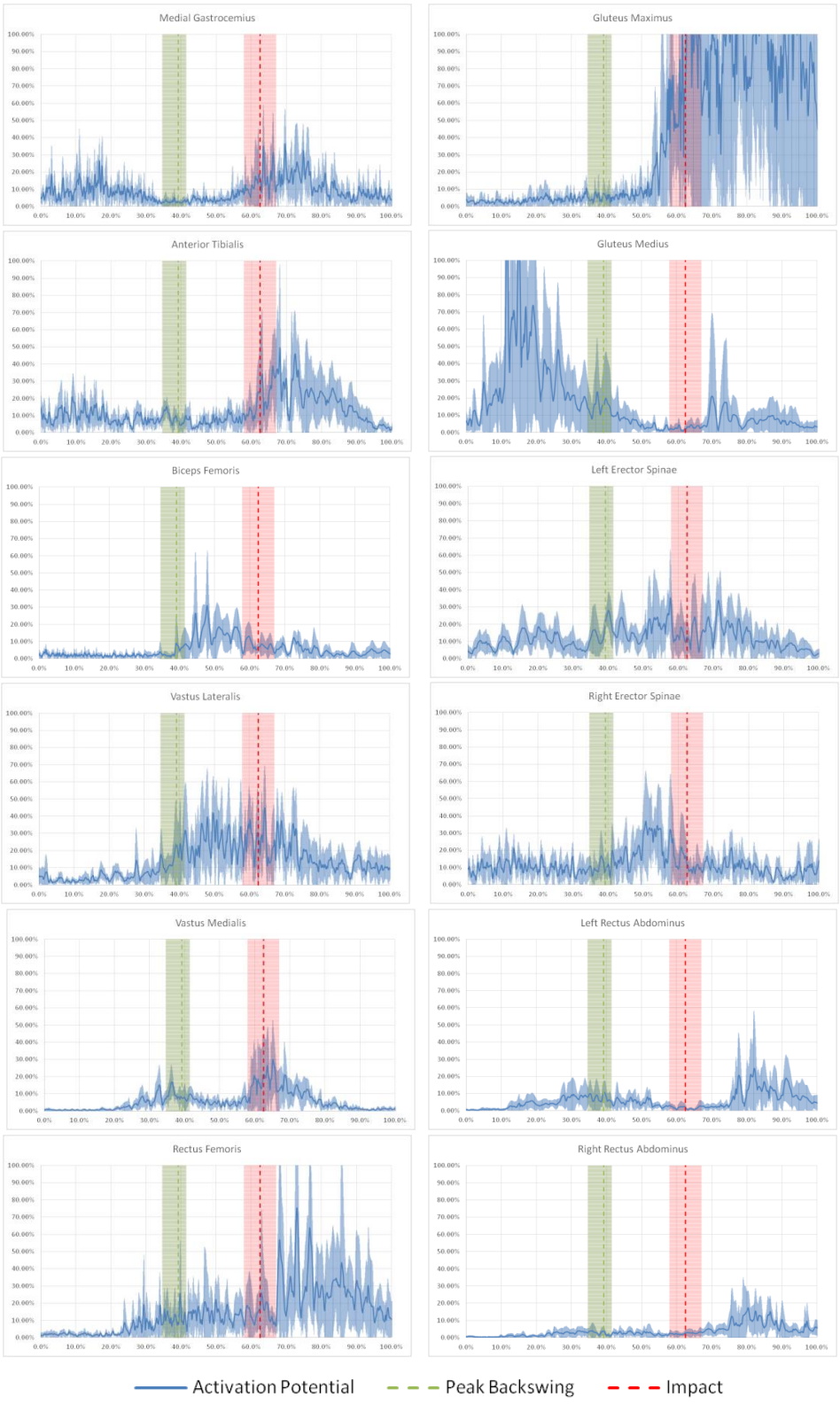

Figure 56 - F03 average PAT EMG activation

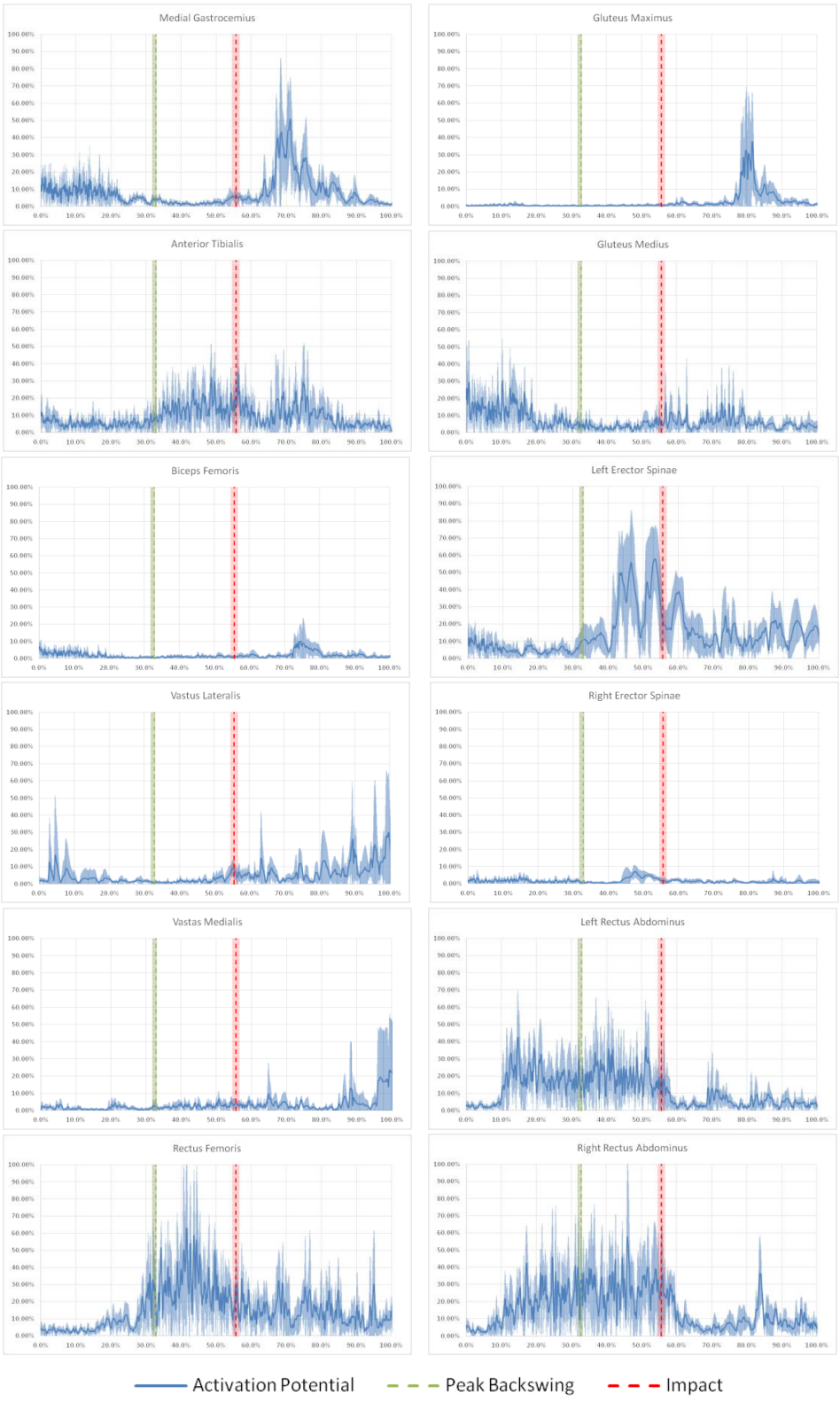

Figure 57 - F04 average PAT EMG activation

5.3 FG Results and Discussion

5.3.1 FG Trajectories

All four participants attempted between 5 and 10 50-yd field-goals. The resulting trajectories for these kicks are presented in Figure 58, Figure 59, Figure 60 and Figure 61. Participant F01 made 4 out of 6 50-yd field-goal attempts. His two misses were accurate enough to go through the goal posts but FG 1 and FG 5 did not have the distance to make it above the crossbar. The tabulated trajectory information for this series of kicks (Table 7) shows that F01 had an average launch pitch angle of 31.3° at an average speed of 31.0 m/s. As previously mentioned, a larger launch pitch angle propels the ball upward more rapidly, thus helping to avoid opposing players who may want to block the kick. However, there is a tradeoff between this launch angle and the horizontal distance the ball can travel. When the launch pitch angle is larger, a greater amount of the ball velocity is in the vertical direction, thus taking away from the horizontal speed of the ball.

F01's launch pitch angle was higher than his average 31.3° during FG 1 (32.5°) and FG 5 (32.4°). Along with this higher launch angle, the ball speed for these kicks was lower than the average at 28.6 m/s and 29.6 m/s respectively. Therefore it is understandable that these kicks did not travel as far, in the horizontal direction, as the other kicks.

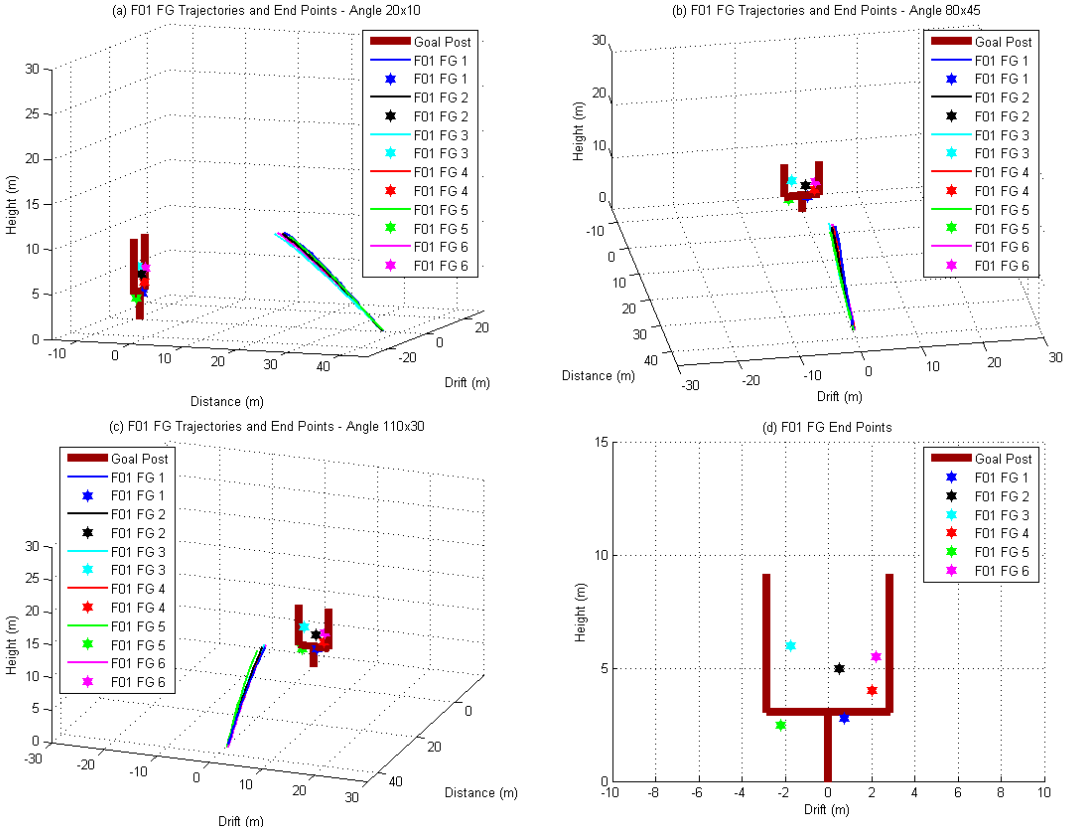

Figure 58 - F01 FG Trajectories (a-c) Depict trajectories and end points, (d) Depicts the end points

Table 7 - F01 FG - Ball Launch Mechanics

Kick	1	2	3	4	5	6	Average	STDV
Pitch (deg)	32.5	31.6	29.6	31.0	32.4	30.5	**31.3**	**1.1**
Roll (deg)	-0.9	-1.6	-4.8	-2.6	-4.8	-2.0	**-2.8**	**1.7**
Resultant Magnitude of Velocity (m/s)	28.6	29.5	30.1	31.6	29.6	29.7	**29.9**	**1.0**

Participant F02's field-goal kicks resulted in much different trajectories than those of the other participants (Figure 59). This participant's field-goal trajectories showed many similarities to that of a punt. Punts are not examined in this study, but a punter is trained to 'glance' the ball off the side of his foot. This action typically causes the ball to shank to the right (if you are a right footed kicker) before establishing a spiral and cutting

back to the left in the air. A similar flight pattern was observed with F02's field-goal attempts. For example, an average launch roll angle of 26.6° was found. The other three participants showed a roll between -3° and 3°. In the displayed trajectories, it is evident that the ball travels approximately 25 m with positive drift before straightening out.

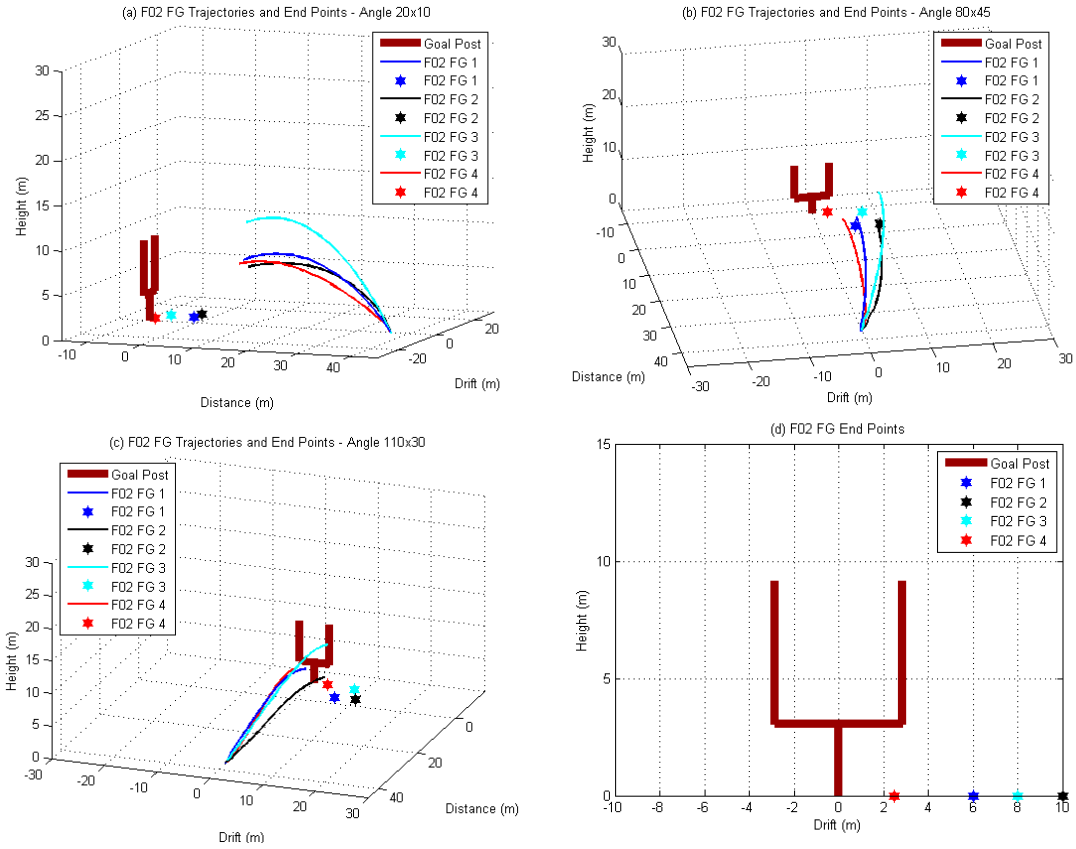

Figure 59 - F02 FG Trajectories (a-c) Depict trajectories and end points, (d) Depicts the end points

Table 8 - F02 FG - Ball Launch Mechanics

Kick	15	16	17	18	Average	STDV
Pitch (deg)	33.8	34.9	40.5	26.6	**34.0**	**5.7**
Roll (deg)	16.7	38.5	31.0	20.2	**26.6**	**10.0**
Resultant Magnitude of Velocity (m/s)	24.6	22.9	25.0	22.8	**23.8**	**1.1**

Participant F03 demonstrated a very similar launch pitch angle to that of F01 at 31.6° and made one out of four 50-yd field-goals. The lone made field-goal was barely long enough to make it through the goal-post. FG 4 was notably different from the first three with a pitch 5.2° less than his average, a roll of 6.7° less than his average, and a resultant magnitude of velocity less than that of the average. Though the ball velocity was lower than the other kicks, FG 4 crossed the plane of the field-goal noticeably higher than the other field-goal attempts. Meaning that it traveled the farthest in the horizontal (distance on the plots) direction. FG 2 and FG 4 have nearly identical ball speeds, which further demonstrates the impact of launch pitch angle on kick distance.

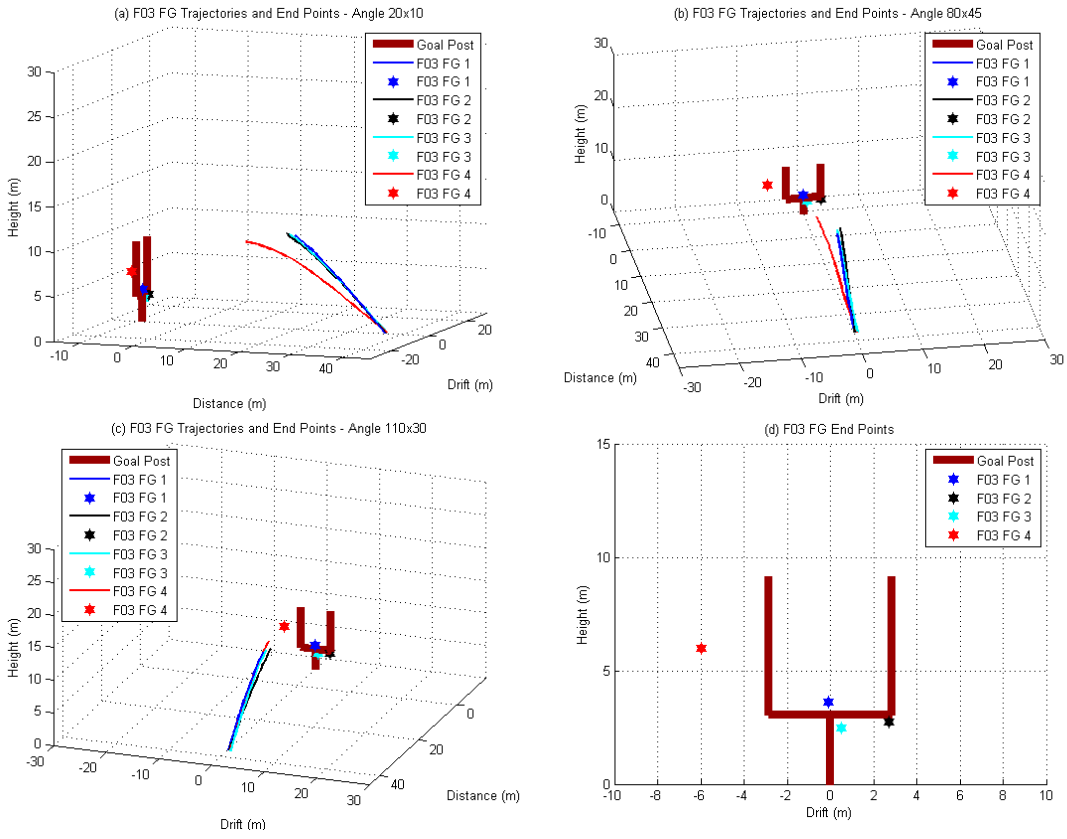

Figure 60 - F03 FG Trajectories (a-c) Depict trajectories and end points, (d) Depicts the end points

Table 9 - F03 FG - Ball Launch Mechanics

Kick	1	2	3	4	Average	STDV
Pitch (deg)	34.4	32.6	32.8	26.4	**31.6**	**3.6**
Roll (deg)	-0.4	3.0	-1.4	-8.5	**-1.8**	**4.8**
Resultant Magnitude of Velocity (m/s)	24.7	23.0	25.2	22.9	**23.9**	**1.2**

Participant F04 showed both an average lower launch pitch angle and a larger ball speed after impact. It was clear that this combination allowed for F04 to kick the ball noticeably farther than the other participants. F04 missed one out of five field-goal attempts, passing to the right of the goal post. Similar to F03's FG 4, this miss crossed the plane of the goal-post higher than any of his other kicks. There is little difference in the launch pitch angle from FG 8 and the average, but the roll was greater than one standard deviation from the average, which likely contributed to the inaccuracy of the kick. Additionally, FG 8's ball speed (32.2 m/s) was 1 m/s faster than any of F04's other FG attempts which may in part be due to a smaller component of velocity going to the y-direction (due to roll). This is likely why this kick went further than the others in the horizontal direction.

The two groupings of kicks to the left side of the field-goal (FG 6 & FG 10) and to the right side of the field-goal (FG 7 & FG 9) had similar launch roll angles with around 0 degrees and 4.5 degrees respectively. These kicks occurred separately from each other as if the participant is trying to compensate for being left or right of the field-goal centerline.

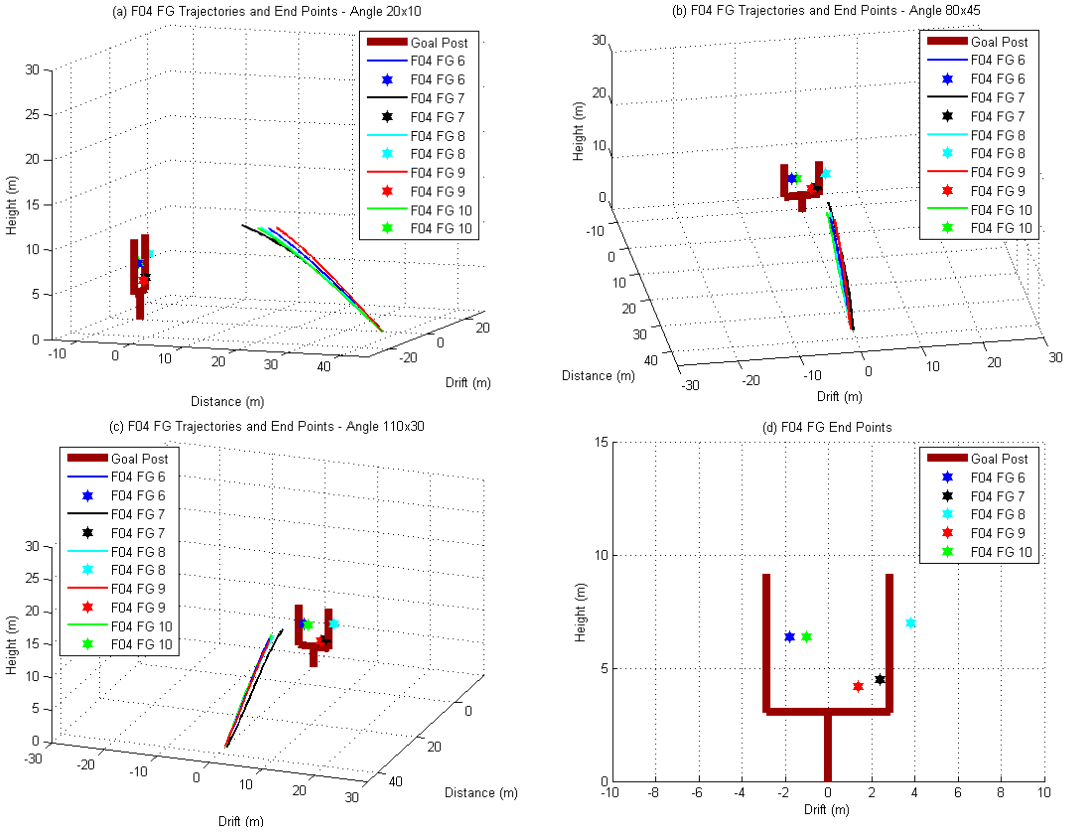

Figure 61 - F04 FG Trajectories (a-c) Depict trajectories and end points, (d) Depicts the end points

Table 10 - F04 FG - Ball Launch Mechanics

Kick	6	7	8	9	10	Average	STDV
Pitch (deg)	29.0	27.0	28.0	31.0	27.6	28.8	1.7
Roll (deg)	1.8	5.0	-0.5	4.3	-0.9	2.6	2.5
Resultant Magnitude of Velocity (m/s)	30.2	29.7	32.2	31.1	31.5	31.0	1.1

5.3.2 FG Kinematic Tracking Data

As previously mentioned, the kinematic tracking data was processed to give segment speeds, joint angles, and joint power for the kicking leg. Other useful information from the field-goal attempts such as impact location and velocity, as well as relevant plant leg information, will be addressed as well.

Body Segment Velocity

Similar to what was previously presented for PATs, the average magnitude of resultant velocity for the pelvis, thigh, shank, and foot are plotted through the defined kicking phase for the field-goals (FG) in Figure 62.

Participants F01and F04 displayed deviation from their average greater than what was observed for PATs. The timing of peak backswing became more variable when attempting 50-yard field goals compared to PATs. Participants F01 and F03 also displayed much greater variability in when impact happened in the phase. The greater variability was not surprising given that a 50-yd field goal is a maximum effort kick whereas a PAT is more of a minimum effort kick. Slightly faster average foot speeds were observed during the 50-yd field goal kick when compared to PATs, suggesting a trade-off between control and speed when performing a place kick.

The larger kinematic variability also drove the average peak foot speed down since the timing of the peak speeds did not align temporally. Participant F03's time of impact with the ball ranged from 59.5% to 69.3% of the kicking cycle.

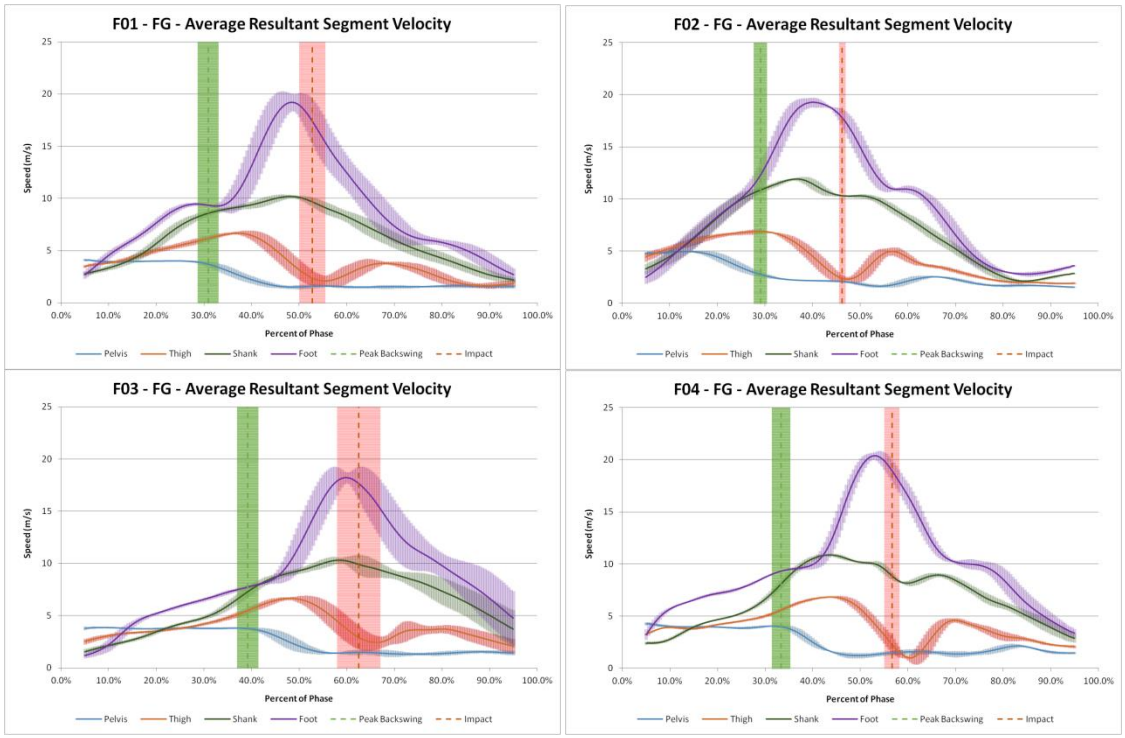

Figure 62 - FG Average magnitude of resultant segment velocity

The increased deviation in kinematics along with impact conditions resulted in a larger deviation in football end points with respect to the goal-post (Figure 63). F03 had the least consistent and accurate end points since he exhibited the most deviation outside of the goal-post. F01 showed accurate kicks with respect to the center of the goal-post but had more deviation outside of the goal-post than F04. This evaluation is in agreement with the observed kicks since F03, F01, and F04 made 25%, 67%, and 80% of their 50-yd field-goals, respectively.

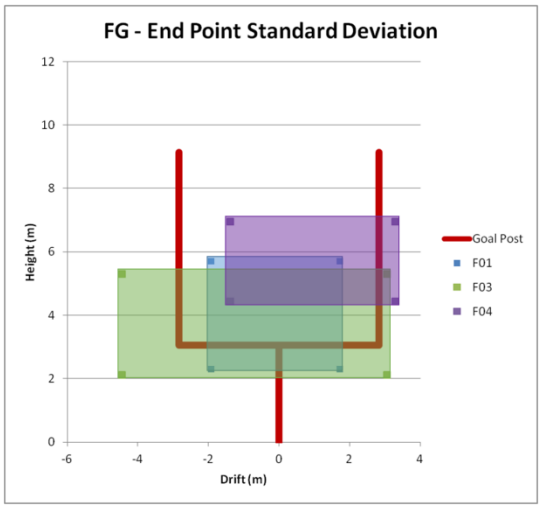

Figure 63 - FG deviation from final End Point

In all four participants the speed of the hip dropped near peak backswing as the non-kicking foot planted and the kicking leg circumducted around the planted foot. Soon after, the speed of the thigh dropped when approaching impact as the shank rapidly extended ("whipped") around the knee. As the knee extended, the foot rotated about the shank's center of mass and accelerated to a maximum speed while approaching impact.

Though the speed profiles for participant F02's pelvis and thigh resemble those of the other participants, a distinct difference in shank and foot speed was observed. F02's foot continuously accelerated up to maximum speed and the shank followed an almost identical profile up to peak backswing. The other participants generally maintained a foot speed larger than that of the shank and there was a clear decrease in the foot speed profile at or around peak backswing.

Kicking Leg Joint Angles

Similar to what was previously presented for PATs, the average joint angles of the kicking leg through the phase were examined and plotted through the defined kicking

phase for the field-goals (FG) in Figure 64. As expected from observing the segment speed plots, there were very few differences in joint flexion between PATs and field-goals (for the participants who performed both) except for the variability in the timing of peak backswing and impact. F04 does show more deviation in hip angle throughout the entirety of the phase as opposed to just the bask swing phase with the PATs and F01 achieves a maximum hip flexion around 60° where 80° of flexion was observed in the PATs. This lower amount of hip flexion suggests that F01 alters his follow-through for longer field-goals by coming to a peak follow-through position lower than that of the shorter PAT.

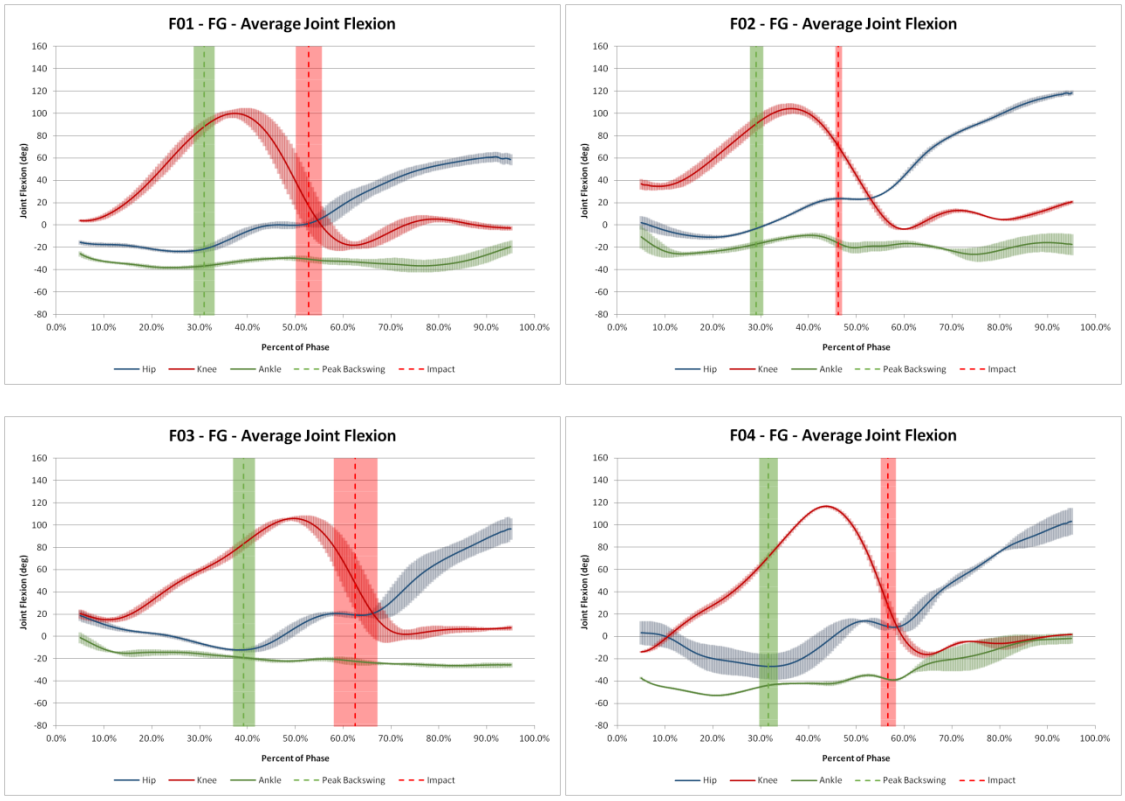

Figure 64 - FG average joint flexion

An interesting observation is that F02 displayed little variability across kicks at each point in the movement cycle, despite not regularly kicking field-goals. Impact also occurred when the knee was still flexed approximately 70°, similar to his impact position during punting. Impact for the other participants occurred a few percent of movement cycle before the hip and knee flexion curves crossed, earlier than their PATs. This did not greatly affect F01's knee flexion at impact but increased F03 and F04's knee flexion by roughly 25° and 7° respectively.

Joint Power

The joint power for the field-goal attempts was also calculated. Several differences between the PATs were observed. Participant F01 demonstrated an average joint power in the backswing phase and into the swing phase that was very similar to what was observed in the PATs. The main difference was the deviation in knee joint power from the average. Little deviation was present in the PATs in contrast to the approximately 10 W of deviation observed in the field-goal attempts. Also (on average), impact occurred while the hip was showing more absorption.

Participant F02 produced joint power curves which reached impact with a neutral hip and a knee joint power around 45 W. Participants F01 and F03 impacted the ball with a knee joint power closer to 35 W and 40 W respectively. F04 reaches a maximum average knee joint power nearing 80 W and impacted the ball with a knee joint power of 76 W and a hip joint power of 12 W. This combination of hip and knee joint power resulted in an average total of 88 W of energy generation at impact, nearly twice the max of the participant with the next highest joint power.

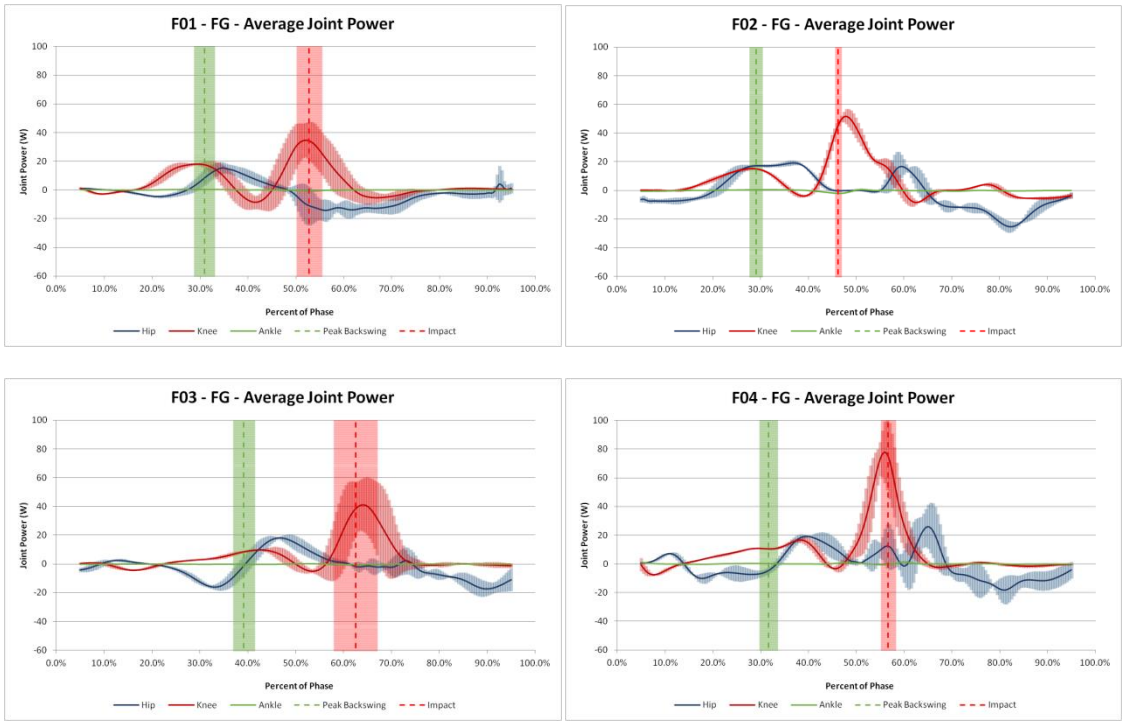

Figure 65 - FG average joint power

These data have shown that F04's body movement in approaching impact for a field-goal produced larger peak foot speeds and joint powers. F02 showed the second highest values in both foot speed and joint power at impact but this production was not translated to ball launch mechanics as F02 produced the lowest ball launch speed at 23.8 m/s. This suggests that other conditions at impact effected the transfer of energy to the football.

5.3.3 Foot-Ball Impact Condition

Though the foot is modeled as a rigid segment, in reality it is far from rigid. The foot is made up of 26 bones (Figure 66) and 33 joints. The model created through V3D estimates the foot's center of mass using an assumption that the foot remains rigid. However, in reality, the malleable nature of the foot means there is undoubtedly movement across the 33 joints during the kick. However, the majority of the foot's mass

is closer to the ankle, thus flexing distal joints such as the toes would do little to alter the center of mass location.

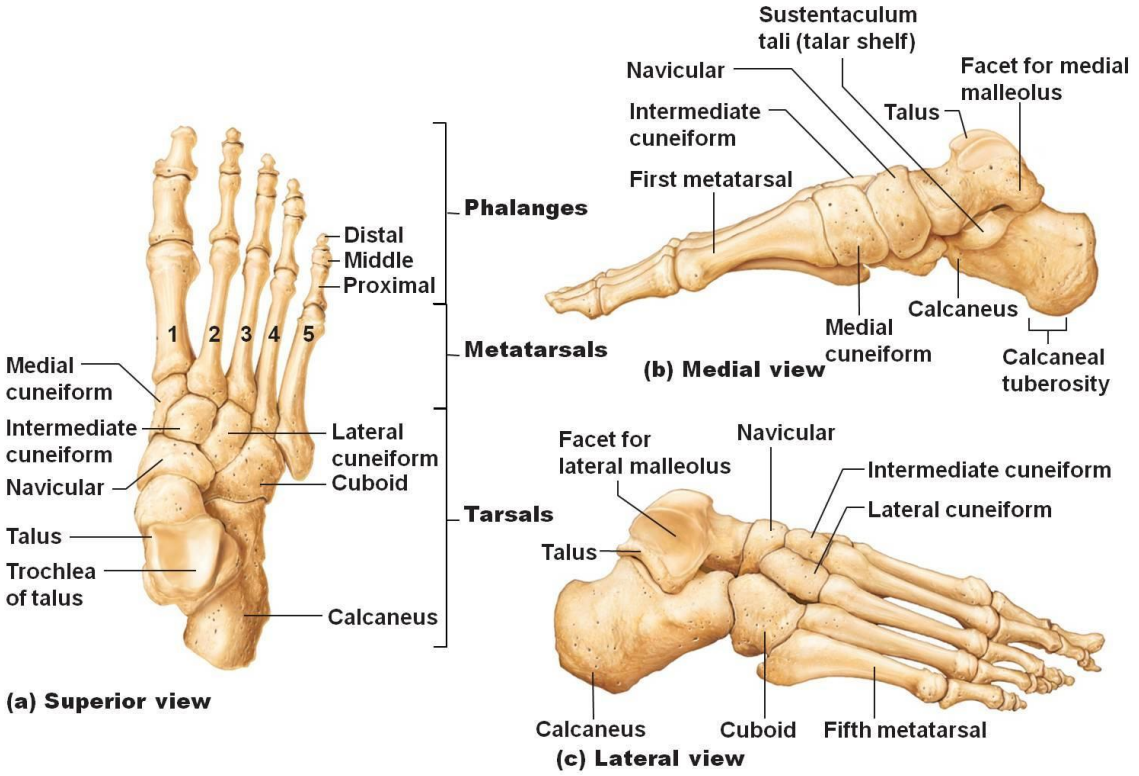

Figure 66 - Skeletal anatomy of the foot (adopted from [7])

At impact the weight of the kicker transfers across the plant foot from the heel to the toes and in this motion the heel of the plant foot is softly lifted. This causes the marker cluster on the heel of the plant foot (this cluster along with the static model outlined in 6.1.2 define the left foot) to be rotated slightly downward. When modeling the foot as a rigid segment this bending of the toes is not observed and the plant foot appears to go underground as evident with the left foot in Figure 67 (left). During the swing phase, the kicker's tight leather soccer cleats would be expected to bind the athlete's foot

very tightly, contributing to mid and forefoot rigidity. Functionally, the mid and forefoot appear more dense when contacting the ball, thus helping reduce the risk of injury.

When observing the interaction between the kicking foot and the ball several estimations needed to be performed resulting in a rectangular shaped "impact zone" where the rigidly modeled foot contacted the ball (similar to Figure 67, left). This rectangular shape is the rough area in which the foot is in contact with the ball.

Initially, an attempt was made to implant an accelerometer in the center of the ball to determine the precise location of initial impact and direction of force. Implantation of a Bluetooth accelerometer was attempted but the device possessed a reading frequency of only 10 Hz, far below a more ideal sampling rate around 100 Hz. This limitation resulted in inconsistent results and significantly slowed the data collection process. Due to these setbacks the position of the foot's center of mass in combination with its velocity was utilized to evaluate the participant’s interaction with the football. This information is presented in the following figures and tables.

Both the *j*-tilt and *k*-tilt of the football were measured and recorded for each kick. The *j*-tilt (forward-negative or backward-positive tilt) of the ball varied greatly amongst the participants, an average of -4.3º for F01, 6.7º for F03, and 0.1º for F04. This pitch angle in the *y-z frame* of reference alters the vertical height of the ball. The *k*-tilt, or tilt left/right, was much more consistent between participants. An average between 6-7° to the right was found for the participants. The average *j*-tilt and *k*-tilt of the ball before impact for each participant are implemented into the following figures.

Participant F01 displayed notable consistency in both impact location and foot velocity greater even then that of F04 who showed the most consistency in kinematics. This consistency at impact demonstrates that consistency in body kinematics does not necessarily correlate to consistency in ball impact. Figure 67(left) depicts an example of F01's foot contact with the ball (with the foot modeled as a rigid segment). Interestingly, F01 missed FG 1 and FG 5 despite the velocity of the foot at impact being very similar across all the kicks. The only noticeable difference from this specific data set was that the foot's center of mass for FG 1 and FG 5 was further to the left of the other kicks. When looking at the ball trajectory data, FG 1 and FG 5 displayed launch pitch angles larger than the other kicks and a ball speed less than the average. This finding highlights that the location of impact on the ball is highly instrumental on the ball launch mechanics and the overall distance and accuracy of the kick.

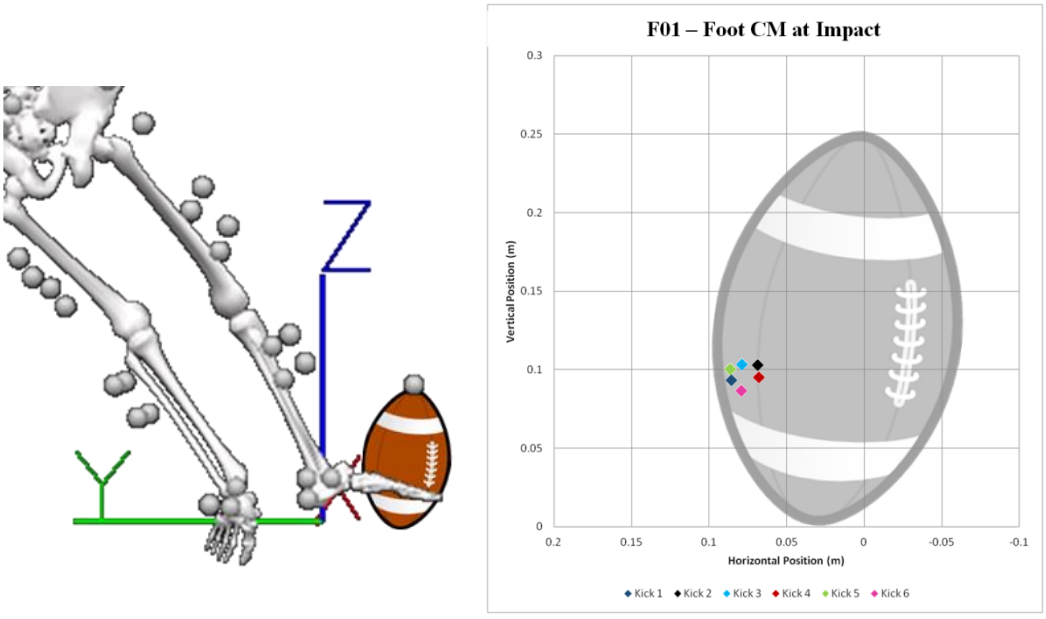

Figure 67 - F01 FG - Kicking foot center of mass at impact

Table 11 - F01 - Kicking Foot CM Velocity at Impact

FG	1	2	3	4	5	6	Average	STDV
x-velocity (m/s)	17.3	17.1	17.5	17.5	17.2	17.5	17.3	0.2
y-velocity (m/s)	-2.5	-1.3	-1.6	-2.4	-1.0	-3.5	-2.1	0.9
z-velocity (m/s)	2.9	2.9	3.5	3.3	4.1	2.6	3.2	0.5

Participant F02 showed a kicking foot center or mass on the far left side of the ball, outside of the ball in the *z-y plane* for all kicks besides FG 18. F02 also showed a foot velocity with a y-component averaging 4.6 m/s off to the right. Therefore it is not unexpected that the ball traveled to the right of the goal-posts for all four kicks. It can also be seen in Figure 68 (left) that there was noticeable knee flexion at impact which correlated with the findings in Figure 64.

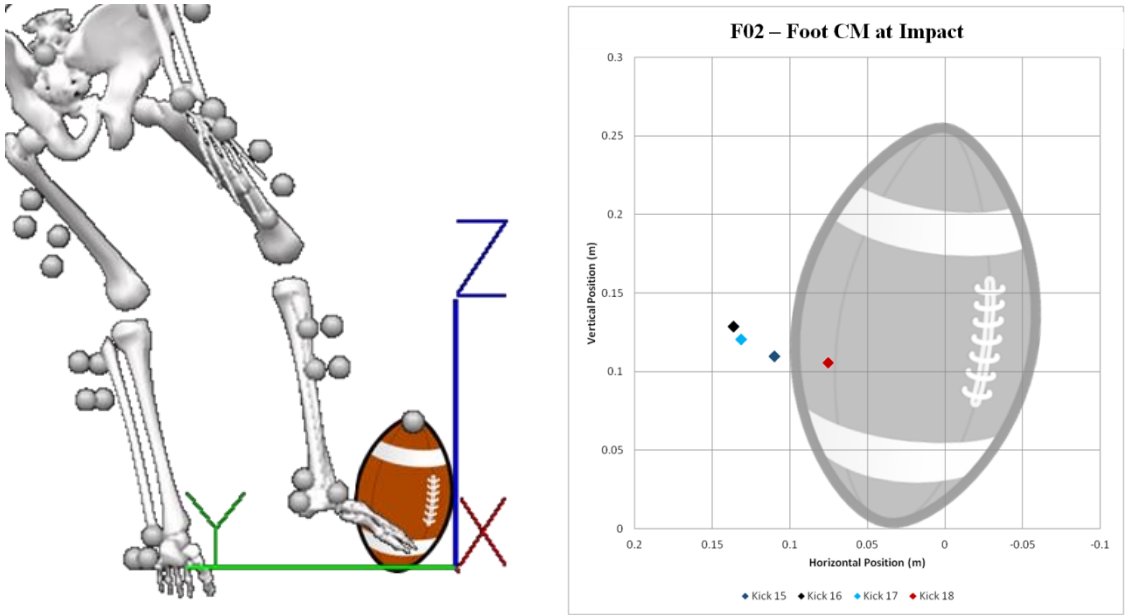

Figure 68 - F02 FG - Kicking foot center of mass at impact

Table 12- F02 FG - Kicking Foot CM Velocity at Impact

FG	15	16	17	18	Average	STDV
x-velocity (m/s)	18.6	19.2	18.3	18.2	18.6	0.5
y-velocity (m/s)	-3.9	-4.6	-5.2	-4.9	-4.6	0.5
z-velocity (m/s)	2.5	2.5	2.2	1.3	2.1	0.6

Participant F03 shows a kicking foot center of mass at impact similar to that of F01 and impacts the ball with in a consistent center of mass location (Figure 69). F03 showed the most deviation from the average throughout the kinematic analysis yet very little deviation with center of mass location data set. F03 made FG 1 but missed the others (refer to the trajectories section). The foot's center of mass in FG 1 was not very different from the other three kicks. What is most noticeable is that FG 1 had the highest *z-component* of velocity when compared to the other kicks. This likely contributed to the direction of impact through the ball and how the foot's velocity translated to the ball.

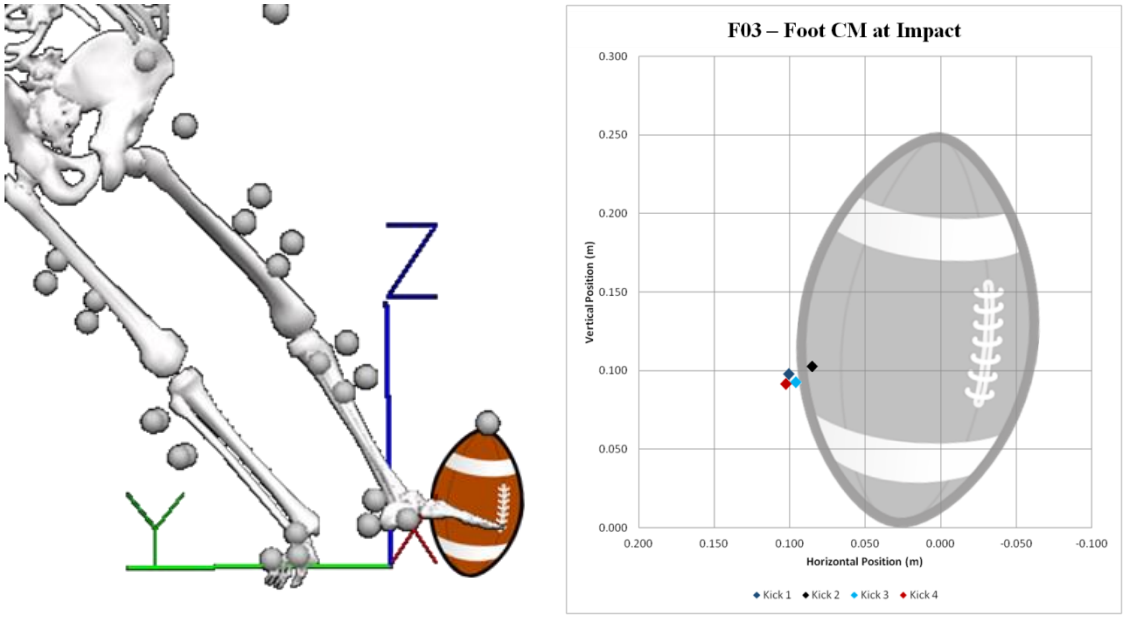

Figure 69 - F03 FG - Kicking foot center of mass at impact

Table 13 - F03 FG - Kicking Foot CM Velocity at Impact

FG	1	2	3	4	Average	STDV
x-velocity (m/s)	15.9	16.7	17.6	18.2	17.1	1.0
y-velocity (m/s)	0.6	-0.6	-2.3	-3.5	-1.4	1.8
z-velocity (m/s)	4.2	3.6	2.2	-0.1	2.5	1.9

Surprisingly, participant F04 had the most variance in foot center of mass at impact and the same amount of velocity variance as F03. The majority of the deviation in foot velocity and location is due to FG 8 which was the F04's single miss. Impact occurred with the foot's center of mass more than 5 cm away from the ball in the *y-z plane*. This arose because impact occurred earlier than average which resulted in the foot traveling down and away from the body at impact. These impact conditions will be examined further when individual kicks are investigated.

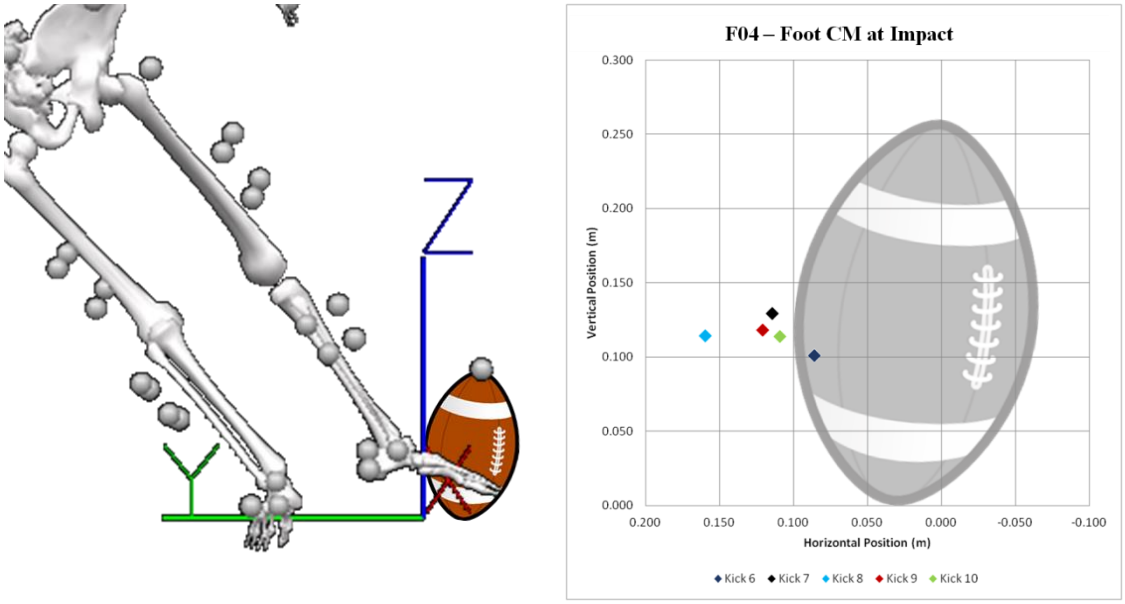

Figure 70 - F04 FG - Kicking foot center of mass at impact

Table 14 - F04 FG - Kicking Foot CM Velocity at Impact

FG	6	7	8	9	10	Average	STDV
x-velocity (m/s)	17.7	18.2	19.4	18.4	18.4	18.4	0.6
y-velocity (m/s)	-1.7	-1.4	-5.9	-2.0	-2.2	-2.6	1.9
z-velocity (m/s)	4.1	4.0	-1.1	3.8	2.9	2.7	2.2

A number of comparisons can be made from this data set. Figure 71 displays the relationship between foot impact speed and ball launch mechanics. Participant F03 showed similar ball launch speed with impact speeds varying by 2 m/s, while the other participants generally showed an increase in ball launch speed when impact speed increased. When looking only at the *x-component* of velocity a strong trend was present across all of the participants. As the horizontal component of their impact speed increased, generally their launch pitch angle decreased.

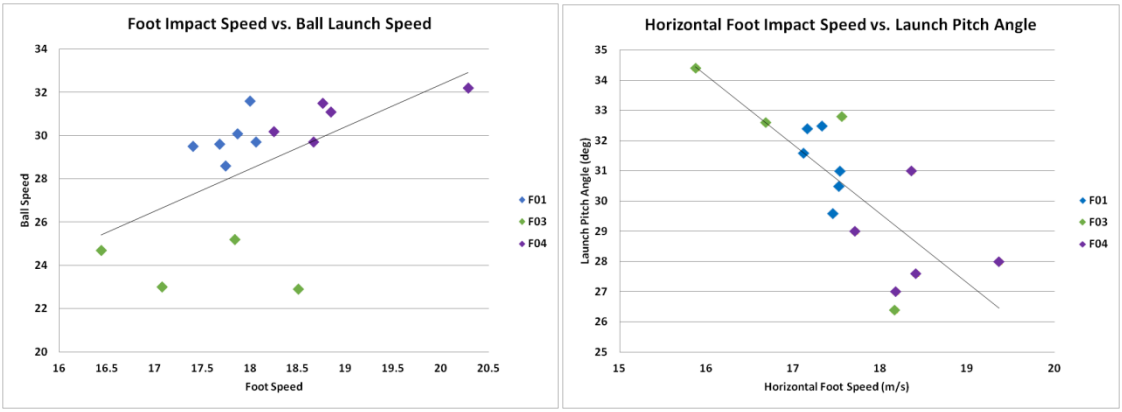

Figure 71 - Correlations between foot speed and mechanics of ball flight

5.3.4 Electromyography

Participant F01 exhibited nearly identical muscle activation patterns while performing field-goals when compared to his PATs. The main difference was that muscle activation levels during field-goal attempts were generally higher than those of the PATs.

Participant F02's EMG data showed activation patterns very similar to that of the model presented in the PAT EMG section despite impacting the ball earlier in the swing phase compared to the other participants (i.e., impact occurs when the knee is still in approximately 70 degrees of flexion. The gluteus maximus begins to activate at impact, acting to slow the kicking leg down as impact occurs.

F03 shows very similar field-goal activation patterns as those recorded in PATs. One noticeable difference is that F03 displayed a higher level of biceps femoris activity throughout all phases of the field-goal kick compared to the relatively brief period of biceps femoris activation during only the swing phase of the PAT. Less rectus femoris activation was observed during the field goal follow-though, but more vastus lateralis and vastus medials activation occurred.

Participant F04, like F01 showed nearly identical muscle activation patterns between the field goals and PATs. Given the greater demand of field-goal attempts, the magnitude of muscle activation was greater during compared to PATs. Gluteus maximus activation for F04 does not occur until late in the follow-through phase, thus not impeding hip flexion until after ball impact.

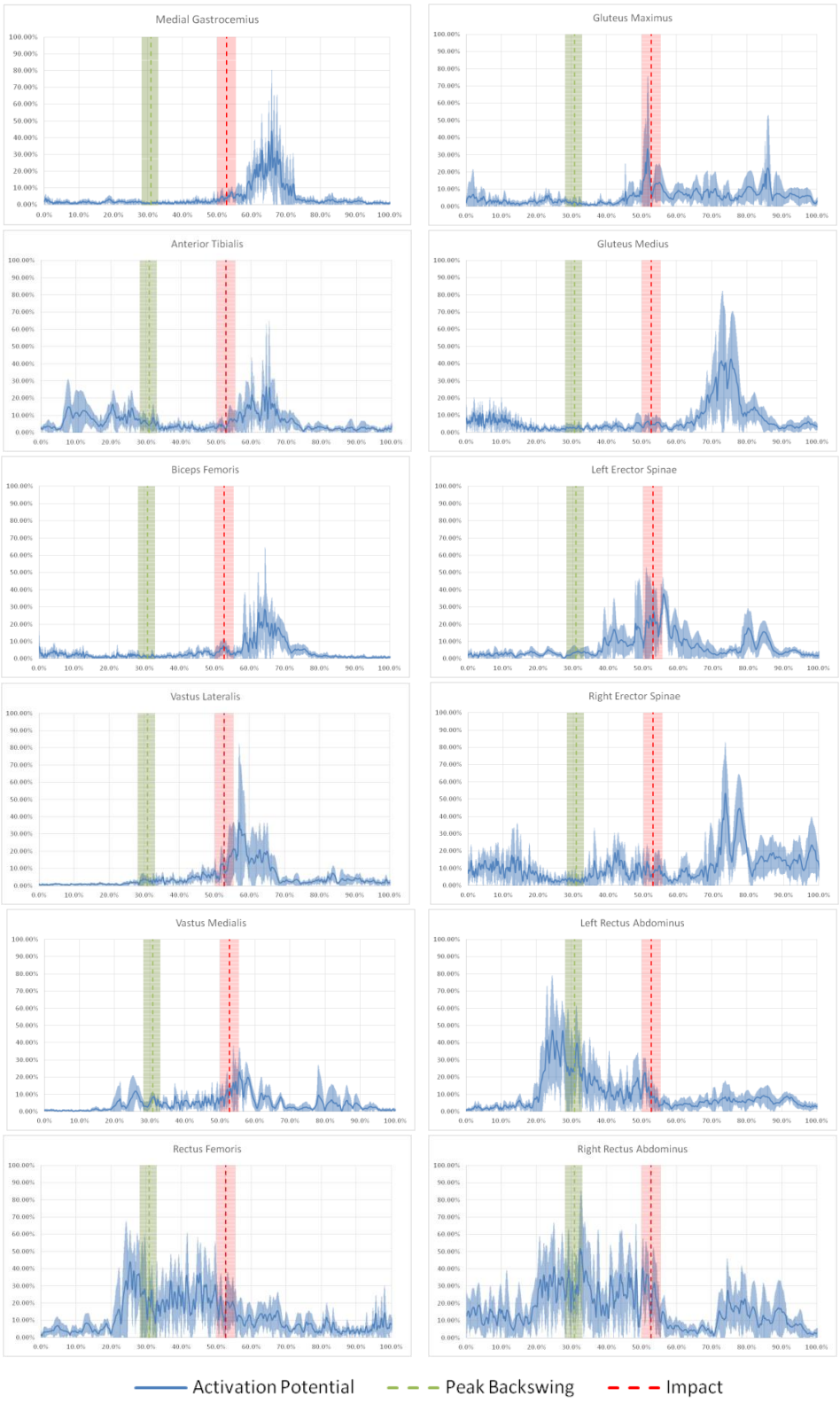

Figure 72 - F01 average FG EMG activation

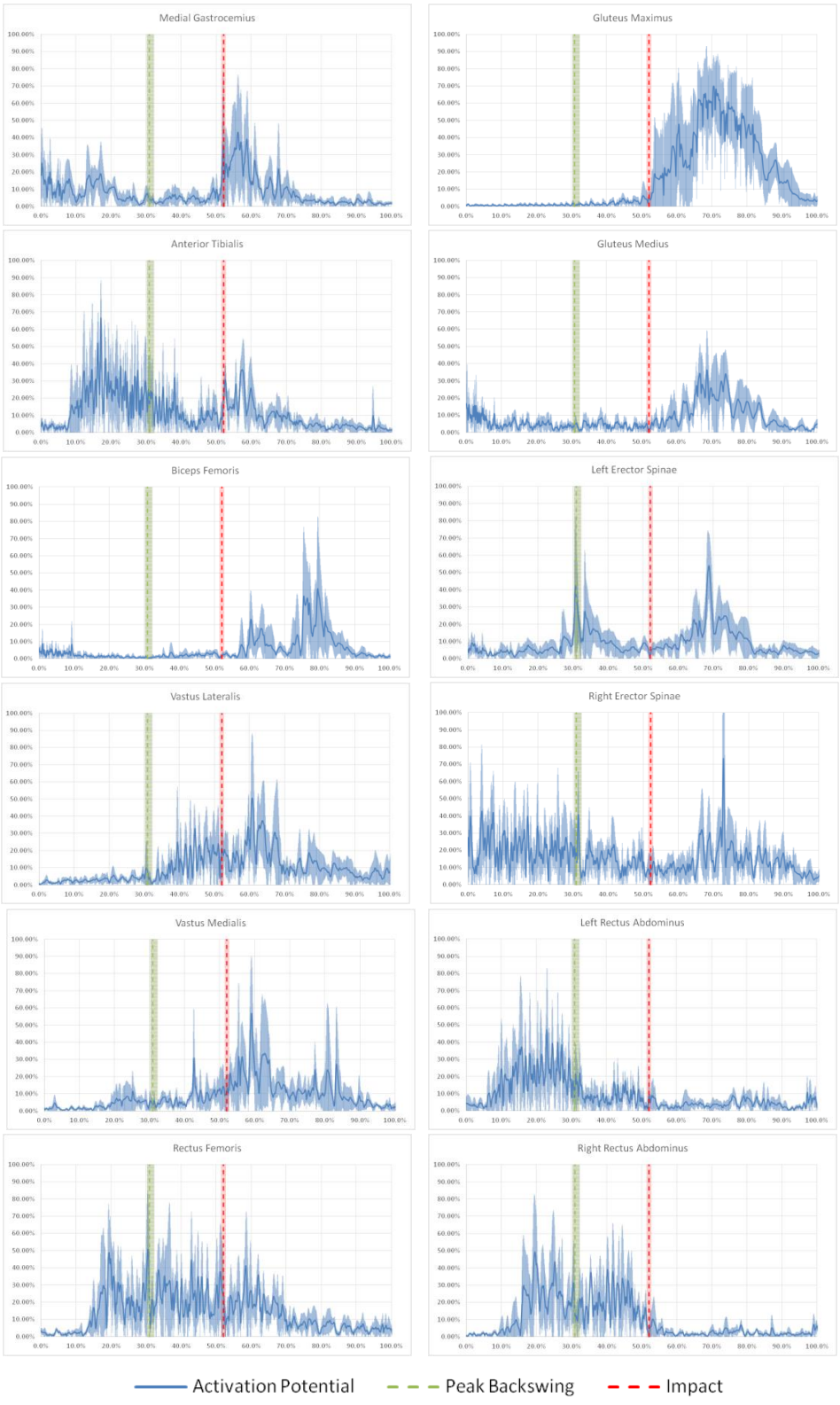

Figure 73 - F02 average FG EMG activation

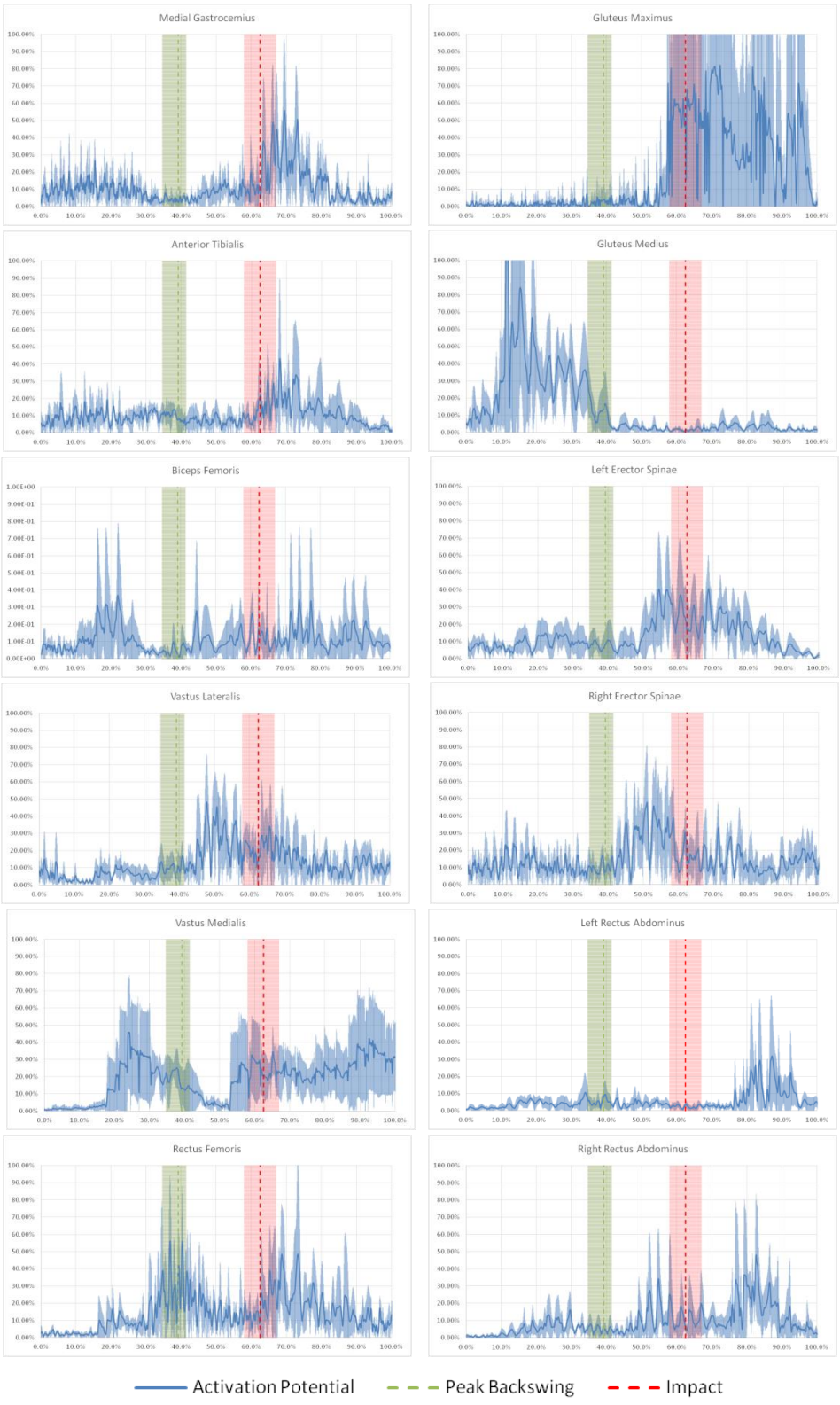

Figure 74 - F03 average FG EMG activation

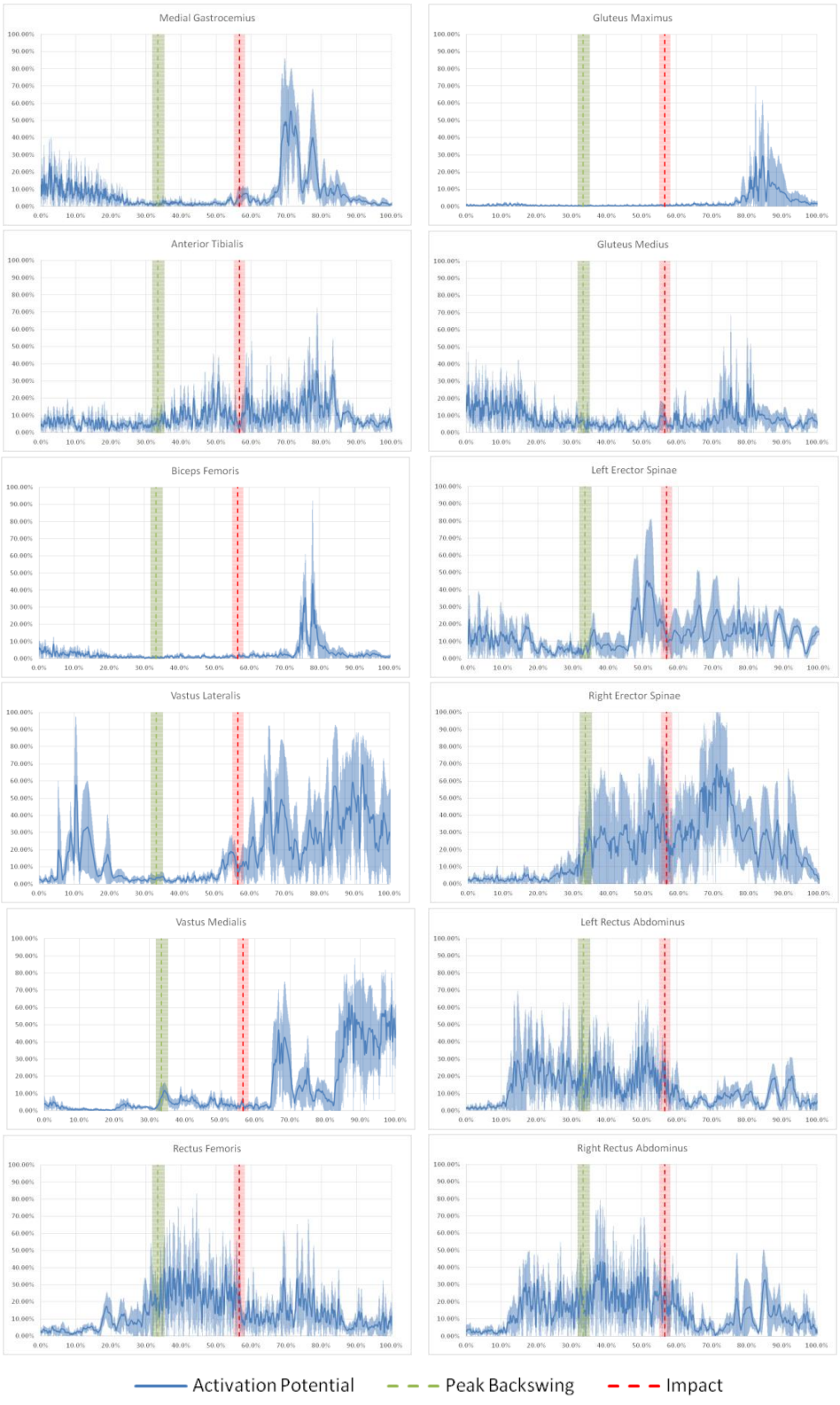

Figure 75 - F04 average FG EMG activation

5.4 Further Investigation of Individual Field-Goal Attempts

5.4.1 F01 – Investigated Field-Goals

Participant F01 made four out of six 50-yd field-goals. FG 3 is examined as F01's *best* kick because it crossed the plane of the goal-post between the uprights and higher than the other kicks. FG 5 is examined as F01's *worst* kick because it crossed the plane of the goal-post below the crossbar (short of the goal-post) and was the least accurate kick because it was the farthest from the centerline of the goal-post.

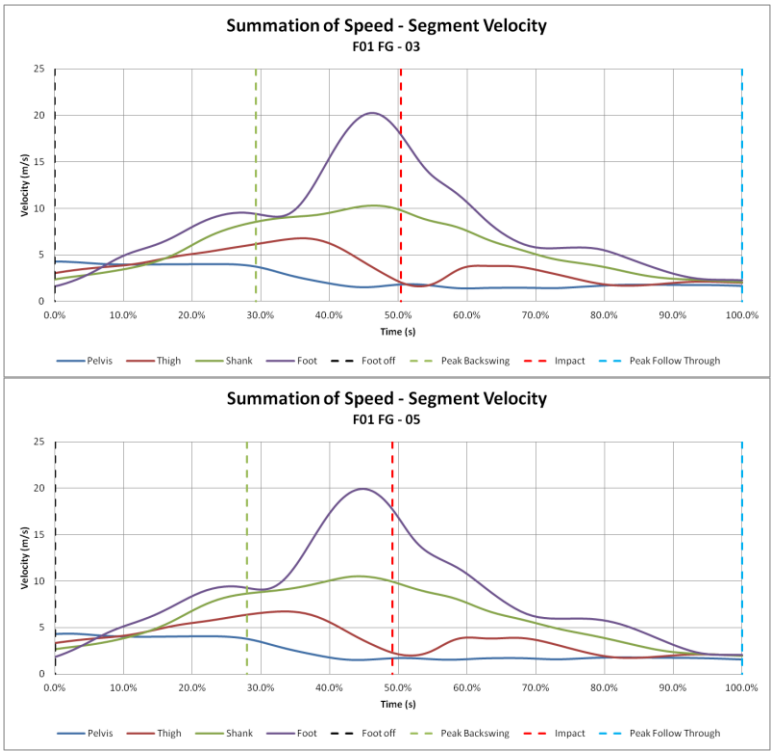

Figure 76 - F01 - Magnitude of resultant segment velocity *best* (top) and *worst* (bottom) kicks

All of F01's field-goal attempts were accurate enough for the ball to travel through the uprights if the ball was kicked far enough. F01's segment velocity for FG 3 and FG 5 (Figure 76) are nearly identical with exception of approximately 1% difference in phase for both the peak backswing and impact which is essentially negligible. FG 3

reaches a slightly higher maximum foot speed resulting in a difference of 0.2 m/s at impact. The *x*, *y*, and *z-components* of the foot velocities were very similar as well (Table 11) but there were noticeable differences in ball launch mechanics (Table 7). Both FG 3 and FG 5 had ball end points on the far left side of the goal-post and understandably exhibited the most negative launch roll angles for F01. FG 3 displayed a ball launch speed 0.5 m/s faster than FG 5 with a 1.8° lower launch pitch angle allowing more of the ball speed to be in the horizontal direction, 26.2 m/s compared to 25.0 m/s. This lower launch pitch angle would be more susceptible to being blocked in a game allows for more horizontal velocity.

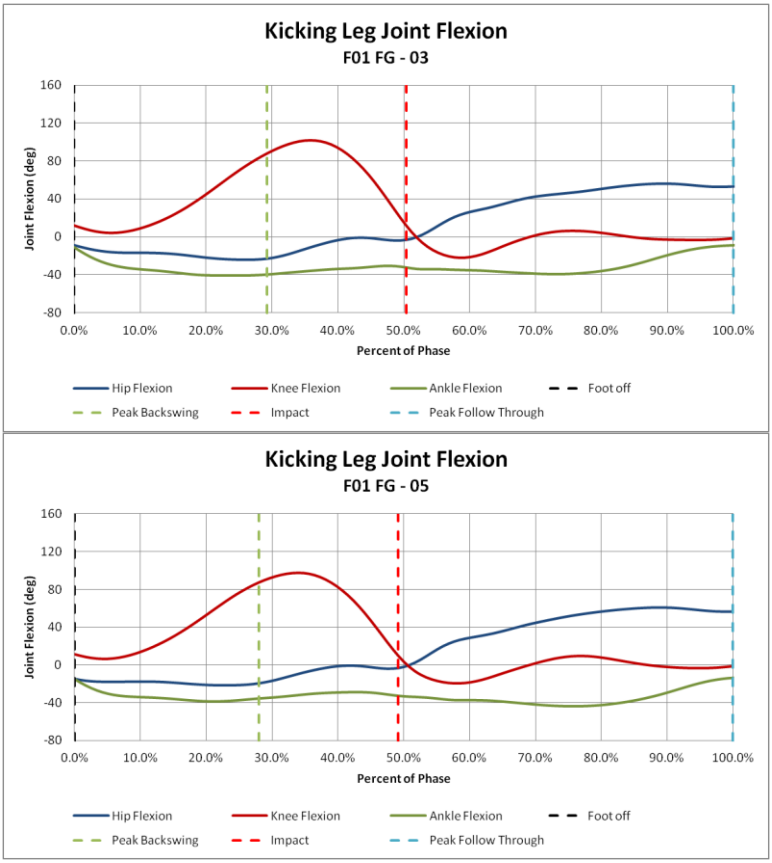

Figure 77 - F01 - Joint flexion *best* (top) and *worst* (bottom) kicks

Joint flexion for the kicking leg of F01 is consistent between FG 3 and FG 5 and no discernible differences are visible (Figure 77). It should be noted that the hip and knee for F01 consistently reach a joint flexion of 0° at the same point in the kicking phase. This motion "whips" the kicking leg into a straightened, more rigid body that the football accelerates off of. When examining these joint angles further, axial rotation and internal rotation (inversion/eversion) of the ankle was investigated.

Figure 78 depicts the point at which the foot impacts the ball in the *x-y plane* with both rear and front views. In this figure the ball is to scale and shows the orientation of the ball at impact (the *k*-tilt). When closely looking at the orientation of the kicking leg at impact, it is difficult to observationally discern significant differences in motion between the *best* (FG 3) and *worst* (FG 5) kicks based on sagittal plane kinematics alone. Future research focusing on variations in frontal and transverse plane motion patterns arising during PATs and field goals may help identify additional factors critical to successful kick outcomes.

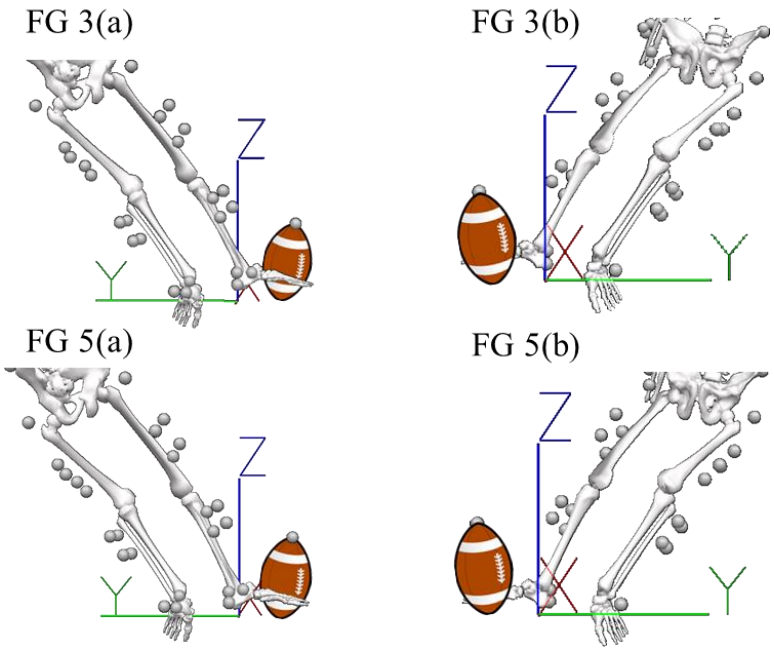

Figure 78 - F01 - View of impact rear (a) and front (b)

The orientation of the foot causing impact to occur lower on the ball may also cause F01 to compensate for more foot velocity in the *z-direction*, trying to kick through the center of the ball, as it is expected that an applied force that is directed through the center of mass of the football would allow for a cleaner transfer of energy. At impact in FG 5 the foot had a *z-velocity* of 4.1 m/s where as FG had a *z-velocity* of 3.5 m/s. The combination of a lower impact location and higher vertical velocity for FG 5 contributes to the larger pitch launch angle of 32.4º when compared to FG 3 at 29.6º.

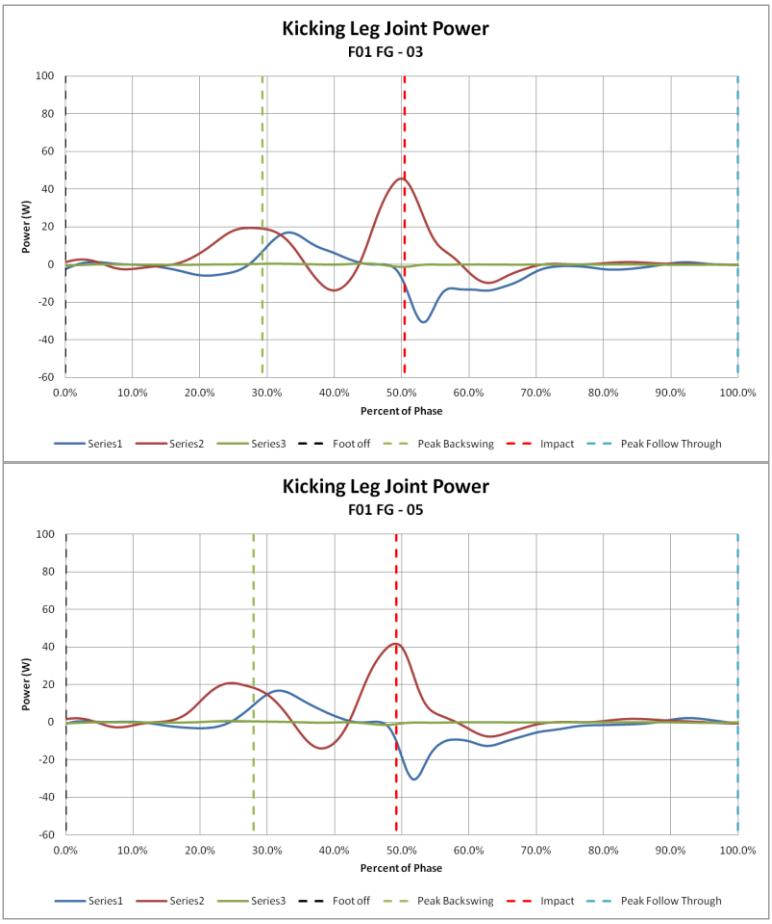

Figure 79 - F01 - Joint power *best* (top) and *worst* (bottom) kicks

The joint powers in the kicking leg for FG 3 and FG 5 follow similar curves as well (Figure 85). F01 impacts the football at maximum knee power but the knee power for FG 5 is slightly lower than that of FG 3. This is a difference of approximately 3.5 W and likely contributes to the slight difference in foot speed at impact.

Similar to the other comparisons, electromyography data remained consistent through these two kicks with exception to the vastus medialis. This muscle is used to extend the knee and therefore activation is typically present in the swing and follow-through phases. This is true for FG 3 but FG 5 displays activation in the backswing

phase. Activation of vastus medialis while the knee was still flexing would likely slow the rate of knee flexion, and secondarily slow the foot speed (by 0.2 m/s).

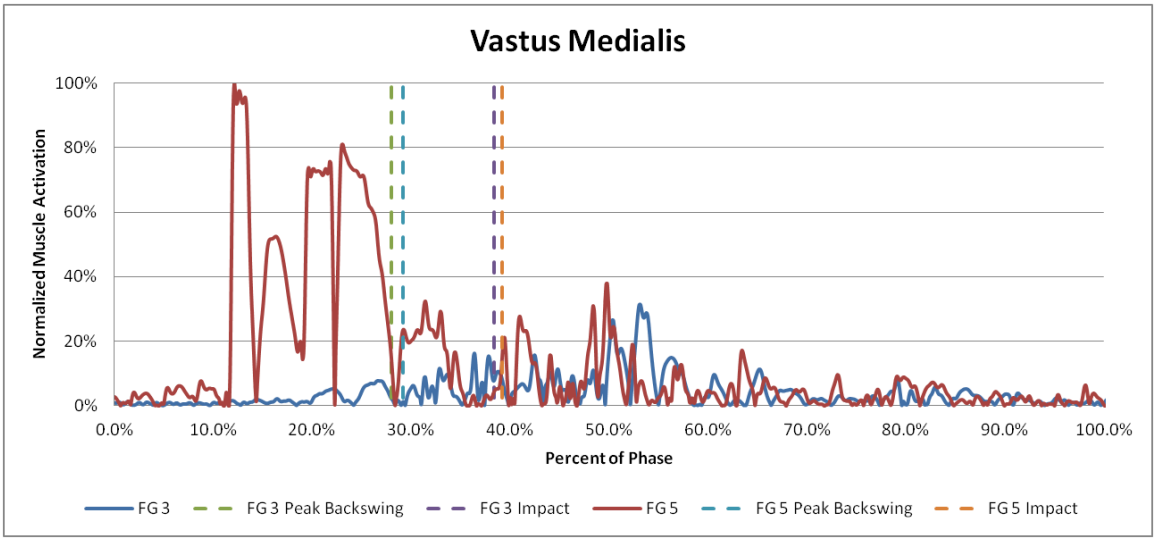

Figure 80 - F01 - Comparison of vastus medialis

5.4.2 F03 – Investigated Field-Goals

Participant F03 made one out of four 50-yd field-goals. FG 1 is examined as F03's *best* kick because it is the one kick that was successful from 50-yds, it was also perfectly accurate, crossing the goal-post at the centerline. FG 4 is examined as F03's *worst* kick because it was highly inaccurate, crossing the plane of the goal-post 6 yards off of the centerline.

Though the segment speed curves of FG 1 and FG 4 are quite similar (Figure 81), the point at which peak backswing and impact occur is quite different. FG 1 shows more of a 'normal' segment speed curve with respect to phase landmarks since pelvis speed begins to drop around peak backswing and impact occurs after the foot has reached its maximum speed. In FG 5 F03 reaches peak backswing earlier in the kick before the pelvis begins to slow, likely before the plant foot becomes planted. This jump causes

impact to occur before reaching maximum foot speed and as a result the foot has a large *y-component* of velocity and a negative *z-component* since the foot is still traveling towards the ground. This type of impact with a negative *z-component* of velocity will be referred to as hitting it 'fat'. Though there are components of the foot velocity in the *y* and *z-directions* much different from the average, likely contributing to the inaccuracy of the kick, FG 4 is impacted with a foot speed of 18.5 m/s whereas FG 1 was impacted at 16.4 m/s.

Differences in segment speed at impact were observed for both the thigh and shank as well. The thigh and shank traveled at 4.5 m/s and 10.6 m/s at impact respectively. The combination of segments speeds results in a total speed of 29.4 m/s for FG 1 and 35.0 m/s for FG 4. Even though the ball is impacted at a higher foot speed and overall kicking leg speed the ball is launched at 22.9 m/s, 1.8 m/s slower than FG 1. Impacting the ball while having a negative *z-velocity* contributed to the ball launching at a pitch angle of 26.4º, 12º lower than FG. Therefore, this type of impact may allow for the ball to travel further but is more difficult to control and can greatly affect the launch angle.

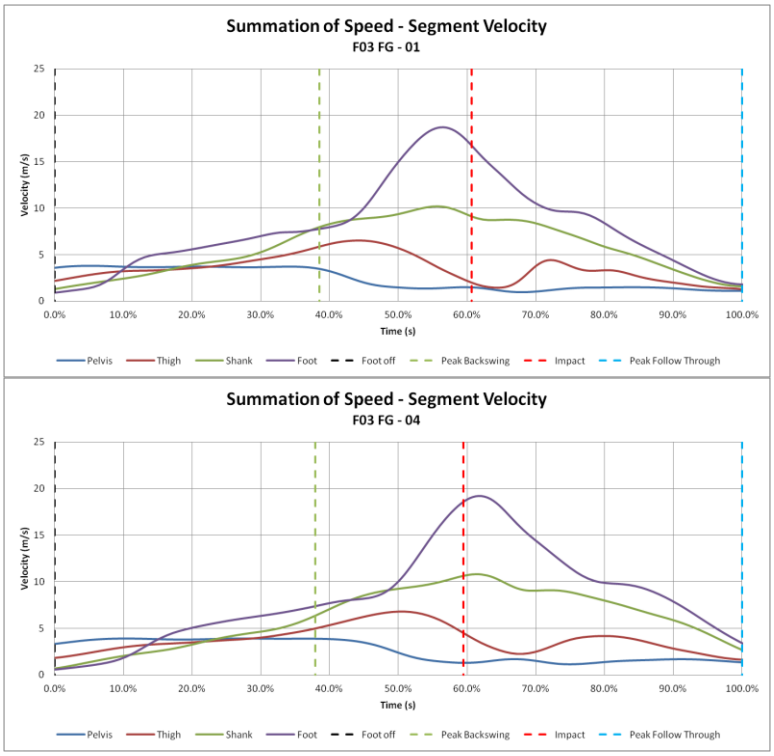

Figure 81 - F03 - Magnitude of resultant segment velocity *best* (top) and *worst* (bottom) kicks

As expected, joint flexion for FG 4 shows peak backswing and impact earlier in the kick as well (Figure 82). This is then translated onto joint power in Figure 83. In FG 4 F03 displays his "whipping" motion much later in the kick and makes initial impact when the hip, knee, and ankle are at nearly 0 W. This information supports the notion that a higher joint power at impact more closely correlates to higher ball launch velocity than foot speed.

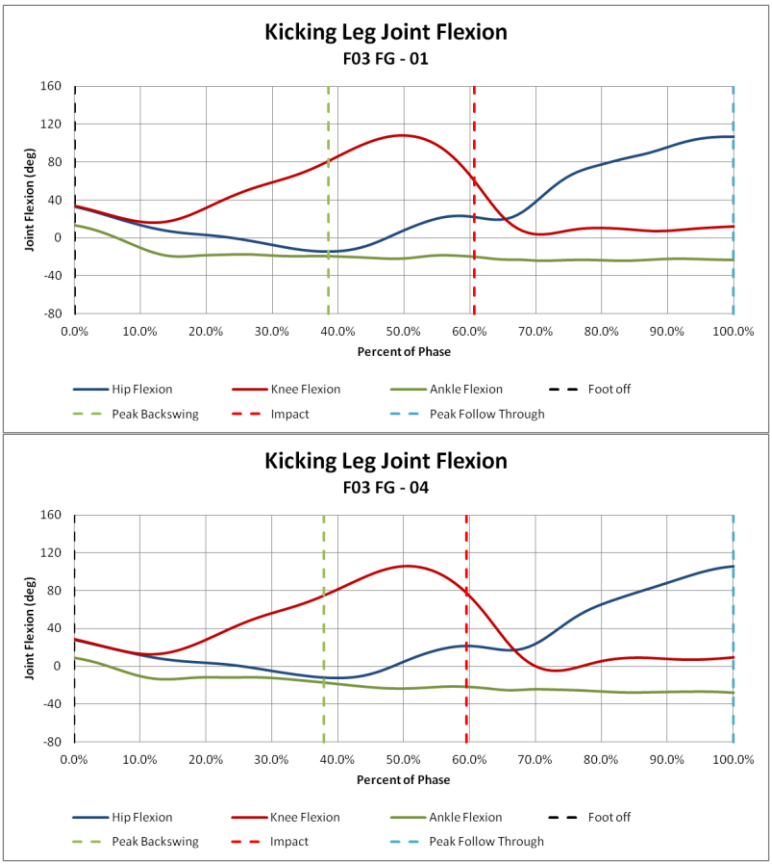

Figure 82 - F03 - Joint flexion *best* (top) and *worst* (bottom) kicks

F03 was the only participant who oriented the ball tilted backward (positive *j*-tilt), an average close to 7º. In comparison F01 shows an average pitch of -6.6º and F04 shows an average of 0.1º, essentially vertical. It has been determined that the location of impact on the ball can play a large role in the successfulness of the kick. Therefore consistency in how the ball is oriented at impact can be just as important as consistency in kinematics.

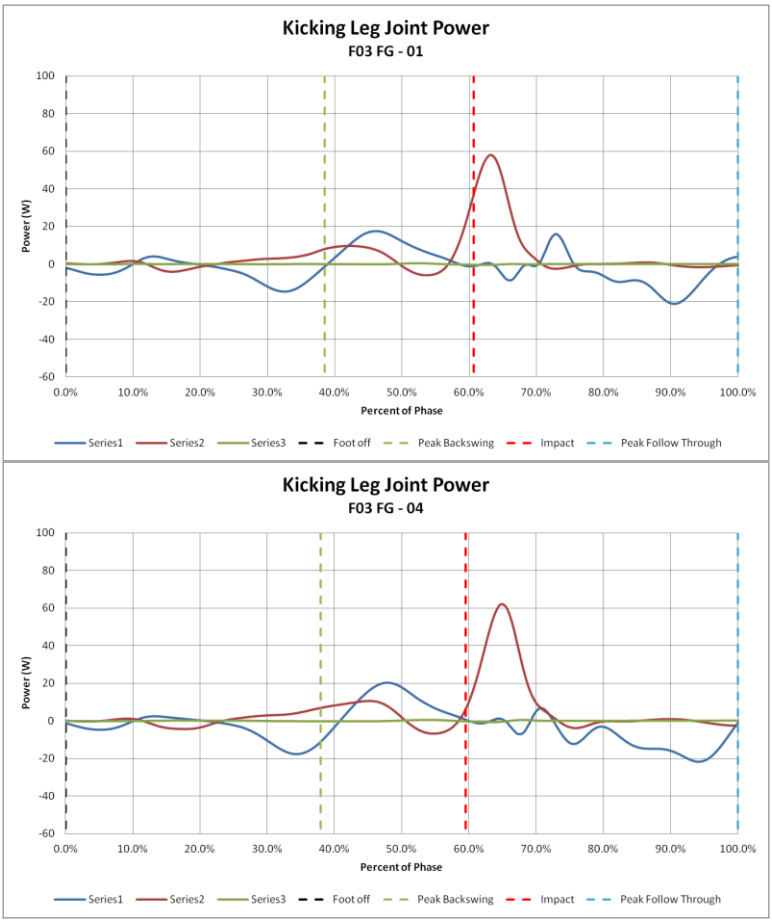

Figure 83 - F03 - Joint power *best* (top) and *worst* (bottom) kicks

In FG 1 the ball is oriented with a *j*-tilt of 9.6º and a *k*-tilt of 3.7º. In this orientation the ball is tilted backwards towards, and tilted to the right side, away from the kicker. In FG 4 the ball is oriented with a *k*-tilt of 6.6º and a *k*-tilt of 8.8º. This orientation is similar to the last but the ball is tilted much farther to the right before impact (this can be observed in Figure 84). This extra tilt causes the foot's center of mass to be farther away from that of the football and may affect the transfer of energy to the ball on impact. It should also be noted that in FG 1 (the only field-goal that F03 made) the ball was oriented with the most *j*-tilt (3.3º more than the next highest) and the least *k*-tilt (1.2º less

than the next lowest). Perhaps just changing the orientation of the ball at impact would increase F03's chances of successfully making a 50-yd field goal.

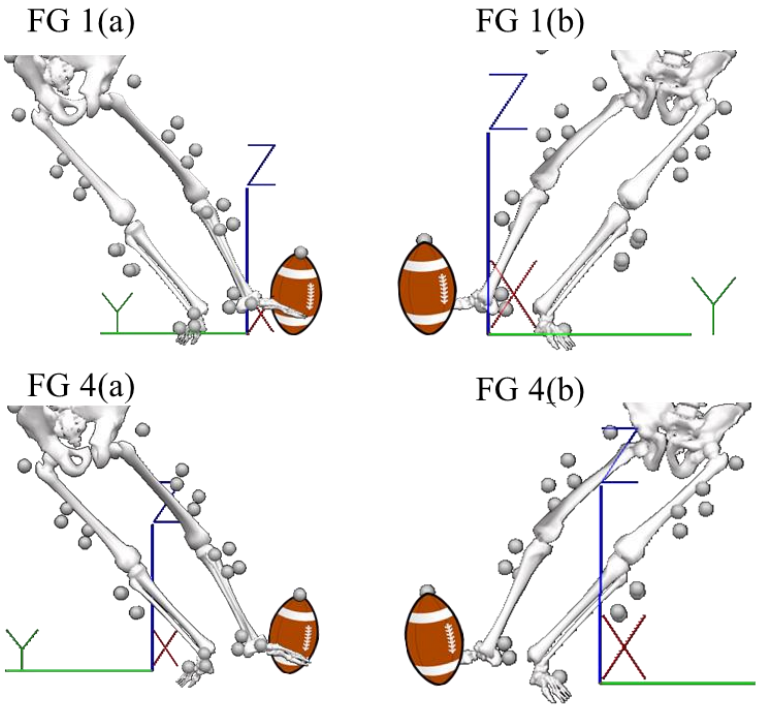

Figure 84 - F03 - View of impact rear (a) and front (b)

5.4.3 F04 – Investigate Field-Goals

Participant F04 made four out of five 50-yd field-goals. FG 10 is examined as F04's *best* kick because it crosses the plane of the goal-post closest to the centerline while also crossing over 6 m above the ground. FG 8 is examined as F04's *worst* kick because it was his only miss, roughly 4 m from the centerline of the goal-post.

Similar to what was observed with F03, F04's *worst* kick showed impact earlier in the kicking phase with respect to maximum foot speed. For F04's FG 8 this resulted in the ball being impacted at over 20 m/s, nearly the peak foot speed. FG 10 was impacted at 18.8 m/s which was the median for his field-goal attempts (Figure 85). These two kicks

also launched the ball with the highest speeds of the 5 field-goal attempts at 31.5 m/s and 32.2 m/s for FG 10 and FG 8 respectively.

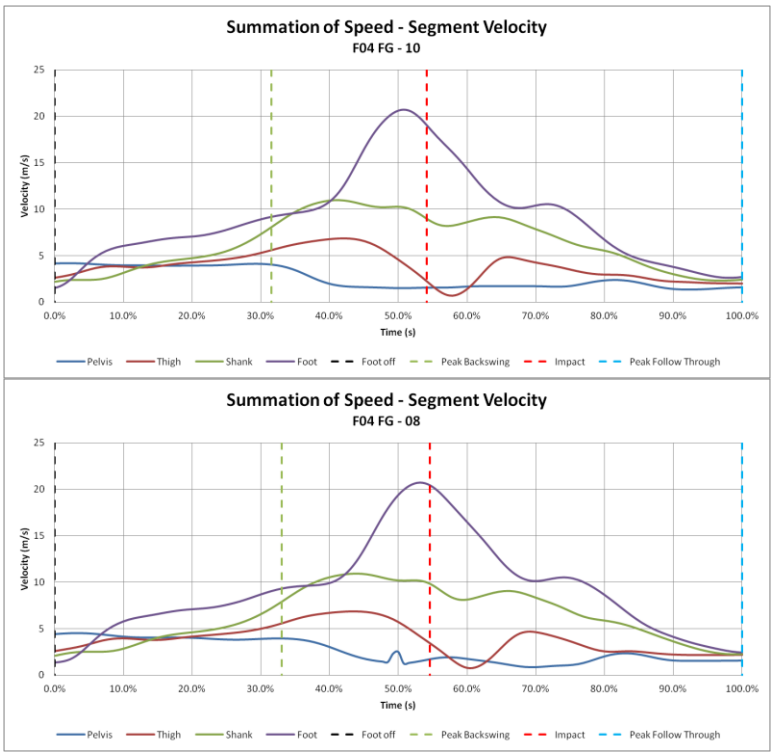

Figure 85 - F04 - Magnitude of resultant segment velocity *best* (top) and *worst* (bottom) kicks

As expected from observing the segment speed plots for FG 8, impact occurred farther away from the straightening of the kicking leg (hip and knee flexion both equaling zero) as seen in Figure 86 (note: because of aberrant data possibly arising from movement artefact in the hip flexion curve for FG 8, this curve was not included in the averages presented earlier). Therefore the foot is still clearly traveling down and away from the hip and knee giving it a *z-velocity* component of -1.1 m/s and is impacting the ball 'fat'. There is also a large *y-component* of velocity at -5.9 m/s, a magnitude of 3.7 m/s more than the closest kick. Negative *y-velocity* would be to the right of the kicker and FG

8 is missed to the right of the goal-post. These ball launch mechanics are similar to what was observed in FG 4 with F03, negative *z-velocity* and the largest magnitude of *y-velocity*.

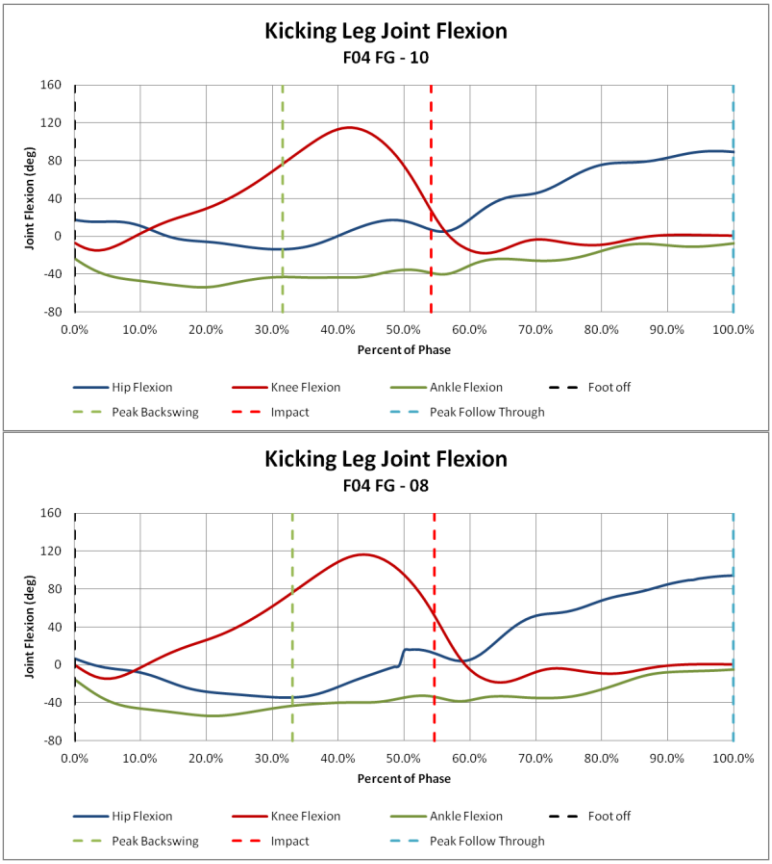

Figure 86 - F04 - Joint flexion *best* (top) and *worst* (bottom) kicks

F04 shows the steepest knee flexion slopes of all the kickers examined in this study. This slope of the knee flexion curve relates to the angular velocity about the knee joint and in turn, how fast the shank and foot move. The physical size of all the participants was very similar (1.84±0.04 m tall and 89.1±3.4 kg in mass). Additionally, the moment of inertia between the kicking legs of participants varied only slightly (F01 - 0.815 kg*m^2, F02 - 0.932 kg*m^2, F03 - 0.879 kg*m^2, and F04 - 0.862 kg*m^2) with a

standard deviation of 0.048 kg*m^2. Therefore, the driving factor in determining joint power was angular velocity and angular acceleration (EQ 10). Since F04 displays the largest change in knee flexion over time it is not surprising that he also exhibits the largest knee joint power (Figure 87).

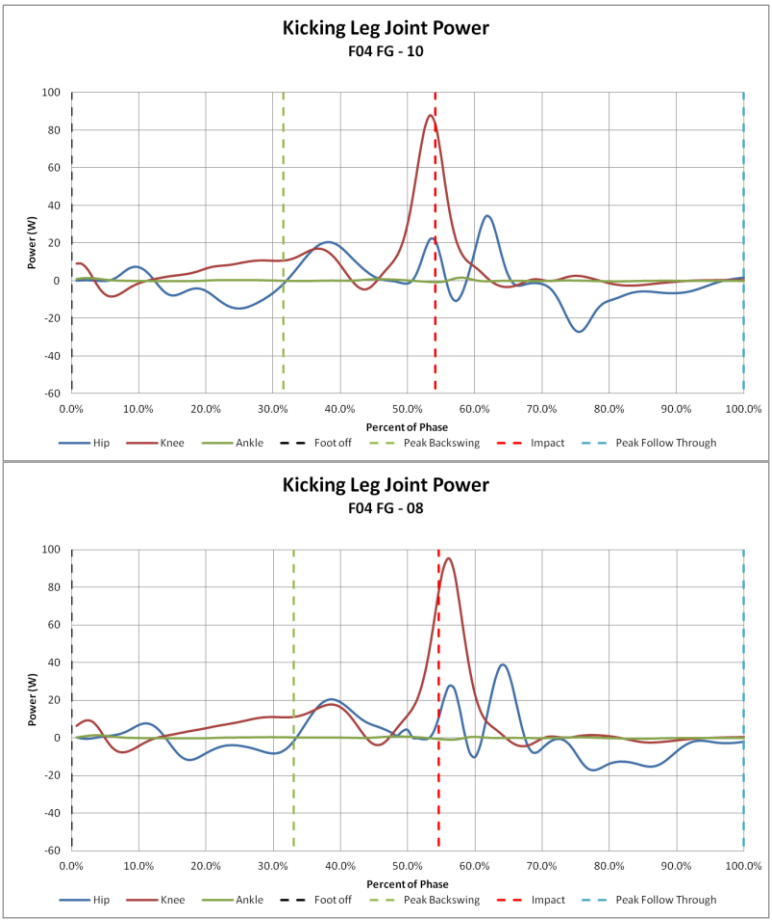

Figure 87 - F04 - Joint power *best* (top) and *worst* (bottom) kicks

F04 displayed both hip and knee joint powers larger than the other participants and on average made contact with the ball shortly after reaching the peak of these powers. What also stands out besides the magnitude of the joint power is that the initial peaks in power at the hip and knee occurred nearly simultaneously. This was not

observed with the other participants and may likely contribute to the higher foot speeds and ball launch speeds measured for F04.

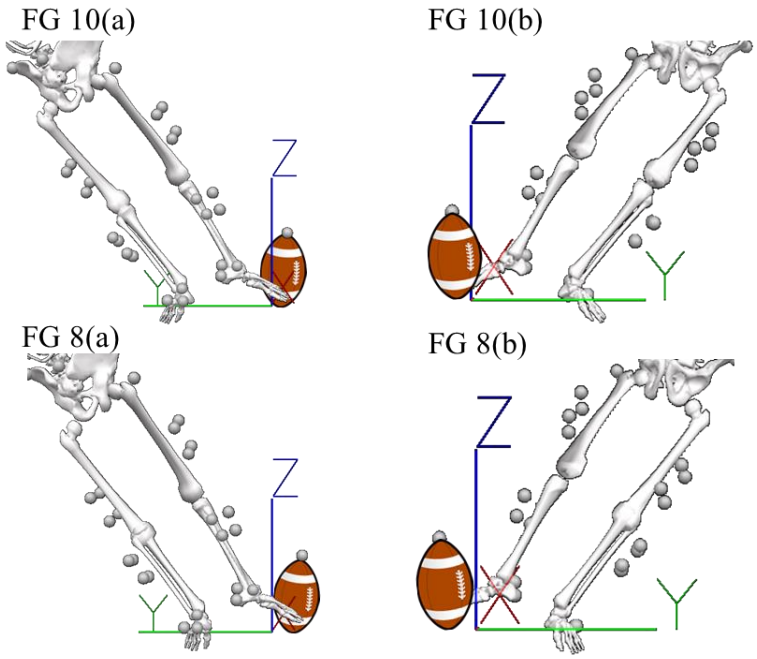

Figure 88 - F04 - View of impact rear (a) and front (b)

The orientation of the foot, as calculated through the Qualisys and Visual 3D software, is presented in Figure 88. In this figure F04 appears to impact the ball with more of the top surface of the foot when compared to the other participants impacting the ball with the side of the foot (this orientation at impact was confirmed with the videos of the kicks). Impacting with the top of the foot requires plantar flexion (extension) and pronation of the ankle. As observed in the average joint flexion plots (Figure 64), F04 shows the largest amount of ankle plantar flexion with an average near 40° where F01 achieved only approximately 30° and F03 and F02 displayed approximately 20°.

Impacting the ball with the side of the foot places a larger load on the muscles, tendons, and ligaments that control internal rotation and adduction. The muscle groups controlling the leg (e.g., quadriceps, hamstrings, pretibial muscles and plantar flexors) generally function as synergists for flexing and extending the leg's joints. Thus impacting the ball with the top surface of the foot would place less of an internal rotational load on the kicking leg and direct more of the load through the muscles designed for flexion.

It is also evident from Figure 88 that F04 impacts the ball closer to his toes. This corresponds to the foot center of mass plot in Figure 70 where F04 foot's center of mass is on average 10 cm from the center of the ball. If we observe the kicking leg as a single rotating rod, the end of the rod (farthest from the point of rotation) would have the highest linear velocity at any given point, thus promoting greater efficiency.

5.4.5 Kinetic Energy

Calculating the kinetic energy (KE) through the kick considers both the linear segment speeds and angular velocities of the segments about the joints. Linear kinetic energy is a function of the mass and linear speed of the segment. The three components of the leg (thigh, shank, and foot) were used in the kinetic energy analysis. EQ 11 was used to calculate the linear kinetic energy for each segment

$$KE_{linear} = \frac{1}{2}mv^2 \qquad \{\text{EQ 11}\}$$

where m is the approximated mass of the segment and v is the linear velocity of the segment.

Similar to linear kinetic energy, angular kinetic energy was calculated using EQ 12. Angular kinetic energy is composed of two variables, the moment of inertia of a segment about the axis of rotation and the rotational velocity of the segment about that axis.

$$KE_{angular} = \frac{1}{2} I \omega^2 \quad \{EQ\ 12\}$$

where I is the approximated mass moment of inertia of the segment and ω is the rotational velocity of the segment about the body's center of mass.

Multiple studies have been performed to give an average percent mass and length for most body members as well as an average mass moment of inertia of each body member about the body's center of rotation [1].

Table 15 - Segment percentages with respect to the individual's height and weight [1]

Member	Length (L%)	Mass (m%)	Inertia (I%)
Thigh	25.4%	9.9%	32.3%
Shank	23.3%	4.6%	30.2%
Foot	11.7%	1.4%	47.5%

To calculate the length of each member the corresponding length percent was taken from the height of the kicker. Similarly, the mass of each member was calculated by taking the corresponding mass percent from the total mass of the kicker. EQ 13-16 step through the process of finding the length, mass, and mass moment of inertia for each body member examined.

$$L_{segment} = H_{kicker} * L\% \quad \{EQ\ 13\}$$

where $L_{segment}$ is the length of the member, H_{kicker} is the measured height of the kicker, and $L\%$ is the corresponding length percentage from Table 15.

$$m_{segment} = m_{kicker} * m\% \quad \{EQ\ 14\}$$

where $m_{segment}$ is the mass of the member, m_{kicker} is the measured mass of the kicker, and $m\%$ is the corresponding mass percentage from Table 15.

$$I_{segment} = I\% * m_{segment}L^2{}_{segment} \quad \{EQ\ 15\}$$

where $I\%$ is the percent mass moment of inertia from Table 15. The total kinetic energy for each segment was found by combining the linear and rotational kinetic energies EQ 16.

$$KE_{Total} = KE_{linear} + KE_{angular} \quad \{EQ\ 16\}$$

This methodology was used with the average linear and rotational segment velocities for participants F01, F03, and F04 to calculate the kinetic energy of the thigh, shank, and foot. These segment kinetic energies were then combined to produce an estimated kinetic energy for the kicking leg (Figure 89). The point of impact in the phase was synchronized for the participants so that the kinetic energies at impact could be compared. Consistent with what has been presented for foot speed and kicking distance, F04 displays the highest kinetic energy at impact and F03 displays the lowest.

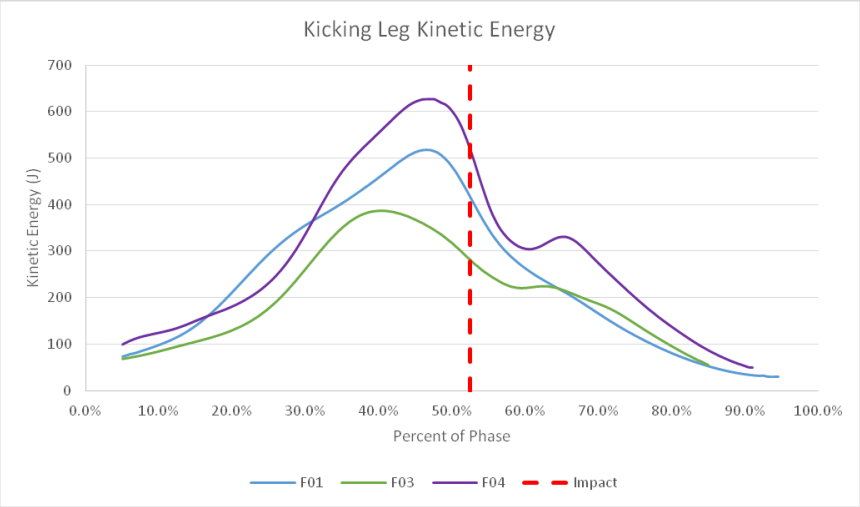

Figure 89 - Estimated kinetic energy of the kicking leg

A similar calculation can be made using EQ 11 to determine the kinetic energy of the ball just after being launched (Figure 90). As expected participant F04's ball had the most kinetic energy while F03 showed the lowest kinetic energy. Comparing the kicking leg kinetic energy to that of the football, participant F01's football's kinetic energy was 45% that of his kicking leg at impact. Participants F03 and F04 showed 43% and 39% respectively. Though there are differences in how the participants made contact with the football at impact, these numbers imply that the relationship between energy created by the body and energy delivered to the football is non-linear.

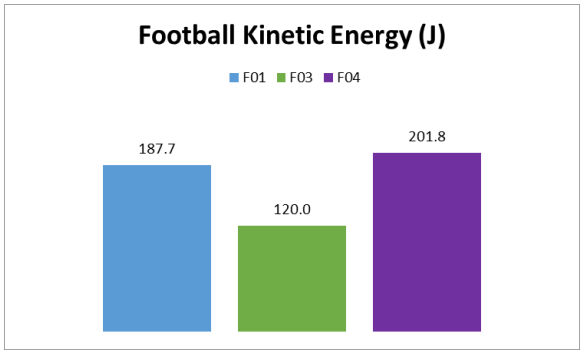

Figure 90 - Estimated kinetic energy of the football after launch

Chapter 6: Conclusion

As emphasized at the beginning this dissertation, the kicking motion is a unique, highly specialized form of striking [12]. As variable after variable was measured, evaluated, and presented in this study (e.g., electromyography, joint kinematics and kinetics, ball orientation), it becomes apparent that place-kicking is an incredibly high speed, complex motion, that tests the limits of the human body..

Chapter 3 introduced a low cost post-processing technique for accurately tracking the trajectory of an object in 3D space. There are a number of 3D tracking systems currently on the market but they can be very expensive and are commonly restricted by capture volume or what types of objects are compatible for tracking. The tracking program developed in this dissertation relies on the uncomplicated post processing of two 2D videos at perpendicular angles to each other, which recreate the viewed 3D space. This technology was then used throughout this dissertation to track football flight. This information was critical in determining the effectiveness of the kick.

In Chapter 4 a mechanical field-goal kicker was utilized to perform controlled place kicks. In this simplified pendulum based model, the impact location, angle, and ball tilt were varied while the impact velocity from the mechanical kicker remained constant. This study highlighted the importance of impact location, over impact angle and ball tilt, when wishing to maximize kick distance and height. When observing a range of impact locations along the bottom half of the ball, it was found that an impact at 5.5 cm from the bottom of the ball consistently results in a farther kick.

It was also found that, under the experimental conditions, a positive or negative *k*-tilt resulted in the ball drifting off to the right or left respectively. If the ball was in the air long enough, this drifting motion hooked the ball back towards the centerline on its descent. Due to the pendulum dynamics of the mechanical kicker, this information cannot be directly related to the instep kick in human subject field-goal kicking, but can help us to understand the dynamics of end-over-end football flight in a controlled environment.

The overall intention of Chapter 5 was to determine factors leading to successful long distance field-goals. The information presented, aligning with the findings in Chapter 4, suggests that impact conditions are the independent variables that drive the ball launch mechanics, and ultimately the trajectory of the football. A number of actions that control these variables were measured and analyzed in this study. Kinematic tracking (inverse dynamics) and electromyography allows for evaluation of the summation of speed principle contributing to segment velocity, calculation of joint angles and powers, as well as foot orientation and velocity, to assess impact conditions.

As observed in the Chapter 4 and in individual kick comparisons (Chapter 5.4), the orientation of the football at impact can have noticeable effect on its trajectory. Unlike many of the biomechanical factors present in performing a place-kick, this variable can easily be adjusted and tested through practice to find the ball orientation that works best for an individual's kicking style. Through each kicker oriented the ball differently, all participants oriented the football with a slight positive *k*-tilt when performing their field-goal attempts. Orienting the football this way allows a kicker to

impact the football with their foot more perpendicular to its long axis, similar to a 0° *k*-tilt impact with the mechanical kicker.

When observing the percentage of 50-yd field-goals made, the end points, and more collectively the deviation plot for field-goal trajectories in Figure 63, it is clear that participant F04 made a higher percentage of his attempts and consistently kicked the ball farther than the other participants. Participant F01 proved to be the most accurate, by sending every attempt between the uprights of the goal-post but missed two attempts short of the cross-bar.

Using F04 as the model, the kinematic re-creation shows that he impacts the football consistently lower than the other participants with a foot center of mass farthest away from the middle of the football. Due to the more planter flexed and pronated orientation of the ankle and foot, F04 is able to apply a more direct load to the football by reducing internal rotation of the joints transferring the impact load to the larger muscles designed for sagittal plane advancement. This orientation makes the kicking leg more rigid and allows F04 to make solid contact with a foot center of mass farther from the ball.

This more efficient orientation at impact also showed a higher impact velocity and as a result a higher ball launch speed. The higher foot speed is made possible due to a superior display of the summation of speed principle. Ideal timing of muscle activation translates the body towards the football and rotates the hip and knee so that the kicking foot starts to accelerates while the shank displays its maximum speed. This timing of

segment speed increases the angular velocity of the knee joint which in turn creates a spike in knee joint power through impact. Increased linear and angular velocities heavily contribute to the higher kinetic energy observed in F04's kicking leg at impact which in turn allows for more energy delivered to the football.

6.1 Future Directions

One limitation of this study is the number of participants. Increasing the number of participants would allow for more variation in kicking style to be observed and superior verification of the findings. Participants of different skill levels, lower level such as high school or higher level such as professional kickers could be examined to map a progression of skill acquisition, muscle demand, joint motion and body control.

It was determined that the interaction between the kicking foot and ball is very important. Instrumenting the ball with a high frequency accelerometer would allow for a more precise evaluation of impact location as well as the rotation of the ball in flight. Such a measurement device would allow for a better understanding of the foot to ball interaction and the dynamics of ball flight.

This study takes steps to examine the summation of speed principle on a number of different levels with respect to place-kicking. The protocols developed for this study could easily be applied to other complex activities that exhibit proximal-to-distal motion. For example, these protocols could be adjusted and applied to a throwing motion whereas little adjustment would need to be made to investigate a corner kick or penalty kick in soccer.

References

1. "Inverse Dynamics." *Clinical Gait Analysis*.<http://www.clinicalgaitanalysis.com/teach-in/inverse-dynamics.html>.
2. "Sensor Loacations." *SENIAM*. N.p., n.d. Web. 30 Mar. 2015.
3. "Types of Body Movement." CNX. N.p., n.d. Web. 7 Oct. 2015. <http://cnx.org/>.
4. Andersen et al. "Biomechanical Differences Between Toe and Instep Kicking - Influence of Contact Area on the Coefficient of Restitution." *Football Science* Vol. 5 (2008): 45-50.
5. Appleton, Brad. "Stretching and flexibility." (1993).
6. Barfield, William Roy, Donald T. Kirkendall, and Bing Yu. "Kinematic Instep Kicking Differences Between Elite Female and Male Soccer Players." *Journal of Sports Science and Medicine* 1.3 (2002): 72-79.
7. *Bone Structure Skeleton of Left Foot*. Digital image. *Foot and Ankle Bone Anatomy*. N.p., n.d. Web. 20 Oct. 2015.
8. Brancazio, Peter J. "The physics of kicking a football." *The Physics Teacher* 23.7 (1985): 403-407.
9. Brown, Douglas. Tracker. Vers. 4.29. 2015. http://physlets.org/tracker/.
10. Bull-Andersen, T., Dorge, H. and Thomsen, F. (1999) “Collisions in soccer kicking.” *Sports Engineering* 2, 121-125.
11. Bunn J. “Scientific Principles of Coaching.” Englewood Cliffs, NJ: Prentice-Hall, 1972
12. Butterfield, Stephen A., and E. Michael Loovis. "Influence of age, sex, balance, and sport participation on development of kicking by children in grades K-8."*Perceptual and Motor Skills* 79.1 (1994): 691-697.
13. Cesar, Guilherme Manna. *Development of postural strategies for the control of forward momentum*. University of Southern California, 2014.
14. *Concentric and Eccentric Muscle Loading*. Digital image. *StudyBlue*. N.p., n.d. Web. 10 Nov. 2015.

15. Delsys® Tringo™ Wireless EMG Sensor. Digital image. Delsys. N.p., n.d. Web. 1 Aug. 2015.
16. DeProft, E., Cabri, J., Dufour, W. and Clarys, J.P. (1988a) Strength training and kick performance in soccer players. In *Science and Football*. Eds: Reilly, T., Lees, A., Davids, K., and Murphy, W.J. New York: E & F.N. Spon, 108-113.
17. DeProft, E., Clarys, J.P., Bollens, E., Cabri, J. ad Dufour, W. (1988b) Muscle activity in the soccer kick. In *Science and Football*. Eds: Reilly, T., Lees, A., Davids, K., and Murphy, W.J. New York: E & F.N. Spon, 434-440.
18. Dorge, H. et al.(1999) "EMG activity of the iliopsoas muscle and leg kinetics during the soccer place kick." *Scandinavian Journal of Medicine and Science in Sports* 9, 155-200.
19. Gabbard, Carl. "Foot laterality during childhood: a review." *International Journal of Neuroscience* 72.3-4 (1993): 175-182.
20. Gay, Timothy. *Football Physics*. N.p.: Holtzbrinck, 2004. Print.
21. Gesell, Arnold, and Louise B. Ames. "The ontogenetic organization of prone behavior in human infancy." *The Pedagogical Seminary and Journal of Genetic Psychology* 56.2 (1940): 247-263.
22. Haubenstricker, J., et al. "Preliminary validation of a developmental sequence for kicking." *Midwest District convention of the American Alliance of Health, Physical Education, Recreation, and Dance, Chicago, IL*. 1981.
23. Holden, John P., and Steven J. Stanhope. "The effect of variation in knee center location estimates on net knee joint moments." *Gait & Posture* 7.1 (1998): 1-6.
24. Huang, T., Roberts, E. and Youm, Y. (1982) "Biomechanics of kicking." *Human body dynamics: impact, occupational, and athletic aspects*. Ed: Ghista, D. Oxford: Clarendon Press. 407-443.
25. Kellis E, Katis A. "Biomechanical characteristics and determinants of instep soccer kick." *J Sports Med Phys Fitness.* 2007 6, 154-165.
26. Kollath E: Analyse des Innenspannstoßes aus biomechanischer Sicht.Fußballtraining 1983, 2(5):15-20.

27. Lee, W. M., A. P. Mazzoleni, and M. A. Zikry. "Aerodynamic effects on the accuracy of an end-over-end kick of an American football." *Sports Engineering*16.2 (2013): 99-113.
28. Lees A, Nolan L. "The biomechanics of soccer: A review." *J Sports Sci* 1998, 16:211-234.
29. Lees A: (2003) "Biomechanics applied to soccer skills." *In Science and Soccer* 2nd Edition. Edited by: Reilly T, Williams A. London, Routledge; 2003:123-134.
30. Levanon J, and Dapena J. "Comparison of the kinematics of the full-instep and pass kicks in soccer." *Medicine and Science in Sports and Exercise* 1998 30, 917-927.
31. Marshall RN, Elliott BC. "Long-axis rotation: the missing link in proximal-to-distal segmental sequencing." *J Sports Sci.* 2000 Apr;18(4):247-54.
32. Mello, Roger GT, Liliam F. Oliveira, and Jurandir Nadal. "Digital Butterworth filter for subtracting noise from low magnitude surface electromyogram." *Computer methods and programs in biomedicine* 87.1 (2007): 28-35.
33. Naito, Kozo, Yosuke Fukui, and Takeo Maruyama. "Multijoint kinetic chain analysis of knee extension during the soccer instep kick." Human Movement Science 29.2 (2010): 259-276.
34. Nunome H, Asai T, Ikegami Y. and Sakurai S. "Three-dimensional kinetic analysis of side-foot and instep soccer kicks." *Medicine and Science in Sports and Exercise* 2002 34, 2028-2036.
35. Plagenhoef, S. (1971) "Patterns of human motion." Englewood Cliffs, NJ: Prentice-Hall.
36. Roberts, E. Mortimer, and A. Metcalfe. "Mechanical analysis of kicking." (1969): 315-319.
37. Robertson G, "Body Segment Parameters." Presentation: School of Human Kinetics, University of Ottawa.
38. Rodano, R. and Tavana, R. (1993) Three dimensional analysis of the instep kick in professional soccer players. In: *Science and Football II*. Eds: Reilly, T., Clarys, J. and Stibbe, A. London: E & FN Spon. 357-363.

39. Shan and Zhang. “From 2D leg kinematics to 3D full-body biomechanics-the past, present and future of scientific analysis of maximal instep kick in soccer.” *Sports Medicine, Arthroscopy, Rehabilitation, Therapy & Technology* 2011, 3:23.
40. Shan G. and Westerhoff P. (2005) “Full-body Kinematic Characteristics of the Maximal Instep Soccer Kick by Male Soccer Players and Parameters Related to Kick Quality.” *Sports Biomechanics* Vol 4 (1) 59-72.
41. Sinclair, Caroline B. *Movement of the young child, ages two to six*. Merrill Publishing Company, 1973.
42. Smith, Christina, et al. "The Application of an Exporatory Factor Analysis to Investigate the Inter-Relationships amongst Joint Movement during Performance of a Football Skill." *Journal of Sports Science and Medicine* 5.4 (2006): 517-524.
43. Smith, N., Dyson, R. and Hale, T. (2002) The effects of sole configuration on ground reaction force measured on natural turf during soccer specific actions. In: *Science and Soccer IV*. Eds: Sprinks, W., Reilly, T. and Murphy, A. London: Taylor and Francis. 44-52.
44. Watkins, James. An introduction to biomechanics of sport and exercise. Churchill Livingstone, 2007.
45. Watts, Robert G., and Gary Moore. "The drag force on an American football." *American Journal of Physics* 71.8 (2003): 791.
46. Weineck J. (1997) Fußballtraining. Teil 1: Konditionstraining des Fussballspielers. Perimed: Spitta Verlag. (In German)
47. Zernicke R, Roberts EM: Lower extremity forces and torques during systematic variation of non-weight bearing motion. Med Sci Sports 1978,10:21-26.